Exploring the Role of Hydrogen in Decarbonizing Heavy Industry

by

Kali Benavides
B.Sc., Massachusetts Institute of Technology (2015)

Submitted to the Institute for Data, Systems, and Society
in partial fulfillment of the requirements for the degree of
Master of Science in Technology and Policy
at the
MASSACHUSETTS INSTITUTE OF TECHNOLOGY
June 2023

Authored by: Kali Benavides
Institute for Data, Systems, and Society
May 12, 2023

Certified by: Sergey Paltsev
Deputy Director, MIT Joint Program
on the Science and Policy of Global Change
Senior Research Scientist, MIT Energy Initiative
Thesis Supervisor

Certified by: Howard Herzog
Senior Research Engineer, MIT Energy Initiative
Thesis Supervisor

Accepted by: Noelle Eckley Selin
Professor, Institute for Data, Systems, and Society
Professor, Department of Earth, Atmospheric
and Planetary Sciences
Director, Technology and Policy Program

Exploring the Role of Hydrogen in Decarbonizing Heavy Industry

by

Kali Benavides

Submitted to the Institute for Data, Systems, and Society
on May 12, 2023, in partial fulfillment of the
requirements for the degree of
Master of Science in Technology and Policy

Abstract

Hydrogen is increasingly being seized upon as a widespread decarbonization solution. There are a number of potential applications for hydrogen and investments are being funneled into demonstration projects. In this thesis work I explore the economic competitiveness of hydrogen in two heavy industry applications; steelmaking and high temperature heating. These processes rely on fossil fuels for multiple attributes and there is not another low carbon alternative fuel that has all of these characteristics. I find that in all regions, low carbon hydrogen production costs are currently more expensive than fossil fuels. High temperature heating with hydrogen increases the cost of clinker by 58-225%, and raw glass by 16-73%. Applications of hydrogen in steelmaking increase steel costs by 24-90%. Cost ranges represent the different costs when using Blue or Green H_2. As a competing low carbon steel production pathway, I also assessed steelmaking with CCS which increased steelmaking costs by ($\sim$14%). Using the MIT Economic Projection and Policy Analysis (EPPA) model, I examined the deployment of H_2 based steelmaking and steelmaking with CCS under a deep decarbonization policy scenario. Results show that at current costs deployment is limited prior to 2050. However, if costs are reduced then these technologies can deploy rapidly (achieving up to 100% of the share of global steel production by 2050). Adoption of decarbonization technologies is regionally specific and there can be regional advantages to deploying certain production pathways.

Thesis Supervisor: Sergey Paltsev
Title: Deputy Director, MIT Joint Program on the Science and Policy of Global Change
Senior Research Scientist, MIT Energy Initiative

Thesis Supervisor: Howard Herzog
Title: Senior Research Engineer, MIT Energy Initiative

Acknowledgments

I would first like to sincerely thank my advisors Sergey Paltsev and Howard Herzog for their guidance and insightful teachings. I have learned from them how to conduct research in a methodical and inquisitive manner. I am also grateful to Jennifer Morris and Angelo Gurgel for lending me their expertise in modeling and helping me navigate the EPPA model. I truly could not have done this work without them. I also want to thank Bryan Mignone, Bryan Chapman and Haroon Kheshgi for their invaluable insights and collaborative discussions. I am also very appreciative of the funding provided by ExxonMobil to complete this research.

Thank you to the TPP staff for keeping the gears of this multifaceted program running smoothly. Thank you Barb for your bright outlook and quick problem solving. Thank you to Frank for giving us an introduction into the policy realm and nurturing the program's core purpose. Thank you to Elena for being such a delightful resource in the TPP offices as well as leading an amazing fitness class. Thank you to all my TPPers! Your friendship was an unexpected surprise of graduate school. Though there were weekends spent working, there were plenty of memorable social gatherings. I am grateful to have found a cohort of deeply supportive peers and I hope that the TPP network continues to thrive in the future.

Of course, no one knows better the work that went into this thesis than Nick. Thank you for your support and love throughout graduate school. I'm excited to see what the next chapter brings. Last but not least, my family. Thank you Mom and Dad for your unwavering support. You have always been my greatest cheerleaders and provided essential advice for all of my big life choices. Thank you to my sister, Sylvia. Going back to school is never easy but you provided me with an excellent example of how worthwhile it can be. And thank you to my grandparents, Japo and Papa, for all of your love and guidance. I am so excited to celebrate with you in person at my graduation. And thank you to my Grandma and Grandpa, who have always loved me unconditionally. I know Grandpa would have fully supported me going another round at MIT.

Contents

List of Figures

List of Tables

0.1 Acronyms

ATR : Autothermal Reforming

BF-BOF: Blast Furnace - Basic Oxygen Furnace

CCS: Carbon Capture and Storage

CO_2 : Carbon Dioxide

DOE: Department of Energy

DRI-EAF: Direct Reduced Iron - Electric Arc Furnace

EIA : Energy Information Administration

EJ: Exajoule

EPPA : Economic Projection and Policy Analysis model

GHG: Greenhouse Gas

GJ : Gigajoule

H_2 : Hydrogen

IAM : Integrated assessment model

IEA : International Energy Agency

IGSM: Integrated Global Systems Model

IPPC : United Nations Intergovernmental Panel on Climate Change

IRENA : International Renewable Energy Agency

ISPT : Institute for Sustainable Process Technology

kg: kilogram

kt : kilotonne

LBNL : Lawrence Berkeley National Laboratory

Mtpa : Megatonnes per annum

MWh: Megawatt-hour

NETL : National Energy Technology Lab operated by the U.S. Department of Energy

NREL : National Renewable Energy Laboratory

PEM: Proton Exchange Membrane or Polymer Electrolyte Membrane

PJ : Petajoule

PNNL: Pacific Northwest National Laboratory

PSA: Physical Adsorption System

SMR : Steam Methane Reforming

t cs : Tonnes of Crude Steel

t hrs : Tonnes of Hot Rolled Steel

USGS : United States Geological Survey

WSA : World Steel Association

Chapter 1

Introduction

The Intergovernmental Panel on Climate Change (IPCC) concluded in their most recent report that net zero greenhouse gas (GHG) emissions need to be reached by mid-century in order to limit warming to 1.5 degrees Celsius (IPCC (2022)). Global CO_2 emissions in 2022 were estimated to be roughly 34 billion tonnes (IEA (2022a)). To reach net zero in just a few decades will require drastic decreases in emissions across all sectors of the economy. One key sector is heavy industry which emits 40% of global CO_2 emissions (Gross (2021)).

Heavy industry typically encompasses sectors such as cement, steel, petrochemicals, glass/ceramics, refining and other energy intensive manufacturing processes (Friedmann et al. (2019)). The majority of the heavy industry's CO_2 emissions come from three sectors: cement, steel and chemicals (Gross (2021); IEA (2022)). These sectors are classified by the IEA as "hard to abate" because their production processes depend on carbon compounds as key reagents in chemical reactions which makes it difficult to reduce all process emissions (Mandova et al. (2020)). In addition, these processes require high temperature heating and these sectors make products that are traded on an international market which makes their production very competitive (Friedmann et al. (2019); Mandova et al. (2020)). Therefore, in order to compete globally and to be economic these processes must operate with high capacity factors and using the most cost effective processes. Also, these sectors utilize plants with long economic lifetimes and so turnover of the

infrastructure occurs slowly (Mandova et al. (2020)).

Hydrogen is a promising alternative to fossil fuels because when combusted it emits zero greenhouse gas emissions and it is versatile because it can be used for energy generation, energy storage or as a feedstock chemical. While renewable electricity can provide a zero carbon source of energy, not every process can be electrified. Hydrogen is able to provide high heat and energy fluxes similar to fossil fuels. Hydrogen is also able to be transported and stored in a manner that electricity cannot. It can also replace fossil fuels as both a chemical feedstock in certain reactions and as a combustion source for industrial heating processes. Hydrogen gas can even be directly blended into some existing processes that use natural gas, essentially acting as a drop in fuel to reduce CO_2 emissions. New hydrogen technologies are being explored in many sectors such as steel production, chemical production (CCUS with H_2), heating, transportation, power generation and long term energy storage (IEA (2019)). In my thesis, I will focus on two emission intensive heavy industry processes; iron & steel production and industrial high temperature heating. This thesis work aims to understand the current techno-economic competitiveness of hydrogen applications in heavy industry processes as compared to other promising decarbonization pathways. The objectives of this thesis are to:

1. Explore the role that hydrogen may play in decarbonizing heavy industry
2. Assess the costs of different hydrogen production technologies.
3. Determine the cost of hydrogen-based technologies to decarbonize steel production and high temperature heating.
4. Evaluate the role that hydrogen will play in decarbonizing the steel sector by implementing the results of my techno-economic analysis into an integrated assessment model under a deep decarbonization policy scenario.
5. Analyze global and regional steel decarbonization pathways.

I focus on these sectors because currently the iron and steel sector is the highest emitter amongst all heavy industry sectors (Mandova et al. (2020)). There are limited

decarbonization strategies because iron and steel production relies on fossil fuels not only as a source of energy but also to produce the reducing agent needed to convert iron ore to iron (IEA (2020)). Coking coal or natural gas are typically used to generate the reducing agent (IEA (2020)). Carbon is also essential for the strength of steel, with different types of steel containing 0.002%-1.2% carbon by weight (Hosford (2012)). Steel can be recycled via electric arc furnace (EAF), which requires much lower energy and emissions output than primary steel production however, current scrap stock is not sufficient to meet steel demand (IEA (2020)). One decarbonization strategy is to utilize hydrogen as the reducing agent to produce iron. Unlike fossil fuels when hydrogen reacts to reduce iron ore it does not emit any CO_2 (Cavaliere (2019)). The process will still require a source of carbon input to ensure the necessary carbon content in the steel. Another decarbonizing strategy that has been implemented in a few steel plants is carbon capture where the CO_2 is captured directly from the process and then transported for future use or stored indefinitely. In my thesis I will conduct a techno-economic assessment of two steelmaking pathways; one utilizing hydrogen and the other applying carbon capture & storage (CCS).

Heating is another important component of industrial processes due to the amount of energy it requires and represents another hard to abate industrial process. Industrial processes consume roughly 40 percent of global energy demand (IEA (2021)) and two-thirds of that energy is utilized to generate heat (Bellevrat & West (2018)). Due to its current reliance on fossil fuels, the industrial heating sector emits 10 percent of global greenhouse gases (Friedmann et al. (2019); IEA (2021)). The majority of the energy needed for industrial heating is used to generate temperatures greater than 400 Celsius (IEA (2018a)). At these higher temperatures there are fewer available low carbon heating alternatives (Friedmann et al. (2019)). One potential low carbon alternative is H_2 because its combustion does not emit any direct greenhouse gases and because it can generate high temperatures rapidly (Friedmann et al. (2019)).

My thesis is organized in the following way. In Section 2.1 I will detail hydrogen production pathways. In Section 2.2 I will outline existing data on traditional steelmaking processes and in Section 2.2.1 I will describe advanced steel production

pathways. In Section 2.3 I discuss decarbonization pathways for high temperature heating. Section 3.1-3.3 presents my methodology in calculating the levelized costs of hydrogen production, advanced steelmaking and high temperature heating costs. Section 3.4 describes my implementation of these costs into the MIT Economic Projection and Policy Analysis (EPPA) model. Section 4 presents modeling results for decarbonization policy scenarios generated by the EPPA model. Lastly, in Section 5 I will present my conclusions for this thesis work including my key findings as well as policy implications.

Chapter 2

Assessing the State of Knowledge

2.1 Hydrogen Production Pathways

In order for hydrogen to be a decarbonization solution, the production of the hydrogen must also be a low carbon process. There are several production pathways for hydrogen and their emission intensities vary a great deal. Today, the majority of hydrogen is produced from natural gas in a process that emits roughly 10 kg CO_2/kg H_2 (IEA (2019)). The second most common hydrogen production pathway uses coal and emits 19 kg CO_2/kg H_2 (IEA (2019)). These fossil fuel reliant processes are termed Grey hydrogen and Brown hydrogen respectively (IEA (2019)). When carbon capture is applied to either of these processes to capture the majority of direct emissions, then the pathway is called Blue hydrogen. Today only 0.1 % of global hydrogen production is produced via a dedicated water electrolysis process with 2% of global production produced as a byproduct of chloro-alkali electrolysis (IEA (2019)).

An electrolyzer powered by renewable electricity is termed Green hydrogen and can produce hydrogen with zero CO_2 emissions. However, if the electrolyzer is powered by grid electricity then it is referred to as Yellow hydrogen because the emissions intensity of the production pathway will be dependent on the emissions intensity of the electricity generation source (H2GreenSteel (2022)). The IEA calculated that an electrolyzer powered by grid electricity in China would have

indirect emissions of greater than 30 kg CO_2/kg H_2 (IEA (2019)). In addition to a range of emissions intensities, the different hydrogen production pathways also have significantly different levelized costs of hydrogen. The cost of the natural gas-based production route can be as low as $ 1/kg H_2 (IEA (2019)), while electrolysis powered by renewable energy in the U.S. is estimated by the Energy Futures Initiative to cost anywhere from $3-$8/kg H_2 (Breckel et al. (2021)).

2.1.1 Natural Gas Reforming with and without Carbon Capture

Currently the majority of hydrogen is produced from natural gas in a process called steam methane reforming (SMR) (IEA (2019)). In the SMR process natural gas acts as both the fuel to heat the process and the feedstock that reacts with the steam to produce CO_2 and hydrogen (Sadler & Anderson (2018)). An alternative process that also uses natural gas is autothermal reforming (ATR), which uses steam and oxygen injections to produce CO_2 and H_2. As demonstrated in Figure 2-1, unlike the SMR process the ATR process has just one chamber where both the combustion reaction and the reforming reaction take place (Sadler & Anderson (2018)).

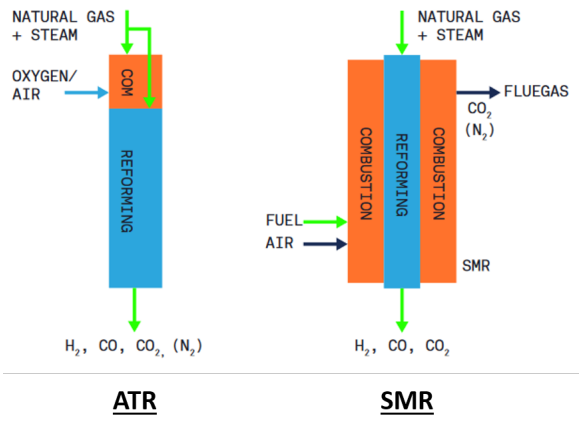

Figure 2-1: Simplified figures of the ATR and SMR processes. Figure from Sadler & Anderson (2018)

In the SMR process only ~60% of the CO_2 can be recovered from the syngas stream (Lewis et al. (2022)). To reach higher overall capture rates requires another

capture unit on the flue gas (Lewis et al. (2022)). The flue gas has a lower pressure and a lower concentration of CO_2 than the syngas stream which makes it a more challenging capture point (Sadler & Anderson (2018); Lewis et al. (2022)). Due to these differences in the process, ATR has a higher potential CO_2 capture rate using just a capture unit on the syngas stream as compared to SMR (Sadler & Anderson (2018)). SMR with CCS and ATR with CCS are both commercial scale ready technologies. There are three SMR plants with CCS in operation today and an estimated six ATR plants with CCS under development (Lewis et al. (2022)). A 2022 report commissioned by the Department of Energy (DOE) on fossil-based hydrogen production concluded that an SMR with two capture units could achieve a 96% capture rate at a levelized cost of ~$1.57/kg H_2 (2016 USD) as compared to ~$ 1/kg H_2 for SMR without CCS (Lewis et al. (2022)). The study found that ATR with one capture unit could achieve a 94% capture rate with a levelized cost of ~$1.52/hg H_2 (2016 USD) (Lewis et al. (2022)).

2.1.2 Electrolysis

(a) Alkaline electrolysis cell

(b) PEM electrolysis cell

Figure 2-2: Conceptual diagrams of two types of electrolysis cells. Figures from Schmidt et al. (2017)

Electrolysis is a less widely used hydrogen production pathway, however it is not a novel technology. Alkaline electrolyzers were invented in the 1920s and have a long history of commercial applications (IEA (2019)). Proton exchange membrane (PEM) electrolyzers were invented around 1960 and are now being deployed at a commercial scale. Another electrolyzer technology is the solid oxide electrolysis cells (SOECs),

however this technology is still in the nascent stages of development and has not yet been commercialized at scale. See Figure 2-2 for diagrams of the PEM and Alkaline electrolysis cells.

While the PEM electrolyzer is currently more expensive than the alkaline, it has some operational advantages. The PEM electrolyzer can operate at a higher pressure which reduces the amount of compression needed to store or transport the hydrogen product (IEA (2019)). PEM electrolyzers do not require an alkaline solution that requires treatment to recycle and they can operate at a wider range of their total load (IEA (2019)). Importantly, PEM electrolyzers have a higher current density and smaller footprint (Iyer et al. (2022)). The PEM electrolyzer is also more adaptable to a grid with intermittent renewable energy than the alkaline electrolyzer because it has a faster start up time and is able to ramp up and down to handle a range of loads (Iyer et al. (2022)).

Recent projects are setting new records for capacity sizes for electrolyzers. The largest green hydrogen project is currently a 150 MW alkaline electrolyzer, brought online by a Chinese chemical manufacturer at the end of 2021 (FuelCellsWorks (2022)) and the largest PEM electrolyzer is 20 MW located in Canada (Collins (2022)). However, electrolyzer costs are predicted to decrease in the future and several electrolyzer manufacturers have announced plans to build GW scale factories including Cummins, ITM Power, ThyssenKrupp, Nel, Plug Power, and McPhy (Collins (2022)). The IEA's Hydrogen Projects Database reports 26 PEM electrolyzer projects and 9 Alkaline electrolyzer projects currently under construction (IEA (2022c)).

The levelized cost of Green hydrogen varies greatly depending on the electricity price and utilization rate. Electrolyzers have a high electrical demand with electricity consumption in the range of ∼48-59 kWh/kg H_2 (IEA (2019)). Recent research into the levelized cost of electrolytic hydrogen production has produced wildly different results. The National Renewable Energy Laboratory (NREL) calculated a levelized cost of $ 4.83/kg H_2 for a PEM electrolyzer powered by grid electricity which enabled the system to operate with a utilization rate of 97% (Saur et al. (2018)). In order for

hydrogen to be produced with no carbon emissions it will need a source of electricity that emits no greenhouse gases. Renewable energy such as solar or wind can supply low carbon electricity but due to their intermittent nature it would be challenging to achieve high electrolyzer utilization rates without energy storage or over sizing of the renewable plant.

A study by Lazard calculated a levelized cost assessment of electrolytic hydrogen production with a sensitivity analysis to account for a range of electricity costs, capital costs and utilization rates. For a 100 MW PEM electrolyzer, the Lazard study calculated a range of hydrogen production costs from \$1.97 to \$5.24 per kilogram of H_2 (2016 USD) (Lazard (2021)). True production costs may be even higher than those estimates, Khan et al. (2021) calculated costs exceeding \$8/kg H_2 for solar PV powered PEM electrolyzers and costs exceeding \$ 6/kg H_2 for wind powered systems (Khan et al. (2021); Friedmann et al. (2019)). In addition, these production costs do not include the cost of transporting and storing the hydrogen.

2.1.3 Other Considerations to Adopting Hydrogen as a Decarbonization Solution

While hydrogen combusts without emitting greenhouse gases, there are other attributes that should be considered before adopting it for new uses as a decarbonization solution. Hydrogen has different storage and transportation specifications than traditional fossil fuels. Due to hydrogen's small molecular size it is more prone to leaks than, for example, methane gas. Hydrogen gas can also embed within certain types of material and has been known to cause metal embrittlement which degrades the material (Parfomak (2021)). Proposals to utilize existing natural gas pipeline networks will need to consider that most of these can only be blended with ∼20% hydrogen before requiring more intensive pipeline upgrades (Parfomak (2021)). Hydrogen leaks are also difficult to detect because the gas as well as its flame is colorless and odorless (Parfomak (2021); IEA (2019)). However, there are cost effective hydrogen detectors being developed (Arrigoni & Bravo Diaz (2022)). Most

recently the DOE's National Energy Technology Laboratory (NETL) announced a breakthrough in a hydrogen detector system (NETL (2023)). Hydrogen is also very flammable but does disperse rapidly once at atmospheric pressure. Long distance transportation of hydrogen can be done via pipeline, which is challenging for the reasons listed previously and requires the correct pipe material and gaskets to prevent leakages. Other more costly options include trucking or shipping as a gas, liquid or by converting hydrogen into another chemical prior to transport (Ex. as liquid ammonia or methanol (IEA (2019); Breckel et al. (2021)). For these reasons, I explore industrial uses of hydrogen where theoretically the hydrogen could be produced and used within the same industrial facility. Today most hydrogen is utilized by large industrial facilities that are well equipped to manage the gas and located to avoid long distance transportation (Breckel et al. (2021); IEA (2019)).

Other concerns with increased usage of hydrogen are its potential impacts as an indirect greenhouse gas. Hydrogen in the atmosphere reacts readily with hydroxyl radicals (OH) to form water vapour (Arrigoni & Bravo Diaz (2022)). The hydroxyl radical is also a primary sink for methane and some models estimate that an increase of H_2 in the atmosphere would make less OH available to react with methane and that this would extend the life of methane in the atmosphere (Arrigoni & Bravo Diaz (2022)). The leakage rate for hydrogen production from electrolysis is estimated at ∼0.2% and methane reforming typically flares any gaseous releases (Arrigoni & Bravo Diaz (2022)). However, further losses can occur through the transportation and supply of hydrogen; estimates range from ∼4% for compressed gas transported via trucking, ∼10-20% for liquid H_2 transported via trucking or shipping and ∼1% for gaseous pipelines (Arrigoni & Bravo Diaz (2022)).

2.2 Iron and Steel Production Pathways

The production of steel requires three main steps: the preparation of the raw materials (Coal, Iron Ore, Lime, Scrap), ironmaking and steelmaking (Figure 2-3). The production pathway that is utilized to produce ∼70 % of global iron and steel

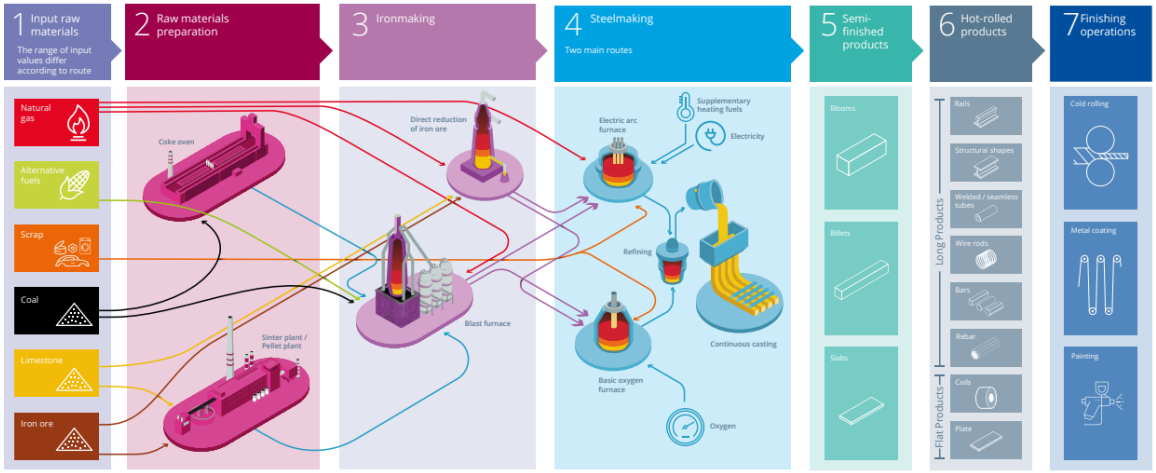

Figure 2-3: Conventional ironmaking and steelmaking pathways. Infographic from World Steel Association (WSA (2023))

production is the blast furnace and basic oxygen furnace pathway (BF-BOF) (IEA (2020)). Coke and iron ore pellets or fines are fed into the top of the blast furnace while air is pumped through the bottom. The air reacts with the coke to form a reducing gas (CO) which then reacts to reduce the iron ore to iron (Cavaliere (2019)). The molten iron (also termed pig iron) then enters the basic oxygen furnace where oxygen is injected to further reduce the carbon content and produce crude steel. The energy intensity of the BF-BOF route is currently ∼21 GJ/t crude steel (IEA (2020)). The IEA estimates that this pathway has an emissions intensity of 2.2 t CO_2/t crude steel when accounting for direct emissions and indirect emissions resulting from grid electricity based on the global average for electricity generation (∼500 kg CO_2/MWh) (IEA (2020)). The IEA estimates that the cost of the BF-BOF pathway ranges from ∼$340-460/tcs (IEA (2020)).

Other primary steel production pathways include the Direct Reduced Iron and Electric Arc Furnace (DRI-EAF) process. The DRI-EAF production pathway currently makes up 7% of global steel production (WSA (2022a)), but is growing rapidly. From 2015 to 2019 the production of DRI increased by 49% (Midrex (2019)). The majority of DRI shaft furnaces use natural gas as the reducing agent and heating fuel but the process can also use coal (India is an example of one region that relies heavily on coal-based DRI for ironmaking (Paltsev et al. (2021a)). The iron produced

called direct reduced iron (DRI) is then fed into an electric arc furnace (EAF) to be converted into steel. Lime, graphite electrodes and fossil fuels are also often added to the EAF to supply chemical energy for heating and promote slag formation. The IEA reports the average energy intensity of the DRI-EAF route as 17 GJ/t crude steel and resulting emission intensity of 1.4 t CO_2/t crude steel (IEA (2020)). The IEA estimates that the cost of the gas based DRI-EAF pathway ranges from ∼$400-600/tcs (IEA (2020)).

The EAF steelmaking pathway is used to produce 29% of global steel production (WSA (2022b)). The EAF can use DRI as mentioned previously but can also utilize up to 100% scrap steel as the metallic input (IEA (2020); Cavaliere (2019)). The EAF melts the scrap steel along with additives such as coal, natural gas, lime, and graphite. These additives add additional carbon content, provide chemical energy for heating and form a foamy slag which helps to transfer heat more efficiently (Cavaliere (2019)). The EAF's process emissions vary depending on the specific operations. On average globally, scrap steel-electric arc furnace processes utilize 150 kg coal/tonne crude steel (WSA (2021)); however, plants can also lower emissions by utilizing natural gas (WSA (2014)). Estimates for direct emissions from a scrap fed EAF process range from 0.1-0.5 tCO2/t steel (WSA (2014); Reimink & Maciel (2021)); with the IEA reporting the average emissions intensity inclusive of direct and indirect emissions as 0.3 t CO_2/t crude steel (This estimate is based on an assumed global average grid electricity emissions intensity of 540 kg CO_2/MWh) (IEA (2020)). The EAF uses electricity as the main source of its energy and the indirect emissions from the electricity can be significant depending on the source of the electricity generation. Scrap can also be used to reduce the energy intensity of the BOF pathway but can only make up lower percentages of the total metallic input (15-25%) (IEA (2020); Cavaliere (2019)). Compared to the other conventional steelmaking processes, the scrap fed EAF process is the most energy efficient with an energy intensity of only ∼2-6 GJ/t crude steel (IEA (2020); WSA (2014)). The IEA estimates that the cost of the scrap-based EAF pathway ranges from ∼$340-490/tcs (IEA (2020)).

All of these pathways produce crude steel which then must undergo additional

processing to form the final steel product. A key part is the rolling process which is common to all production pathways (IEA (2020); Fischedick et al. (2014)). Hot rolling involves heating and pressing the crude steel to reduce the thickness (Worrell et al. (2007)). After the hot rolling step, the additional finishing processes are specific to the end use of the steel (IEA (2020)).

2.2.1 Advanced Low Carbon Iron and Steel Production Pathways

Primary steel production pathways will need to be decarbonized in order to keep global warming below 1.5 Celsius. There are a number of pathways which are capable of partially reducing the carbon emissions of steel production. The BF-BOF process can reduce its CO_2 emissions through top gas recovery & recycling, through carbon capture & sequestration, by using biomass fuels or through injection of hydrogen. However, estimates predict that the highest emissions reduction that can be achieved are ∼72% reduction from H_2 injection and ∼65% reduction from carbon capture. This would not eliminate emissions and the BF-BOF typically has a higher emission intensity than the other EAF pathways (Laguna et al. (2021)). Furthermore, carbon capture is challenging in a BF-BOF plant because the largest source of CO_2 is the blast furnace (BF) off gas that is typically reused in various processes which creates multiple lower CO_2 concentration point sources (including the power plant stack, coke oven gas, blast furnace stove, sinter stack, blown oxygen steelmaking stack, hot strip mill stack, plate mill stack and lime kiln) (Hughes & Zoelle (2022); Yu et al. (2021)). The power plant stack, coke oven gas, and blast furnace stove have the highest CO_2 concentration in their stream and represent the most promising capture points (Hughes & Zoelle (2022)). The DOE's National Energy Technology Laboratory (NETL) calculated the cost of capture to retrofit a BF-BOF plant with two capture plants (each capture plant having 99% capture efficiency) to be 65-90 USD/tonne CO_2 (depending on the scale of the plant). Smelting reduction with BOF is another pathway that when paired with CCS can achieve similar emissions intensity

as DRI-EAF with CCS however its implementation readiness is lower (Laguna et al. (2021)).

The DRI-EAF process can also be equipped with carbon capture, generally capturing the direct emissions from the DRI shaft furnace and the process is more easily configured to directly capture the CO_2 emissions from one source. There are two primary DRI shaft furnace processes: Midrex which accounts for ∼80% of DRI production and the Hyl/Energiron process (Midrex (2019)). The Midrex shaft furnace could be equipped with a capture plant on the shaft off gas however in this process not all of the CO_2 can be captured from a single stream (LBNL (2010)). The Hyl/Energiron process already selectively removes CO_2 from the reduction system. In addition, up to 90% capture rates can be achieved by incorporating a physical adsorption system (PSA) which separates the hydrogen from carbon containing compounds. This allows even more CO_2 to be removed from the capture unit as seen in Figure 2-4. The Hyl/Energiron DRI shaft furnace with carbon capture technology has already been implemented at a commercial scale, however currently all operating plants have commercialised the CO_2 for utilization rather than storage (Duarte et al. (2010)). There are several Hyl/Energiron plants which sell the CO_2 for use in the food and beverages industry (Duarte et al. (2010)). Emirates Steel has two Hyl/Energiron plants located in Abu Dhabi which have been capturing CO_2 since 2016 and transporting the CO_2 to an oil field for enhanced oil recovery (IEA (2020)). Estimates by the Hyl/Energiron company are that there would be minimal additional costs to implement a carbon capture unit into the existing Hyl/Energiron process (Duarte et al. (2010)).

However, there has been limited peer reviewed techno-economic assessments on applications of CCS to a DRI shaft furnace process. A study commissioned by the European Parliament calculates the current production cost of the DRI-EAF with CCS pathway at ∼$630/tonne (2016 USD), roughly 40% more expensive than the BF-BOF production pathway (Laguna et al. (2021)). As comparison real prices for hot-rolled coil steel in 2019 ranged from ∼$450 to 700/tonne (Hodges & Anton (2022)). The costs for BF-BOF produced steel in China being the least costly and the U.S.

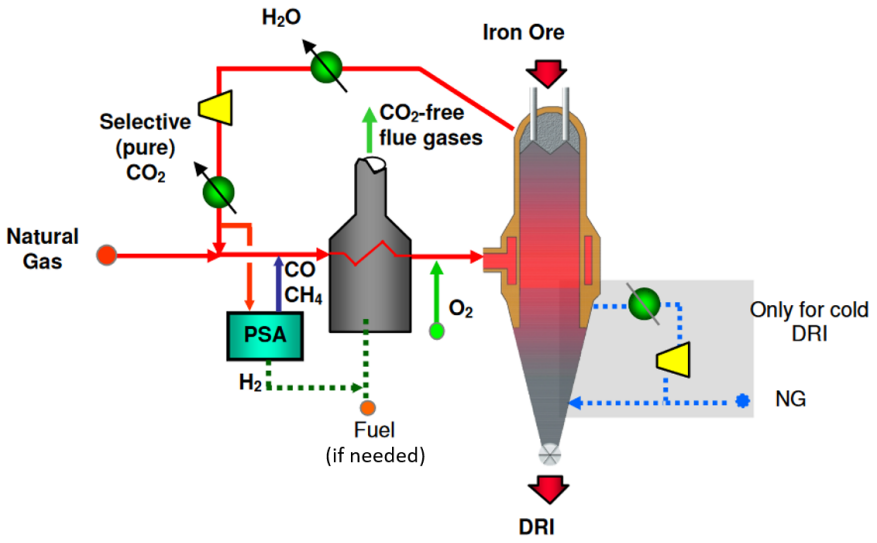

Figure 2-4: Process diagram of ENERGIRON DRI shaft furnace with PSA to achieve ~90% Selective CO_2 Removal. Figure from Duarte et al. (2010)

produced steel being on the higher end of this range.

Complete decarbonization of the primary steel making pathway is theoretically possible although no such pathway has yet been implemented at a full commercial scale. One method is to completely electrify the process using iron ore electrolysis which uses an electro-chemical reaction to reduce the iron ore (Laguna et al. (2021)). However, this technology is still being developed and has only been demonstrated at a pilot plant scale (IEA (2020); Laguna et al. (2021)). Boston Metals is one company working to commercialize this process and in 2023 they received $120 million in funding from the steel company ArcelorMittal (Davey (2023)). Other fuel sources with lower greenhouse gas impacts can also serve as substitutes for fossil fuels. Biomass has been added to existing commercial scale blast furnaces at limited percentages (IEA (2020)) but, to be a 100% substitute for fossil fuels it requires pre-treatment through a process called torrefaction to dry and consolidate the biomass (Lewis et al. (2022)). Costs for torrefied woody biomass are estimated as ~$ 90/tonne (Lewis et al. (2022)). There will also be competition for a potentially limited supply of sustainably sourced biomass (IEA (2020); Yu et al. (2021)).

Hydrogen is another potential substitute for fossil fuels because it can act as both a heating fuel and as the reducing agent in the iron ore reduction reaction. One pathway

is to use H_2 plasma in a smelting reduction process, however this technology is still in the early development phases (Laguna et al. (2021)). Hydrogen can also be injected into a blast furnace, however the BF process is not yet capable of fully substituting H_2 for coal. The more promising route is to use hydrogen as the reducing agent in the DRI shaft furnace process. The natural gas can be replaced with hydrogen except for a minimal amount of natural gas that is still needed to ensure the necessary carbon content in the DRI (0.5-4% (Cavaliere (2019))) as well as to maintain the temperatures needed for the reaction given that the reduction reaction is endothermic (Cavaliere (2019)). The DRI can be formed into steel in an electric arc furnace which when powered by renewable energy allows the entire steel production pathway to theoretically achieve a 100% reduction of emissions (Laguna et al. (2021)). Hybrit is currently leading the way in developing this technology and in 2020 they produced DRI reduced by hydrogen at their pilot plant utilizing the process described in Figure 2-5 (Hybrit (2022)). H2Green is another company that is investing in this technology and they began constructing a DRI plant in Sweden in 2022 (H2GreenSteel (2023)).

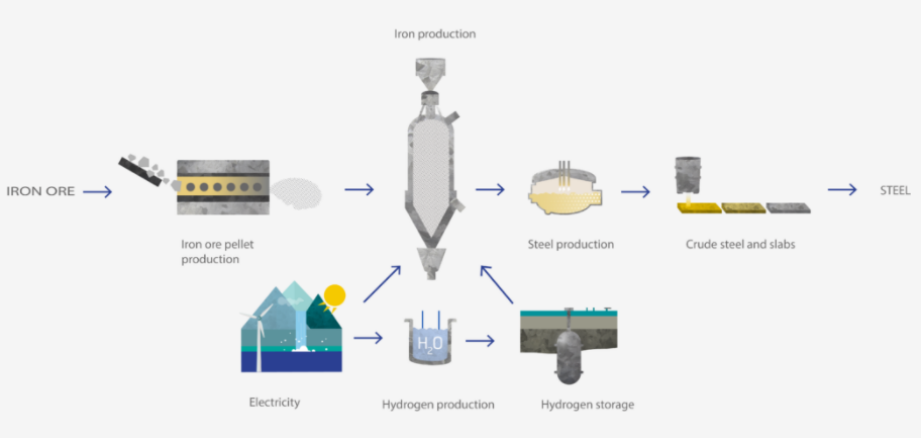

Figure 2-5: Diagram of the Hybrit Process. Figure from Hybrit (2022)

Efforts to quantify the current cost and economic competitiveness of this new technology are more uncertain. Bhaskar et al. (2020) and Cavaliere (2019) have both assessed the technical feasibility of this technology but not the cost. Vogl et al. (2018) assessed the process requirements and cost of a hydrogen-based DRI-EAF pathway and found that the majority of the energy required would be to power the

electrolyzer to produce the hydrogen supply. Since the EAF also relies on electric power, the emissions intensity of this pathway would then be highly dependent on the indirect emissions intensity from the electricity generation. Vogl et al. (2018) found when the EAF is operated on 100% DRI that the break-even grid emission intensity with the BF-BOF pathway is 532 kg CO_2/MWh. Likewise, the electricity price will also highly influence the cost. Vogl et al. (2018) calculated the costs based on 2030 projections for green H_2 DRI-EAF and determined a range of $560-940/tonne liquid steel (2016 USD) based on a range of electricity prices from ∼$28-145 /MWh (2016 USD). Another report prepared on behalf of the European Parliament calculated a steel production cost of $722/t (2016 USD) in 2020 for the hydrogen based DRI-EAF pathway (Laguna et al. (2021)). The cost of the H_2 DRI-EAF is highly dependent on the production cost of hydrogen. In 2019, real prices for conventional production of hot-rolled coil steel ranged from ∼$450 to 700/tonne (Hodges & Anton (2022)).

I selected the DRI-EAF with CCS and H_2 DRI-EAF for my techno-economic assessment and analysis because they have the potential for the greatest emissions reductions while also being more commercially ready than other decarbonization technologies. IEA's assessment in their "Iron & Steel Technology" report forecasts that EAF steel making will contribute the majority of global steel production by 2050 under their sustainable development scenario (IEA (2020)). The IEA also identified CCUS and hydrogen technologies as being important to achieve complete decarbonization of primary steel making (IEA (2020)). Another study commissioned by the European parliament also identified hydrogen as playing a key role in the future decarbonization of steel, specifically citing several ongoing projects in Europe which are developing steel production plants that will utilize hydrogen as the reducing agent (Laguna et al. (2021)). A recent report from the Pacific Northwest National Laboratory (PNNL) assessed global and regional deployment of several different low carbon steel production technologies including biomass, carbon capture & storage, and hydrogen injection (Yu et al. (2021)). Iron ore electrolysis was excluded from their analysis because of its' low technology readiness factor. Yu et al. (2021) found that by year 2050, under the 1.5 Celsius scenario, the DRI-EAF with CCS had the

highest share of steel production out of the advanced steel making technologies and the DRI-EAF with H_2 the second highest. Their analysis predicted that the majority of global steel production would be produced from the EAF scrap pathway (Yu et al. (2021)).

2.3 Decarbonization Pathways for High Temperature Heating

High temperature heating for the majority of industrial processes is currently generated by fossil fuels and this generates a substantial amount of greenhouse gas emissions (Bellevrat & West (2018)). Heavy industry processes such as those for making steel, glass and cement all require temperatures exceeding 1000 Celsius (Friedmann et al. (2019); Vine (2021)). Furthermore, many industrial processes require not only high temperatures but a constant flux of high temperature heat. For high temperature processes, requiring temperatures exceeding 400 Celsius (IEA (2018a)), there are fewer low carbon technology options than for lower temperature heating (Friedmann et al. (2019); Vine (2021)). Some heating technologies that can be utilized to reduce emissions are carbon capture and storage, electrification, nuclear power, solar thermal, biomass, and hydrogen (Friedmann et al. (2019)).

However, each of these options will have challenges to implement. Solar thermal is an intermittent source of heat which will not be compatible with many high capacity industrial process (Friedmann et al. (2019); Vine (2021)). Nuclear power can only supply temperatures up to 850 Celsius (Friedmann et al. (2019)). Solid biomass can supply up to 1,100 Celsius and biofuel can supply up to 2,200 Celsius; however, the carbon avoidance of these fuels is not well defined (Friedmann et al. (2019)) and in the future it will be challenging to ensure a sustainable supply of biomass due to increasing competition (IEA (2020)). Carbon capture and storage is one of the least costly options (Friedmann et al. (2019)), however many regions do not have geological storage options. Electrification of heating processes will in many cases

require major changes be made to the existing process equipment (Friedmann et al. (2019)). In addition, in order to be a low carbon solution the electricity must be supplied without producing greenhouse gas emissions. Solar and wind both supply electricity intermittently, which is not compatible with industrial heating application without other energy storage or back up energy solutions.

Hydrogen is another potential decarbonization pathway for heating and would require fewer retrofits than electrification for some existing processes. However, production of Green hydrogen is expensive compared to conventional fossil fuels. It is likely that it will take a variety of technology options to decarbonize different industrial processes (Vine (2021)). In this research, I will focus on low carbon hydrogen (Green and Blue) as a potential decarbonization pathways for industrial heating and compare the projected heating costs to those using conventional fossil fuels.

Chapter 3

Methods for Base Cost Assessments and Model Implementation

3.1 Levelized Costs of Hydrogen Production

To determine the levelized cost of hydrogen, I consider four different hydrogen production pathways: Green, Blue, Yellow and Grey hydrogen. Because I assume that the hydrogen and industrial end use are collocated, the production cost calculations do not include hydrogen transportation and storage costs. In the same way, electricity transmission and distribution costs for renewable electric energy are not included since I also assume the renewable energy plant is located nearby. A sensitivity analysis explores the additional costs incurred from transportation and storage costs. All costs are for current technology and represented in 2016 USD. The discount rate is 8.5% (Morris et al. (2019a)) and the project lifetime is 20 years (IEA (2020)). The details underlying these calculations are provided in Appendix A. The levelized costs are then utilized to compute a mark up value, which is the ratio of the hydrogen production cost to the cost of a conventional fuel. I use the price of natural gas as the cost of a conventional fuel that hydrogen would be competing with. The markup value is used in the EPPA model to determine the differences in relative costs between technologies (Morris et al. (2019a)). The cost shares determined by the levelized cost calculations are also utilized in the EPPA model to determine the inputs for each

production pathway. Over time, costs evolve endogenously as input costs change and because of learning-by-doing.

The Green hydrogen production pathway is modelled on a Polymer Electrolyte Membrane (PEM) electrolyzer powered by a dedicated onshore wind energy plant. I focus on the PEM electrolyzer technology because of its advantages over the alkaline electrolyzer as described in Section 2.1.2. I assume that the Green hydrogen plant has a capacity of 1 GW, and it produces ∼92,000 tonnes of H_2 annually. This amount is sufficient to supply hydrogen for a 1.14 Mtpa DRI-EAF iron and steel plant. This is a typical size for a DRI-EAF plant capacity. While no electrolyzer facility has yet achieved GW scale capacity, it is presumed to be feasible and H2 Green Steel recently announced plans to construct a 1 GW electrolyzer to power a 2 Mtpa iron plant (Iberdola (2022)).

The wind plant capacity factor is assumed to be 43%, which is the average wind resource level in the United States as reported in NREL's 2021 Annual Technology Baseline report (NREL (2021)). The wind plant capacity factor was calculated using hourly wind resource profiles for 2019 for a location in the continental U.S. with an annual capacity factor equal to the average wind resource level in the U.S. (exact coordinates are listed in Appendix A) (Pfenninger & Staffell (2016); Staffell & Pfenninger (2016)). The wind plant is 1.45 times larger than the electrolyzer's capacity to increase the electrolyzer's utilization rate to 57%. The oversizing ratio was selected by optimizing for the lowest green hydrogen production cost. The wind plant capacity was scaled by the oversizing factor and the electrolyzer utilization rate is determined based on electricity available in each hour. The overnight capital cost of the hydrogen plant is \$1,622/kWe (∼\$2640/kW H_2). This assumes a direct installed capital expense of \$1,065/kWe (ISPT (2020)), indirect capital expense equal to 27% of the direct CapEx (ISPT (2020)), project contingency of 15% of direct CapEx (Rubin et al. (2013); Saur et al. (2018)) and owner's cost of 10.65% of direct CapEx (ISPT (2020)).

The stack replacement cost is estimated at \$331/kWe and the cost is annualized over the stack lifetime of 60,000 hours (Saur et al. (2018); Khan et al. (2021);

Chardonnet et al. (2017)). The electrolyzer electricity consumption is 54.3 kWh/kg (Saur et al. (2018)). The operating costs for the green hydrogen plant consist of fixed O&M of $\sim$ 4% of the capital cost and variable costs due to a water usage of 4.76 gal of water per kg of hydrogen (Saur et al. (2018)). The overnight capital cost and labor costs for the onshore wind system are based on values from the 2021 NREL Annual Technology Baseline (ATB) for a plant of Class 4 resource, moderate rating, in year 2020 (NREL (2021)). The annualized capital and labor costs of the oversized renewable energy system are summed with the annualized capital and labor requirements of the hydrogen plant, and levelized over the plant's annual hydrogen production.

The Yellow hydrogen production pathway represents hydrogen production using a PEM electrolyzer powered by grid electricity. For an initial assessment of levelized cost, I assume a delivered cost of \$69/MWh for grid electricity, which is the average industrial electricity price in the U.S. from 2017 to 2021 (EIA (2023)). Yellow hydrogen is not inherently a low carbon pathway because the indirect emissions due to the electricity vary with the CO_2 intensity of the electrical grid. The initial emission intensity shown in Figure 3-2 is based on the global average for grid electricity emission intensity (504 kg CO2/MWh) (Reimink & Maciel (2021)). In the future, as the electrical grid becomes decarbonized, Yellow hydrogen would also represent a low carbon hydrogen production pathway. Relying on grid electricity enables this pathway to have a higher electrolyzer utilization rate of 90%. The Yellow hydrogen plant only requires a 633 MW electrolyzer capacity to produce the equivalent amount of hydrogen as the corresponding Green hydrogen production pathway.

Electrolysis is one of the methods to produce hydrogen; however, most hydrogen is currently produced using natural gas in a process called steam methane reforming. For an initial assessment of levelized cost, I assume that the cost of natural gas is \$4/MMBtu, which is the average industrial natural gas price in the U.S. from 2017-2021 (EIA (2022b)). The Grey hydrogen production pathway represented in this work is modeled on a single train steam methane reforming plant. The plant design, capital costs, and non-energy operating costs are based on the 2022 DOE/NETL

report on natural gas reforming technologies (Lewis et al. (2022)). The capital costs of ∼$500/kW H_2 include direct capex, indirect capex, owner's cost and contingency costs. This plant produces ∼158,000 tonnes of H_2 annually, operating at 90% capacity factor, which is enough hydrogen to support a 1.96 Mtpa iron and steel plant.

For the Blue hydrogen production pathway, I model a single train autothermal reformer (ATR) with a carbon capture unit using MDEA to remove the CO_2 from the high-pressure syngas stream. This enables the process to achieve a capture rate of 94.5% (Lewis et al. (2022)). I selected the ATR with CCS design over the SMR design due to the advantages I describe in detail in Section 2.1.1. The Blue hydrogen levelized cost is based on an ATR plant which produces 216,000 tonnes of hydrogen annually (this capacity is typical for a single train ATR); enough to supply a 2.68 Mtpa iron and steel plant. The ATR plant design, capital costs, and non-energy operating costs are based on the 2022 DOE/NETL report on natural gas reforming technologies (Lewis et al. (2022)). The capital costs of ∼ $950/kW H2 include direct capex, indirect capex, owner's cost and contingency costs. The cost for the CO_2 transportation and storage is estimated as ∼$10/tonne CO_2 which is based on transporting ∼3.2 Mtpa of CO_2 approximately 100 miles (Smith et al. (2021)).

Figure 3-1 illustrates hydrogen production costs and input shares for the different pathways. Under the baseline assumptions, Grey hydrogen has the lowest cost of $1.08/kg H_2, Blue hydrogen costs $1.70/kg H_2, Yellow hydrogen costs $5.66/kg H_2, and Green hydrogen costs $5.82/kg H_2. Compared to the baseline natural gas price assumed here of $3.79/GJ, Grey H_2 costs are more expensive by a factor of 2, Blue H_2 by a factor of 3.2, Yellow H_2 by a factor of ∼10.7, and Green H_2 by a factor of ∼11.

The 2021 Lazard report on the current levelized cost of hydrogen computes a cost range from $1.96 to $5.24 for hydrogen produced from a 100 MW PEM electrolyzer given a range of assumptions on electrolyzer CapEx ($680-$1,010/kWe), electricity cost ($20-$60/MWh), and electrolyzer utilization (30-90%) (Lazard (2021)). However, they do not calculate a production cost assuming both a high CapEx estimate and a low electrolyzer utilization rate. Utilizing the Lazard's key cost assumptions for

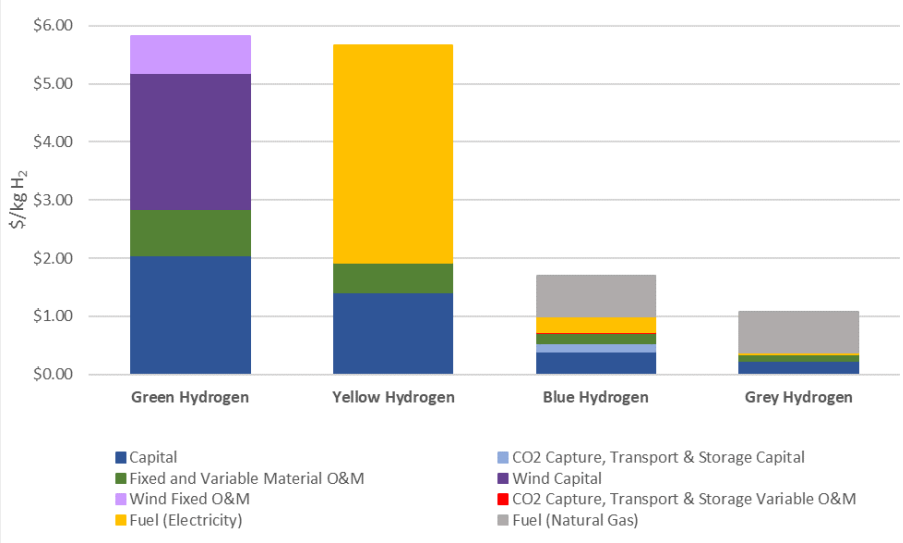

Figure 3-1: Hydrogen production costs and input shares

a medium efficiency electrolyzer yields a hydrogen production cost of \$3.29/kg. My calculated Green hydrogen production cost is on the high end of Lazard's estimates because I have utilized a higher capital cost estimate (\$1622/kWe compared to Lazard's assumed CapEx cost of \$840/kWe), higher fixed O&M cost estimate (∼4% of CapEx compared to their 2.5% of CapEx), and lower utilization rate (∼57% compared to their 98%).

Figure 3-2 provides a comparison of the CO_2 emission intensities for different hydrogen production pathways. Direct emissions are represented by a solid color, and indirect emissions (i.e. from electricity) are represented by shaded areas. The emission intensities for the hydrogen production pathways were calculated based on the energy usage values specified in Section 3.1. The energy emission factors are based on the global average energy emission factors utilized by the World Steel Association for reporting iron and steel sectoral emissions (Grid electricity: 504 kg CO_2/MWh, Natural gas: 56 kg CO_2/GJ) (Reimink & Maciel (2021)). Currently, Yellow hydrogen has the highest emission intensity due to indirect emissions when assuming the global average for grid electricity emission intensity (504 kg CO_2/MWh) (Reimink & Maciel (2021)). It should be noted that indirect emissions would be eliminated with grid decarbonization. Blue hydrogen offers substantial emission reductions relative to

Yellow hydrogen and Grey hydrogen. Since these values do not include emissions associated with the manufacture of equipment, Green hydrogen has zero emissions.

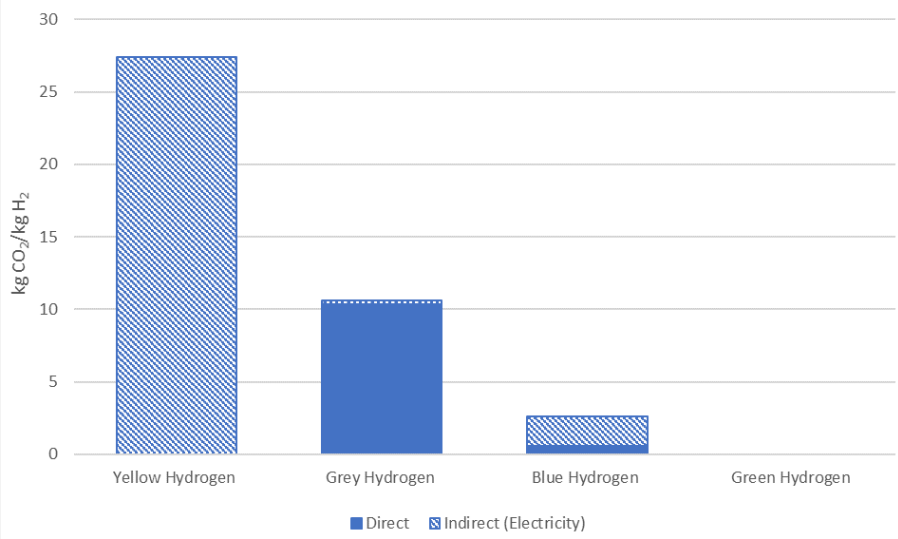

Figure 3-2: CO_2 emission intensity for hydrogen production pathways

3.1.1 Sensitivity of Hydrogen Production Costs to Key Assumptions

The Blue hydrogen production cost varies significantly depending on the natural gas price. As seen in Figure 3-3, the deviation from the baseline natural gas price of \$4/MMBtu can cause large increases in the hydrogen production cost. The high natural gas price of \$32/MMBtu is representative of the natural gas prices seen in Europe in Q1 of 2022 (IEA (2022b)). A decrease in natural gas price to \$2/MMBtu would decrease the hydrogen cost by \$0.35/kg H2. An increase in the natural gas price to \$32/MMBtu would increase the hydrogen production cost by almost \$5/kg H_2. Changes in electricity prices have lesser impacts on the cost of Blue hydrogen production.

Figure 3-4 demonstrates that the Green hydrogen production cost for the integrated plant is dependent on the capacity factor of the renewable energy system. Assuming a low wind capacity factor of 35% results in a higher wind plant oversizing factor of 1.73 which yields an electrolyzer utilization rate of 54%. The increased

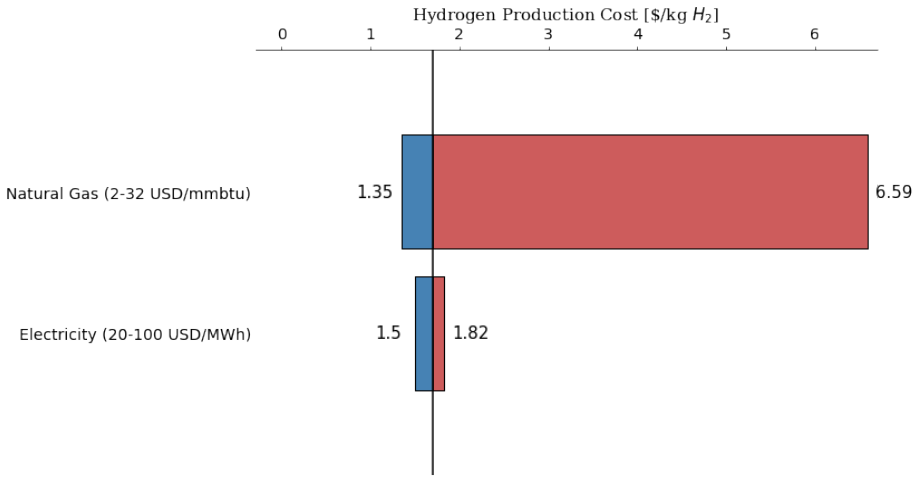

Figure 3-3: Blue hydrogen cost sensitivity to energy prices

capital investment required to enable the higher electrolyzer utilization rate results in an overall increase in the production cost of \$0.90/kg H_2. Alternatively, in a region with a rich wind resource (with a capacity factor of 56%), there is minimal oversizing of the wind plant required (1.18) and the electrolyzer utilization rate is 63%. This reduces the production cost by \$1.01/kg H_2.

Another factor that affects the production cost of Green hydrogen is the plant's capital cost due to electrolyzer and wind capital expenses. Many studies have different scopes for capital costs and may not reflect the actual total capital requirement particularly for an electrolysis-based hydrogen plant. This results in considerable differences in current literature on the levelized cost of electrolytic hydrogen. Cost estimates such as those given by the IEA's "Future of Hydrogen" report (2019) reflects only the direct costs for equipment including the electrolyzer, power electronics, gas conditioning and balance of plant (IEA (2019)). Indirect costs, owner's costs and project contingency costs resulted in a 50% increase in total capital expenses. The IEA estimates that direct capital costs are currently between \$1,100-1,800/kWe and by 2030 could reduce to \$650-\$1,500/kWe (IEA (2019)). Figure 3-4 shows that assumptions for the total capital requirement between \$1,000/kWe and \$2,000/kWe correspond to a range in the green hydrogen production cost of \$5.07 to \$6.27/kg.

The levelized cost of hydrogen calculations assumed that all of the assets were co-

located. However, areas rich in wind resources may not be located where it is most desirable or feasible for steel to be produced. One alternative is to site hydrogen production and renewable electricity generation in one location and then transport the hydrogen to the steel plant. The IEA estimates that pipeline transportation costs for hydrogen can be up to $2/kg if transporting up to 3,000 km (IEA (2019)). Alternatively, the hydrogen plant can be collocated with the steel plant, in which case the renewable electricity must be transmitted to the hydrogen plant. Transmission & distribution costs for renewable electricity can be estimated at $0.03/kWh (Morris et al. (2019a)). Both of these alternatives would increase the levelized cost of hydrogen. In addition, hydrogen storage is currently excluded from my hydrogen production cost estimates. Hydrogen storage might be required in some cases of Green hydrogen production because of intermittent renewable power. The IEA reports costs of $0.59/kg hydrogen for storage in salt caverns, which is one of the most cost-effective options. However, this storage method is only an option in certain regions that have those specific geologic features (IEA (2019)).

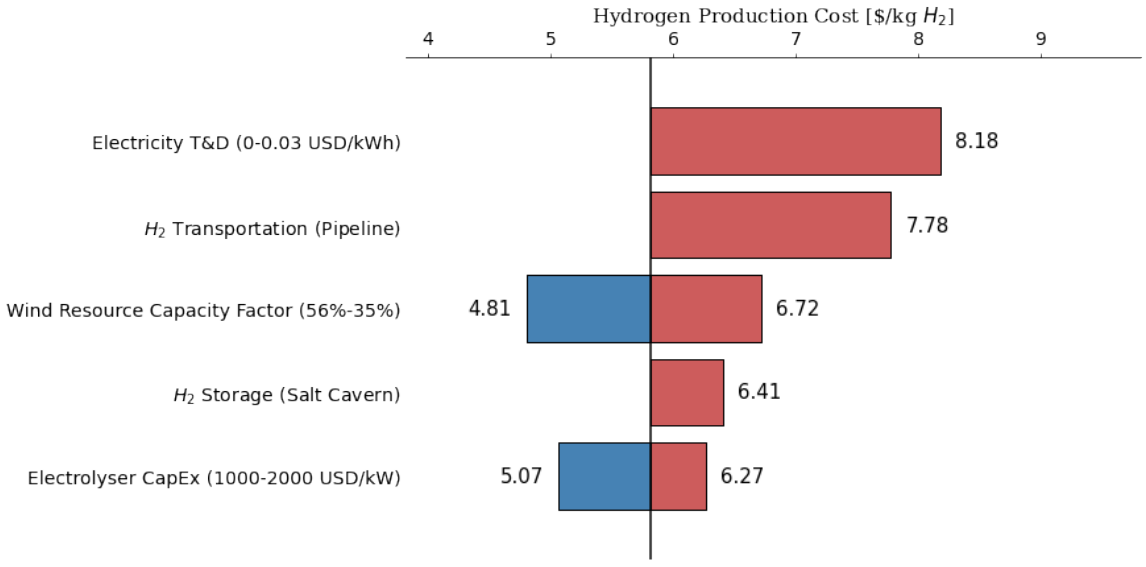

Figure 3-4: Green hydrogen cost sensitivity to various assumptions

3.2 Levelized Costs of Steel Production

Next, I calculate the levelized costs of the two most common conventional steel production pathways: BF-BOF and scrap-based EAF. I then calculate the levelized costs of steel for three different DRI-EAF based production pathways: conventional DRI-EAF, DRI-EAF with CCS, and hydrogen DRI-EAF based on current costs and technology. The ratio of the levelized cost of the advanced steelmaking process to the weighted average cost of conventional steel is utilized in the EPPA model as a markup value. The weighted average conventional steel cost is calculated for each region based on the levelized costs computed in this research for conventional BF-BOF, scrap-based EAF and DRI-EAF; and weighted based on the fraction of total production each process contributes to the region's total steel production. The markup value is used in the EPPA model to determine the differences in relative costs between traditional and advanced steelmaking (Morris et al. (2019a)). If the markup is greater than one, advanced technology is not currently cost-effective unless supported by a policy, such as subsidies, standards, or requirements. The cost shares determined by the levelized cost calculations are also utilized in the EPPA model to determine the inputs for each production pathway. Over time, costs evolve endogenously as input costs change and because of learning-by-doing.

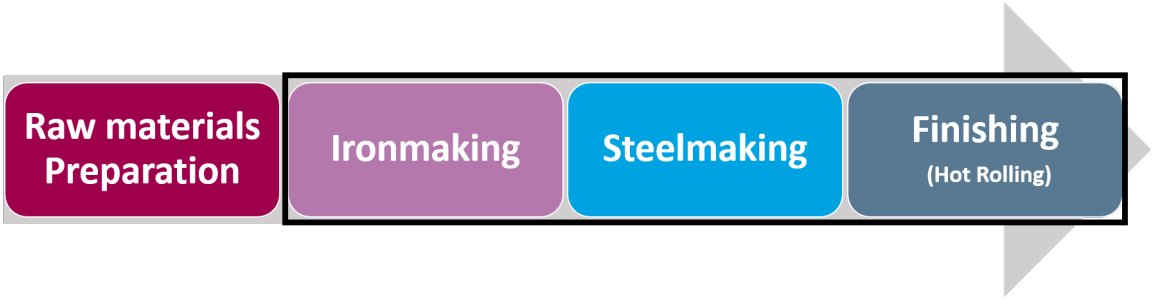

Figure 3-5: Boundaries for ironmaking and steelmaking levelized cost calculations

As shown in Figure 3-5, I include the iron making, steel making, and hot rolling processes in my assessment. I exclude the upstream processes of raw materials extraction and processing (like iron ore mining, agglomeration and pelletizing)

because in the EPPA model these processes are included in the mining sector. For the levelized cost calculations, the iron and steel plant is modelled with a production capacity of 2 Mtpa of hot rolled steel operating at a capacity factor of 90%. The discount rate is 8.5% (Morris et al. (2019a)) and the plant lifetime is 25 years (IEA (2020)). All costs are for current technology and represented in 2016 USD. For an initial assessment of levelized cost, I assume a delivered cost of $69/MWh for grid electricity, which is the average industrial electricity price in the U.S. from 2017 to 2021 (EIA (2023)) and a delivered natural gas cost of $4/MMBtu, which is the average industrial natural gas price in the U.S. from 2017-2021 (EIA (2022b)). In addition, the cost of coal is assumed to be ∼$57/t ($1.83/GJ) which is the average price of bituminous coal in the U.S. from 2010-2019 (EIA (2022a)). The cost of coke is assumed as ∼$200/t based on the price of coke in 2019 (De Clercq et al. (2022)). Other major assumptions are listed in Appendix A. In Section 3.2.1, I vary these price assumptions.

The overnight capital cost for BF-BOF is $588 per tonne of annual capacity (IEA (2019)). The energy usage is modeled on the World Steel reference plant (WSA (2014)). The BF process uses coke as the reducing agent and fuel at a rate of ∼9.8 GJ/tonne crude steel (tcs) (WSA (2014)). The process also uses ∼ 5 GJ/tcs coal and ∼ 0.008 GJ/tcs of natural gas for heating (WSA (2014)). The BF process requires 97 kWh/tcs of electricity (WSA (2014)). The BOF consumes 78 kWh/tcs of electricity and 0.06 GJ/tcs of natural gas. Oxygen is injected into the BOF process creating a very exothermic reaction which requires little energy (Cavaliere (2019)). The BF consumes roughly 1.4 tonnes of iron ore per tonne of crude steel (WSA (2021)). I estimate the base year price for iron ore pellets at $134/t, this is based off of the DRI pellet price utilized by Vogl et al. (2018) and the average difference between the pellet premiums (Barrington (2018)). The BF process can utilize iron ore of lower quality (<62% Fe) than the DRI process (>65% Fe), and the pellet premium for the BF feed is ∼$10/t cheaper (Barrington (2018); S&P Global (2023a)). The BOF also consumes ∼ 45 kg of lime per tonne of crude steel (WSA (2014)). Scrap can also be utilized to further reduce the energy intensity of this process, however typically this

must be limited to less than 25-30% scrap steel (Cavaliere (2019)). For the baseline levelized cost assumptions I assume no scrap steel usage in the BOF. The labor costs are estimated at ∼14% of the total production cost and fixed O&M costs are 3% of the capital expense (Vogl et al. (2018)).

The EAF process has a much lower equipment capital cost of $266 per tonne of annual capacity (IEA (2019)). I assume an EAF process fed 100% scrap steel so that there are no iron ore input costs. The scrap steel usage is 1.1 t/tcs (WSA (2014)). The cost of the scrap steel is ∼$300/t which is representative of the average heavy melting scrap price in the U.S. from 2010-2019 (USGS (2019b)). The primary source of energy to heat the electric arc furnace is electricity and the process requires 520 kWh/t (WSA (2014)). The electric arc furnace also consumes some fossil fuels to provide a source of chemical heating and to promote slag formation (Cavaliere (2019)). I base these calculations on the World Steel reference plant with usages of 0.65 GJ natural gas/tcs and 0.53 GJ coal/tcs. The electric arc furnace also consumes graphite electrodes, lime and alloy materials (Vogl et al. (2018)). The labor costs are estimated at ∼14% of the total production cost and fixed O&M costs are 3% of the capital expense (Vogl et al. (2018)).

The overnight capital cost for the DRI and EAF equipment is $578 per tonne of annual capacity (IEA (2019)). The natural gas usage of the DRI process is modelled on the MIDREX DRI process fed by high quality iron ore pellets (90-94% Fe) to produce 1.4% carbon DRI (Cavaliere (2019)). The DRI process uses 11.52 GJ HHV of natural gas/tcs (Cavaliere (2019)). This natural gas acts as both the reducing agent and fuel for heat. The DRI process also requires ∼100 MWh of electricity/tcs assuming no oxygen injection (Cavaliere (2019)). Injection of oxygen can further lower the electricity requirement for the DRI shaft process (Cavaliere (2019); WSA (2014)). Based on Vogl et al. (2018) the electric arc furnace requires 753 MWh of electricity/tcs when operated with a feedstock of 100% DRI (Kirschen et al. (2011); Vogl et al. (2018); Cavaliere (2019)). Higher DRI purity, higher degree of DRI metallization, feeding steel scrap and injecting fossil fuels for chemical energy can be utilized to reduce the EAF's electricity demand from the baseline I propose here (Kirschen et al. (2011);

WSA (2014); Cavaliere (2019)). The direct reduced iron process consumes 1.5 t iron ore/tcs at a price of $144/tonne iron ore (Vogl et al. (2018)). The process assumes conversion rates of 1.2 t DRI/tcs (IEA (2020)) and 1.03 tcs/tonne hot rolled steel (thrs) (Duarte & Becerra (2011)). The electric arc furnace also consumes graphite electrodes, lime and alloy materials (Vogl et al. (2018)). The labor costs are $76.95/tcs and fixed O&M costs are 3% of the capital expense (Vogl et al. (2018)).

The DRI-EAF with CCS production pathway has a capture unit to achieve 90% capture of CO_2 from the DRI stack gas. As discussed in Section 2.2.1, the Hyl/Energiron DRI process has proven capable of a 90% capture rate utilizing one CO_2 capture unit (Duarte & Becerra (2011)). Since the process is set up to selectively separate CO_2 from the system, there would be minimal capital cost increase to the base plant. For my levelized cost calculations, I estimate the cost of a capture unit on a DRI shaft furnace stack gas. The impact of flue gas composition on the cost of CO_2 capture on DRI facilities is not well studied, so here I assume a constant cost. To estimate the cost of the capture unit, I utilized costs and performance assumptions from a supercritical coal power plant with carbon capture as modelled by James et al. (2019). This process has one CO_2 capture system which uses a Cansolv absorption system, two CO_2 compression systems and achieves a 90% capture rate (James et al. (2019)). James et al. (2019) assumes that the coal power plant stack gas has a pressure of 14.8 psi and 12.46 mol% CO_2. This is representative of a low-pressure capture unit that could be utilized in the DRI process, as the MIDREX DRI stack gas has a pressure of 14.6 psi and contains 24 mol% CO_2 (Ho et al. (2013)).

The capital cost, fixed cost, and variable O&M costs in $/tonne of captured CO_2 are derived from the same study by James et al. (2019) and incorporated into the levelized cost of steel. The electricity usage from the CCS process was calculated to be ∼390 kWh/tonne captured CO_2. This includes the electricity for CO_2 capture, compression, and low-pressure steam generation from a heat pump. The electricity demand for CO_2 capture and compression was based on the 123 kWh per tonne of captured CO_2 reported by James et al. (2019). The low-pressure steam demand is assumed to be 2.4 MJ/kg CO_2 based on analysis by James et al. (2019). If I

assume a heat pump with a coefficient of performance of 2.5 (achievable assuming the thermodynamic efficiency relative to the inverse Carnot efficiency is 50% with a temperature lift of 75 Celsius to heat water from 25 C to 100 C (Yan et al. (2021)), the electricity demand for the heat pump to supply the low-pressure steam needed is ∼267 kWh/tonne captured CO_2. The electricity usage for the DRI-EAF with CCS plant was increased by this amount over the baseline DRI-EAF process. The DRI-EAF with CCS process captures ∼1 Mtpa of CO_2 which is then transported and stored in an underground formation. The cost of CO_2 transportation and storage is ∼\$10/tonne CO_2 which is reflective of costs for onshore pipeline transportation and storage in saline aquifers, for 3.2 Mtpa of CO_2 transported 100 miles (Smith et al. (2021)). The levelized cost of steel from the DRI-EAF with CCS production pathway is ∼7% more expensive than the conventional DRI-EAF production pathway.

The Hydrogen DRI-EAF production pathway utilizes the same processes as the baseline natural gas DRI-EAF pathway, except that hydrogen replaces natural gas as the reducing agent in the DRI process. The assumption for the baseline cost calculations are that the hydrogen plant, renewable energy plant, and steel plant are all collocated. For the MIDREX shaft furnace, approximately 80 kg (11.5 GJ HHV) of hydrogen are required per tonne of crude steel as feedstock for the reducing agent and as a fuel for the reduction gas heater (Cavaliere (2019)). Additionally, 1.89 GJ HHV of natural gas is needed for heating as the DRI cools off during the hydrogen reduction reaction and the addition of natural gas ensures a carbon content of 1.4% in the DRI (Cavaliere (2019)). The hydrogen price for the feedstock is based on the levelized costs of green and blue hydrogen calculated in Section 3.1. The levelized cost of H_2 DRI-EAF utilizing blue hydrogen is 18% greater than the conventional DRI-EAF production pathway, and the H_2 DRI-EAF steel based on green hydrogen has a cost that is 79% greater.

The hot rolling finishing process is assumed to be the same across all steelmaking pathways. Since the markup methodology is used to compute relative costs, my calculations include the energy usage for the finishing process to account for the CO_2 emissions but exclude the capital cost of the finishing plant. The hot rolling plant is

assumed to use 1.05 GJ HHV of natural gas per tonne of hot rolled steel and requires 0.11 MWh of electricity per tonne of hot rolled steel (Duarte & Becerra (2011)).

I compare my calculations with the levelized cost of steel in the 2020 IEA "Iron and Steel Technology" report (IEA (2020)). This report has crude steel production costs with ranges to account for regional variations in cost. Costs for the natural gas-based DRI-EAF process are between ∼$400-$590/tcs. For DRI-EAF with CCS, production costs range from ∼$450-$650/tonne crude steel, and electrolytic hydrogen DRI-EAF production costs range from $500-850/tcs (IEA (2020)). BF-BOF costs range from ∼$340-$460/tcs and scrap-based EAF from ∼$340-490/tcs (IEA (2020)).

My results are summarized in Figure 3-6 (∼$450 for BF-BOF, ∼$560 for scrap-based EAF, ∼$560 for DRI-EAF, ∼$600 for DRI-EAF with CCS, ∼$670 for Blue H_2 DRI-EAF, and ∼$1000 for Green H_2 DRI-EAF). These are generally consistent with the ranges assessed by IEA, although my estimate for Green H_2 DRI-EAF and scrap-based EAF are both higher than IEA. For the Green H_2 DRI-EAF this is driven by differences in the IEA's assumptions around hydrogen production cost. They utilize a lower electrolyzer capital cost (∼$880/kWe versus my ∼$1600/kWe) and higher stack lifetime (95,000 hours versus my 60,000) which results in a lower H_2 production cost. For the scrap-based EAF I assume a scrap cost of ∼$300/tcs which is on the high end of the range that the IEA assumes and I assume higher OPEX costs (Fixed O&M and Labor). In addition, my energy usage assumptions for the EAF are higher (3 GJ/tcs versus 2 GJ/tcs) because it is modeled on the World Steel reference plant and includes inputs of coal and natural gas for additional chemical energy (∼1.5 GJ/tcs). So, while both IEA and my calculations assume that the majority of the energy to the EAF is supplied by electricity, the additional chemical energy input is important for heating and slag formation.

I compute a weighted average cost of conventional steel in the U.S. of $531.91/thrs based on the process share of production in 2019 which was comprised of 30% by the BF-BOF pathway, 67% via the scrap-based EAF pathway and 3% via DRI-EAF (WSA (2022b)). This results in a mark up relative to the conventional steel cost of 13% for the DRI-EAF with CCS pathway, 25% for Blue H_2 DRI-EAF and 90% for

Green H_2 DRI-EAF.

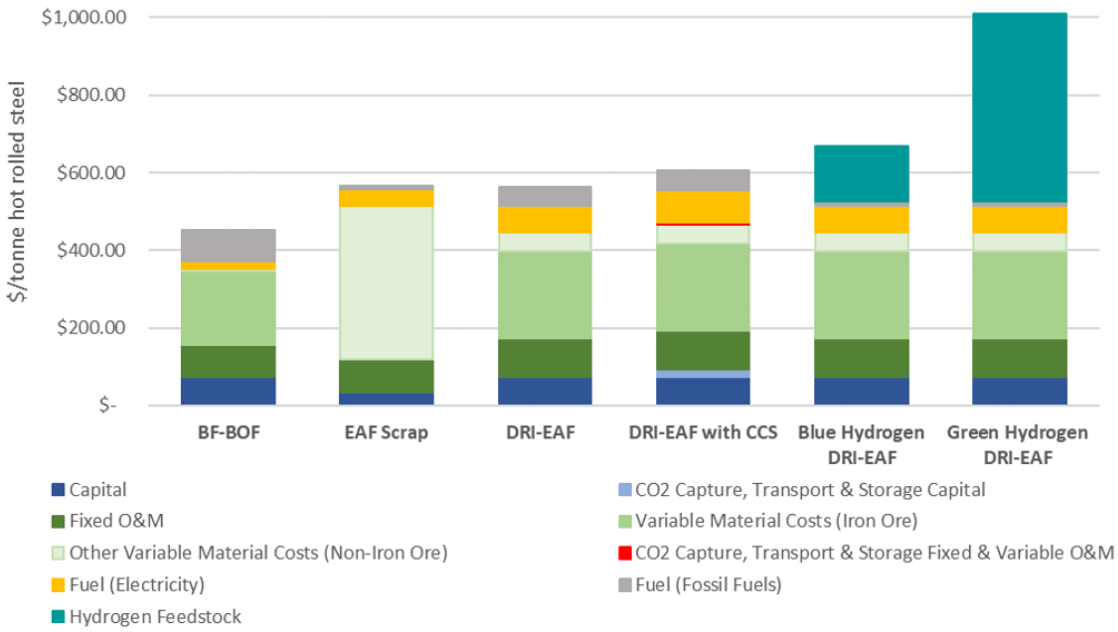

Figure 3-6: Steel production costs and input shares

Figure 3-7 presents the estimated CO_2 emission intensity for different steelmaking pathways, where direct emissions are represented by solid colors, and indirect emissions (i.e., from grid electricity) are represented by shaded areas. These CO_2 emission estimates use the same process boundaries as those used in the levelized cost analysis (iron making to hot rolled steel). The exclusion of the natural gas supply chain emissions more closely aligns with the analytical boundaries used by the IEA and World Steel Association which exclude fugitive methane emissions. The boundaries also align with the distinction in the EPPA model between mining/extraction sectors (raw material processing) and the steel sector (finished steel product). The primary differences between my sectoral boundary and that of IEA and World Steel is that theirs includes agglomeration and coke production which is excluded in ours. The World Steel Association includes finishing processes in their system boundary much like ours; however, the IEA excludes finishing processes. We account for emissions from electricity generation as an indirect emission which aligns with the IEA's accounting. The EPPA model accounts for the direct emissions in all

sectors. The emission intensities were calculated based on the energy usage values specified in the levelized cost calculations. The energy emission factors are based on the global average energy emission factors utilized by the World Steel Association for reporting iron and steel sectoral emissions (Grid electricity: 504 kg CO_2/MWh, Natural gas: 56 kg CO_2/GJ) (Reimink & Maciel (2021)).

The Blue hydrogen DRI-EAF emission intensity in Figure 3-7 includes the direct and indirect (Grid electricity) emissions resulting from the Blue hydrogen production process. As detailed in Section 2.1.1, the Blue hydrogen pathway is modelled on an autothermal reforming plant with CCS which utilizes substantially more electricity than a Steam methane reforming plant with CCS. Figure 3-7 excludes process emissions from lime and graphite in the electric arc furnace because these emissions are dependent on the specific operations. At minimum the emissions resulting from lime and graphite are estimated as 0.03 tCO_2/t steel. However, for the scrap-based EAF pathway I account for the process emissions from the additional fuels added. When electric arc furnaces are fed high levels of scrap steel the process also requires additional carbon to be added as a carburizing agent to create steel with enough carbon content to ensure the desired strength of the steel. Coal or coke is typically injected in the EAF process to form the foamy slag in the electric arc furnace which helps to transfer the heat to the steel and reduce heat loss (Cavaliere (2019)). On average globally, scrap steel-electric arc furnace processes utilize 150 kg coal/tonne crude steel (WSA (2021)); plants can also lower emissions by utilizing natural gas as the source of carbon (WSA (2014)). Estimates for a scrap fed EAF's direct emissions range from 0.1-0.5 tCO_2/t steel (WSA (2014); Reimink & Maciel (2021)). However, for the DRI-EAF pathway we model an EAF with 100% DRI feedstock. The carbon content in the DRI provides chemical energy and helps with slag formation and this reduces the need for injection of coal or other fossil fuels as needed in the 100% scrap fed process (Cavaliere (2019)). More electricity is also utilized in the process using 100% DRI and no scrap steel. Addition of oxygen, high DRI metallization, and feeding hot DRI can all contribute to lower EAF electricity requirements (Cavaliere (2019)).

Even with the current emission intensity of grid electricity generation, advanced steelmaking pathways offer substantial mitigation potential. With full decarbonization of the electric grid, indirect emissions would be eliminated and advanced technologies would provide far greater reductions relative to the traditional steelmaking processes.

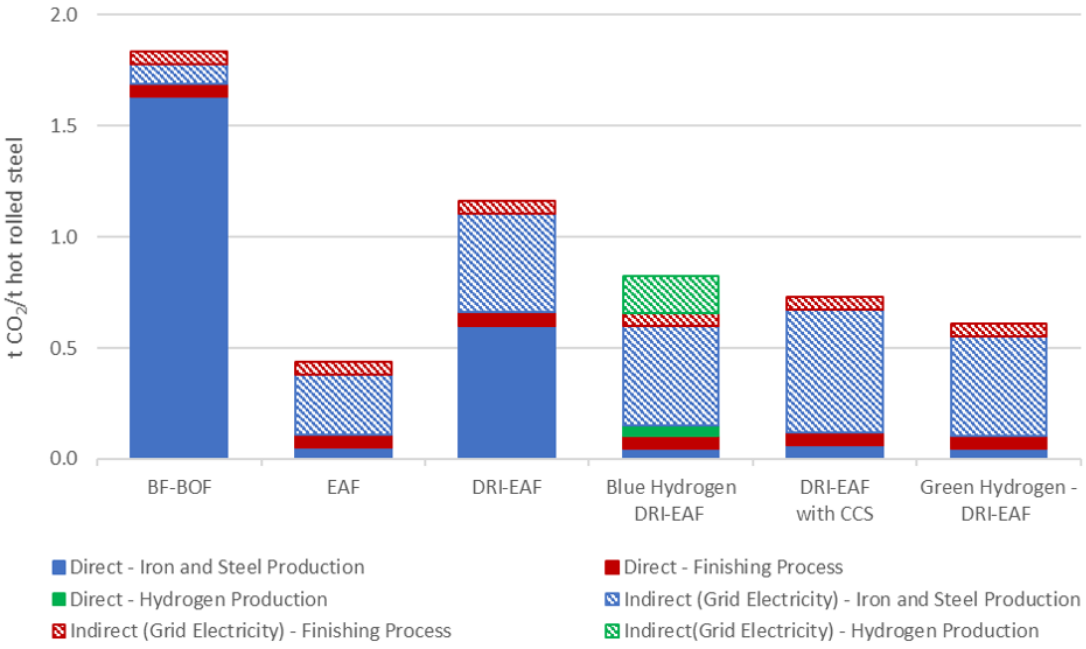

Figure 3-7: CO_2 emission intensity for steel production pathways

3.2.1 Sensitivity of Steel Production Costs to Key Assumptions

The Hydrogen DRI-EAF steel production cost is highly dependent on the cost of the hydrogen feedstock. Figure 3-8 shows the change in the baseline production cost over a hydrogen production cost range of \$1/kg to \$10/kg. The low-end estimate is representative of the current Grey hydrogen production cost. The high end of the estimate is representative of a Green hydrogen production cost using a combination of several factors (low capacity factor wind resource, incurring electricity transmission & distribution costs, utilizing geologic storage for the hydrogen and assuming high capital expense estimates). The baseline H_2 DRI-EAF production

cost is ∼$670/tonne steel, based on the blue hydrogen production cost of $1.70. The high end of the hydrogen production cost estimate increases this cost by an additional ∼$700/tonne steel, essentially doubling the total cost.

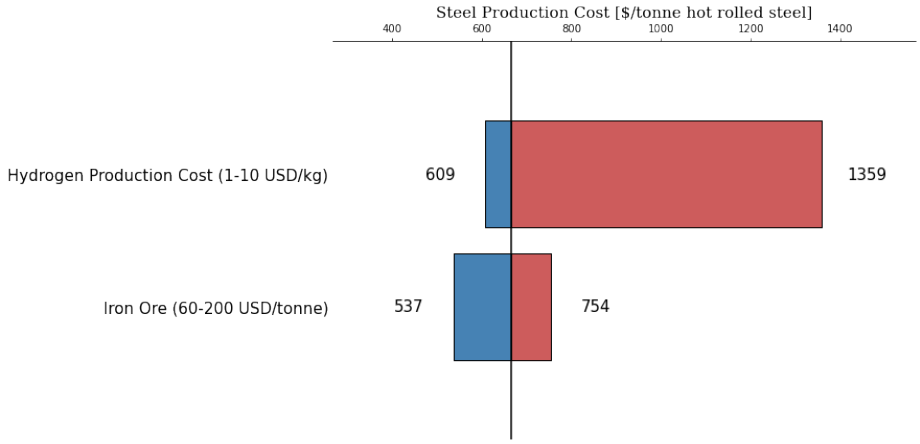

Figure 3-8: Hydrogen based DRI-EAF cost sensitivity to input costs

The iron and steel production cost is highly dependent on the cost of iron ore. Figure 3-8 shows the effect of a range of iron ore prices from $60/tonne to $200/tonne. The low-end iron ore cost of ∼$60/tonne is representative of the average global iron ore (62% Fe) prices from 2014-2019 (World Bank (2022)). The IEA's Future of Hydrogen report (2019) calculates steel production costs based on a price of ∼$60/tonne for iron ore (58% Fe content). The high end of the iron ore price range is $200/tonne which is representative of global iron ore prices in Q2 2021 (World Bank (2022)). The feedstock iron ore in ironmaking typically requires processed iron ore that has been pelletized which incurs an additional pellet premium and the DRI process requires iron ore of higher quality ($>$ 65% Fe) than that required by the blast furnace process (Cavaliere (2019)). Midrex reports pellet premiums for the time period from 2017-2018 of ∼$45/t for lower grade iron ore pellets and ∼$55/t for higher grade iron ore pellets that can be utilized in the DRI process (Barrington (2018); S&P Global (2023a)). My baseline assumptions are based on Vogl et al. (2018) estimates a price of ∼$140/tonne for DRI quality iron ore pellets.

The EAF pathway is most sensitive to the cost of scrap steel as this makes up a large share of the total cost. Figure 3-9 shows the effect of scrap steel prices ranging

from $200/tonne to $400/tonne. The IEA utilizes a cost of $200/tonne in their steel production cost calculations (IEA (2020)). However, prices for shredded scrap steel in the U.S. Midwest have risen to ∼$400/tonne in 2023 (S&P Global (2023b)). The low and high estimate result in a relative change of about -24% and +22% respectively. The scrap-based EAF pathway relies on electricity for most of its energy and so the price of electricity also has an impact on the total cost of the steel.

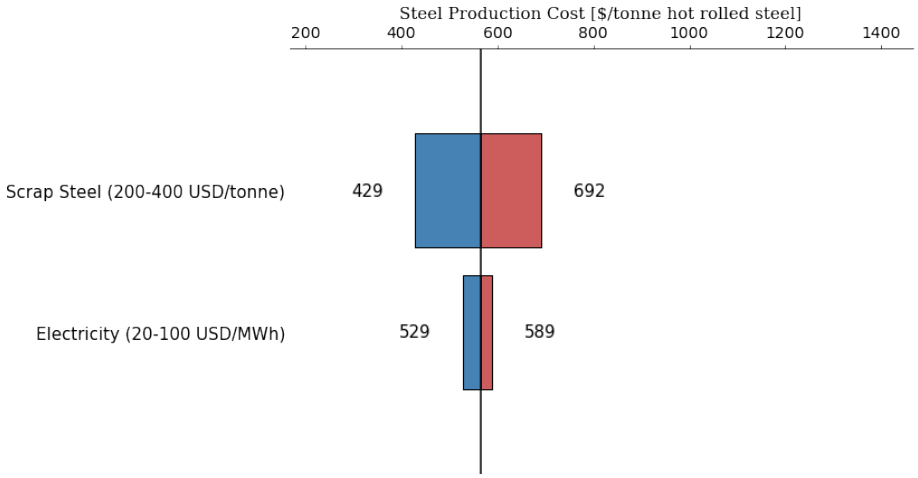

Figure 3-9: Scrap-based EAF cost sensitivity to input costs

The BF-BOF pathway similarly is sensitive to the cost of energy, in this case namely coke and coal. IEA (2020) estimates the price of coking coal from $ 2.56- 5.29 /GJ ($75-155/tce) and the price of coal from $1.19-2.73/GJ ($35-80/tce). However, U.S. coke export prices in 2021 averaged ∼$8.31/GJ (EIA (2022a)). In addition, much like the DRI-EAF pathway, the cost of iron ore greatly impacts the total cost of steel production. Figure 3-10 represents the deviations from the baseline cost assumptions.

Figure 3-11 illustrates the impact of natural gas prices on the levelized cost of steel for different DRI-EAF production pathways. The baseline natural gas price used in my analysis is $4/MMBtu. At this price, the Green Hydrogen DRI-EAF production cost is approximately double the cost of the baseline DRI-EAF process. However, at very high natural gas prices (∼ $50/MMBtu), production costs for these two technologies are comparable. Although these represent very high natural gas prices, Dutch TTF natural gas prices reached $30/MMBtu in Q1 of 2022 and then exceeded

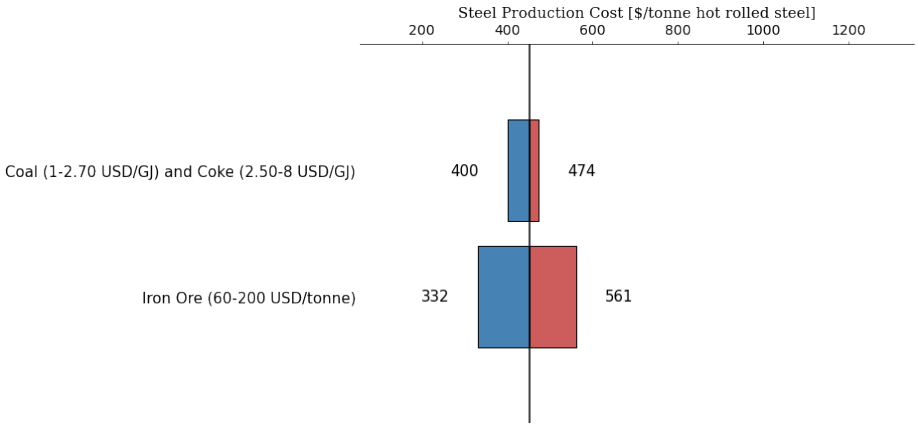

Figure 3-10: BF-BOF cost sensitivity to input costs

$55/MMBtu in Q3 of 2022 (IEA (2022b)). Since Blue hydrogen is produced from natural gas, the cost of Blue H_2 DRI-EAF production also increases with increasing natural gas prices. The positive slope for the cost of Green H_2 DRI-EAF is due to the use of natural gas in the finishing process and DRI heating. Natural gas could theoretically be replaced in these processes by other heating technologies, but I do not explore that possibility in this work.

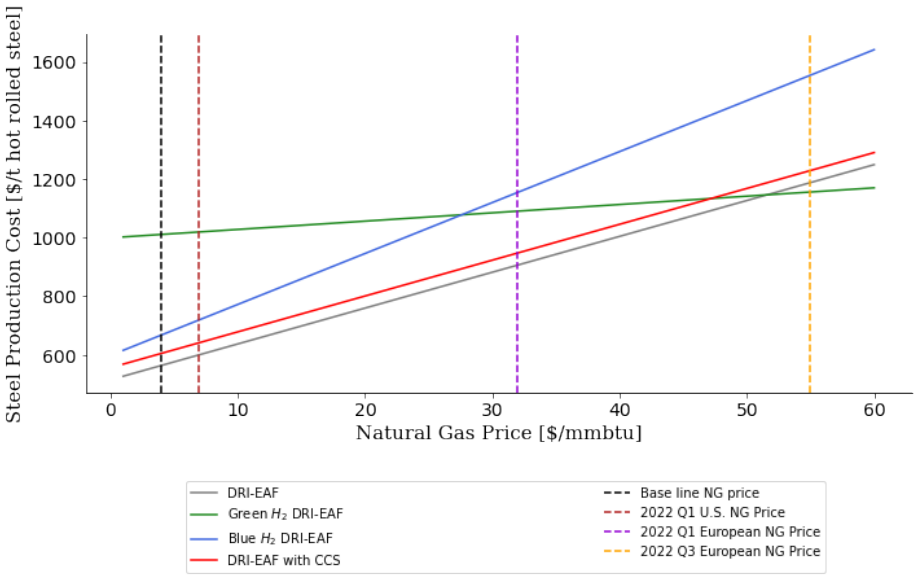

Figure 3-11: Steel production cost sensitivity to natural gas

The impact of carbon pricing on steelmaking costs of the different DRI-EAF production pathways is shown in Figure 3-12. The steel production cost for the

natural gas based DRI-EAF pathway rises the steepest with carbon price, because it has the highest direct CO_2 emissions among the DRI-EAF production pathways that I considered. At a carbon price above \$76/tCO_2, the DRI-EAF with CCS has a lower steel production cost than the conventional DRI-EAF pathway. Making DRI-EAF more expensive than the Blue H_2 DRI-EAF pathway requires a carbon price above \$205/t CO_2, and to make it more expensive than the Green H_2 DRI-EAF requires a carbon price above \$807/t CO_2.

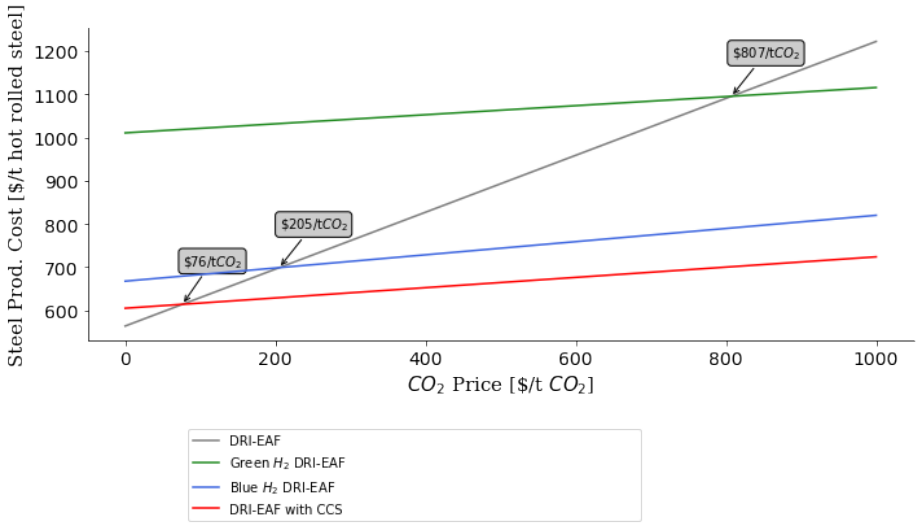

Figure 3-12: DRI-EAF pathways' production cost sensitivity to the carbon price on direct emissions

I also compared all of the technologies to the most carbon intensive and lowest cost pathway (BF-BOF) to understand what carbon price is required to make the other technologies equal in cost to the BF-BOF pathway (Figure 3-13). The scrap-based EAF pathway only requires a carbon price greater than \$71/t CO_2. The DRI-EAF with CCS requires a price greater than \$96/t CO_2, the DRI-EAF without CCS requires greater than \$106/t CO_2, Blue H_2 DRI-EAF requires greater than \$139 and Green H_2 DRI-EAF greater than \$351/t CO_2.

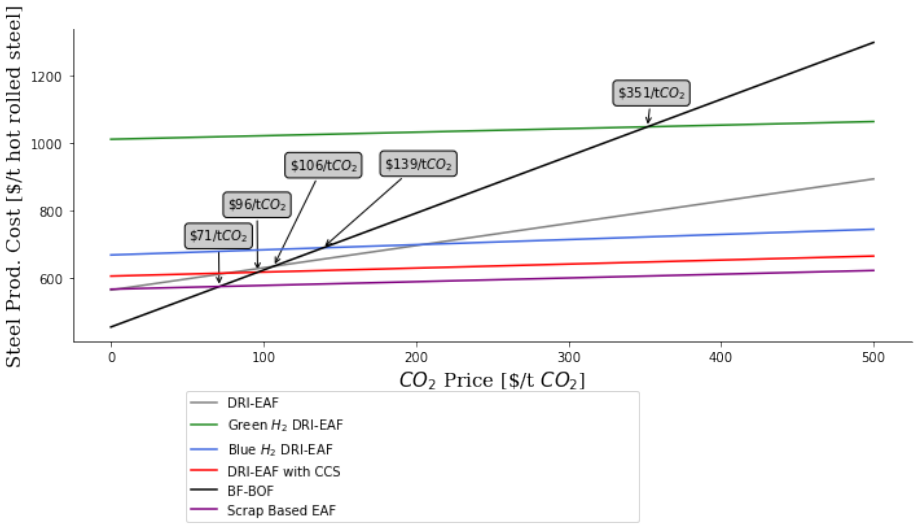

Figure 3-13: Steel production cost sensitivity to a carbon price on direct emissions

3.3 Levelized Costs of High Temperature Heating

I conducted a preliminary assessment of high temperature heating costs for two industrial applications; cement and glass production. I utilized heat usage rates from Friedmann et al. (2019) as reported for each of these processes. I utilize the same assumptions for fossil fuel prices as detailed in Section 3.1 and 3.2 (Natural Gas: ~$3.79/GJ, Coal: $1.83/GJ). These fossil fuel prices are used to compute a conventional heating cost for each of these industrial processes. I then calculate the heating cost if Blue or Green hydrogen were utilized as the heating fuel. The prices for the hydrogen production are those that I calculated in Section 3.1 (Green H_2: $40.97/GJ HHV, Blue H_2: $11.96/GJ HHV)

The cement process is modeled on a cement clinker (dry process rotary clinker kiln) that requires 3.4 GJ of heating per tonne of clinker produced (IEA (2018b); Friedmann et al. (2019)). The clinker process involves high temperature heating of calcium carbonate containing materials to melt the material and complete the calcination process that was initiated in the steps preceding the clinker kiln (IEA (2018b)). The kiln is heated to a temperature of ~1450 Celsius (Friedmann et al. (2019)). This process traditionally relies on coal for heating. The clinker is then blended with gypsum, limestone, and other materials to form cement (IEA (2018b)).

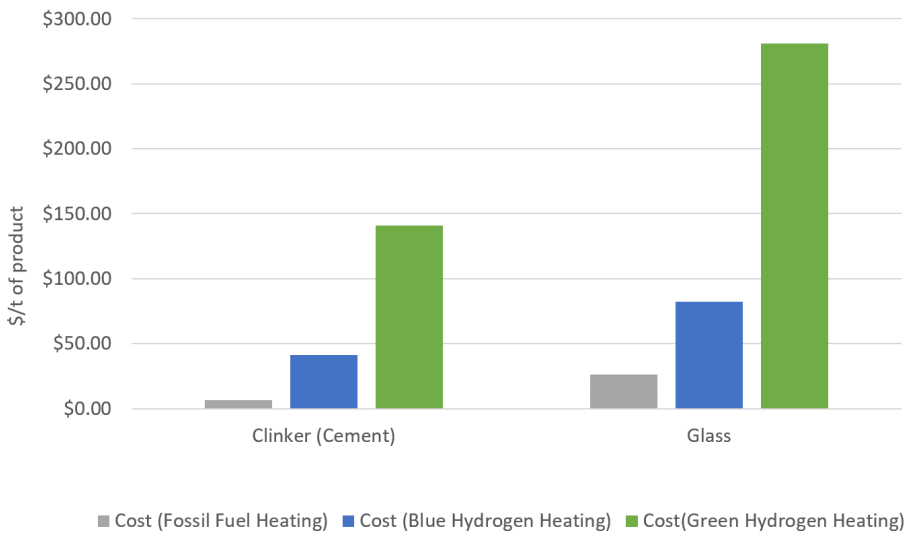

Figure 3-14: Cost of heating for selected energy intensive industrial processes

CO_2 emissions from cement production come from both the chemical reaction to form calcium oxides (60-70% of the total emissions) and from the combustion of fuels (30-40%) (IEA (2018b)). Figure 3-14 compares the heating costs resulting from utilizing different fuels for heating the clinker kiln. The heating cost when using coal ∼\$6/t clinker. However, if utilizing Blue H_2 the heating cost is ∼\$40/t clinker and ∼\$140/t when using Green H_2. Prices for clinker range from ∼\$40-80/t depending on regional variations (U.S. imports being on the higher end of the range and China import prices on the low end) (USGS (2019a); Wood (2023)). The Green and Blue H_2 heating costs would represent a significant increase of current clinker prices, approximately increasing prices by ∼225% and 58% respectively.

The glass furnace utilizes 6.858 GJ/tonne raw glass and traditionally relies on natural gas for heating (Friedmann et al. (2019)). The process requires temperatures of ∼1575 Celsius (Friedmann et al. (2019)). The glass furnace melts raw ingredients (typically silica sand, soda ash, limestone, dolomite and recycled glass) to produce a raw glass product that can be cooled into shape (Glass Alliance Europe (2023)). Heating produces about ∼70% of the emissions associated with flat glass production (Friedmann et al. (2019)). Heating costs with natural gas are ∼\$26/t raw glass, with Blue H_2 ∼\$80/t and with Green H_2 ∼\$280/t. Total costs for raw glass range from

~$300-$400/t (Egenhofer et al. (2014); Friedmann et al. (2019)). Utilizing Green and Blue H_2 at current prices would increase raw glass prices by ~73% and 16% respectively.

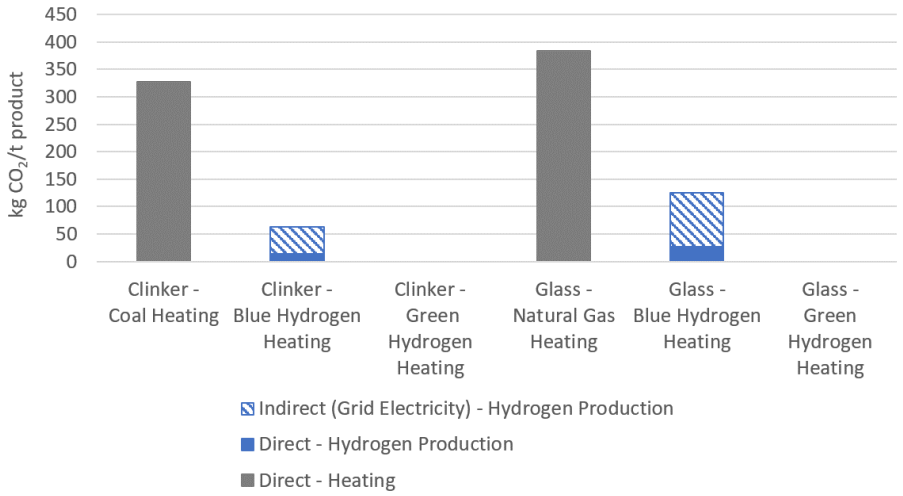

Figure 3-15: CO_2 emission intensity for heating in selected energy intensive industrial processes

I then determined the emission intensity associated only with heating for these processes. I included the direct emissions from the heating fuel and included the associated emissions from Blue hydrogen production. In Figure 3-15, direct emissions are represented by solid colors, and indirect emissions (i.e. from grid electricity) are represented by hatched areas. The emission intensities were calculated based on the energy usage values specified in the levelized cost calculations. The energy emission factors are based on the global average energy emission factors utilized by the World Steel Association for reporting iron and steel sectoral emissions (Grid electricity: 504 kg CO_2/MWh, Natural gas: 56 kg CO_2/GJ) (Reimink & Maciel (2021)). The Blue H_2 emission intensity factors were calculated in Section 3.1.

I determined the CO_2 price on direct emissions required to make the hydrogen heating costs competitive with the conventional fossil fuel heating costs. Since Blue hydrogen is produced from natural gas, the cost of Blue H_2 production also increases with increasing CO_2 price. In Figure 3-16, we see that to make the clinker coal heating cost more expensive than the Blue H_2 heating cost requires a CO_2 price greater than

~$100/t CO_2 and the Green H_2 requires a price greater than ~400/t CO_2.

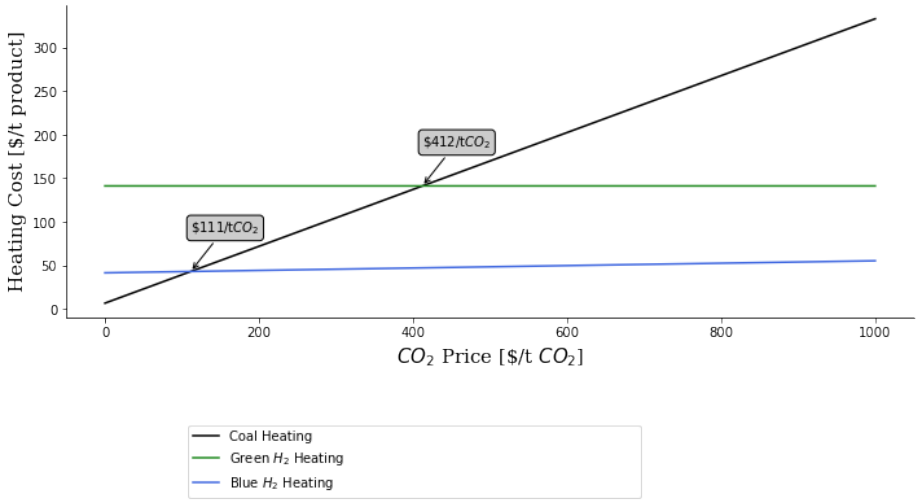

Figure 3-16: Clinker furnace heating cost sensitivity to a carbon price on direct emissions

The glass furnace has a higher heating usage rate per tonne than the clinker furnace; however, it more commonly utilized natural gas for its heating which has a lower emission intensity than coal. In Figure 3-17, we see that to make the glass natural gas heating cost greater than the Blue H_2 heating cost requires a CO_2 price greater than ~$150/t CO_2 and the Green H_2 requires a price greater than ~660/t CO_2.

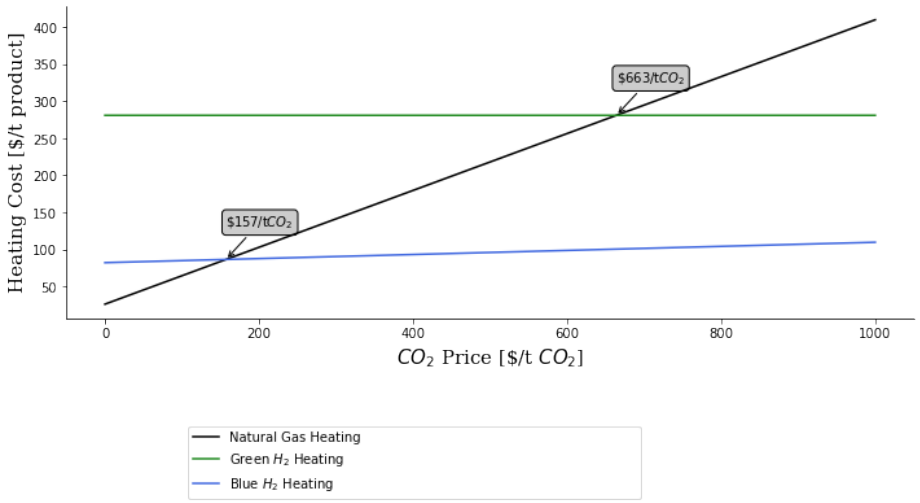

Figure 3-17: Glass furnace heating costs sensitivity to a carbon price on direct emissions

The next section details implementation into an integrated assessment model. However, I focus only on hydrogen and steel production technologies for this assessment. Future work would involve incorporating the details of the levelized cost assessments for high temperature heating into the integrated assessment model.

3.4 Incorporating Base Costs into an Integrated Assessment Model

Integrated Assessment Models (IAMs) have become widely utilized to inform climate policy. Notably, the Intergovernmental Panel on Climate Change (IPCC) has come to rely extensively on different integrated assessment models to conduct their analysis and recommended strategies (van Beek et al. (2020); Krey et al. (2014)). The number of journal publications utilizing IAMs has also increased over time (van Beek et al. (2020)). IAMs can provide great insight into the relationship between different human systems and the environment. However, they are always limited by the level of detail and accurate data that can be incorporated into their structure. Many integrated assessment models present economic sectors in a highly aggregated manner which fails to capture the adoption of specific technologies.

Research which has disaggregated sectors into specific technologies has revealed differences in regional deployment and competition between technologies. Yu et al. (2021) incorporated eight competing steel production technologies into an integrated assessment model. Their research revealed that deployment of technologies varied greatly between different regions indicating that steel decarbonization pathways will be region specific (Yu et al. (2021)). My research seeks to add greater detail on the representation of iron and steel production technologies in IAMs. While I use a particular model (the MIT Economic Projection and Policy Analysis (EPPA) model) as a tool for illustrating my approach, the same approach can be deployed in other IAMs. Representing specific technologies provides greater insight into how these technologies compete for deployment and how regions' decarbonization pathways may

differ. However, as with all integrated assessment models the results are not predictive but rather present possible outcomes for quantifying trade-offs in different scenarios.

3.4.1 Economic Projection and Policy Analysis (EPPA) Model

The EPPA model is a computable general equilibrium model that represents the world economy as multiple sectors and regions (MIT Joint Program (2023); Paltsev et al. (2021b)). The model projects both economic outputs and greenhouse gas emissions as well as other air pollutants (Paltsev et al. (2021b)). The EPPA model is part of an integrated assessment model (IAM) called the MIT Integrated Global Systems Model (IGSM). The IGSM model connects the human systems represented in the EPPA model to the MIT Earth System model (MIT Joint Program (2023)). The EPPA model represents 18 different regions and 16 sectors. Figure 3-18 shows the regional representation in the model. The specific model version utilized in this research also has additional detail on the energy intensive sectors to represent iron & steel production as its own sector. The EPPA model is built upon the GTAP dataset which has data on the inputs and outputs between sectors across the world economy in year 2014 (Aguiar et al. (2019); Purdue University (2023)). The EPPA model then solves from 2020 onwards in 5-year time steps (Morris et al. (2019a)). A public version of this model is available on the MIT Joint Program's website: `https://globalchange.mit.edu/research/research-tools/human-system-model/download`.

The levelized costs calculated in Section 3.1 and 3.2 were based on U.S. energy prices and CO_2 transportation & storage costs. To reflect regional differences when incorporating these costs into the model, input shares and mark ups are computed for each region based on region specific costs for fuels, electricity and CO_2 transportation & storage. Regional energy prices are determined based on the GTAP 10 power database which aligns with the EPPA model's main structure (Aguiar et al. (2019); Purdue University (2023)). Regional CO_2 transportation & storage cost are derived

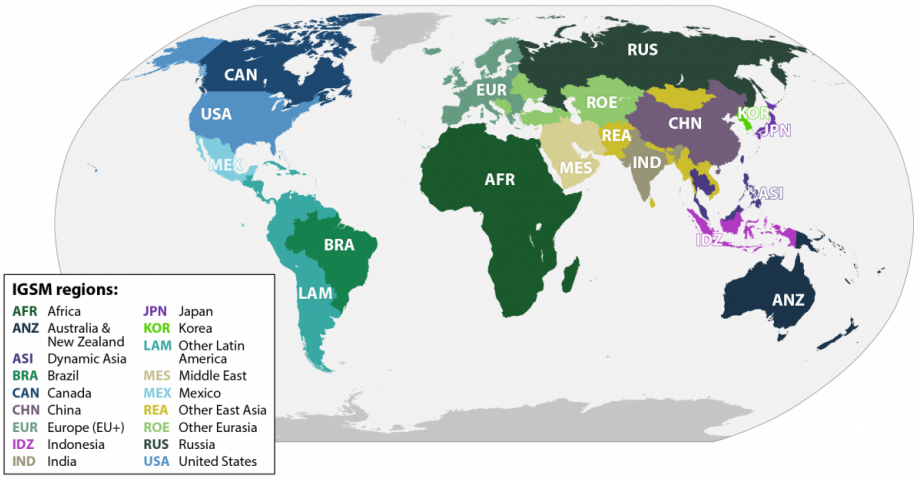

Figure 3-18: Regional representation in the EPPA model (Morris et al. (2019a))

from Smith et al. (2021). However, I assume a constant cost of capital and labor. The base costs derived from these levelized cost calculations for the steelmaking and hydrogen production are then utilized to calculate markup values which are ratios of the cost of the advanced technology to the cost of the conventional technology. This regional specific mark up for each technology in the base year (2020) is determined for all advanced technologies. The markup represents how competitive that technology will be and varies between regions so I expect that the adoption of these technologies will also vary between regions. The input shares for each technology are also incorporated into the production block in EPPA which specifies the different inputs to produce one unit of product. In addition, in the EPPA model, the cost of fuels and electricity are region-dependent and time-dependent. Future technology costs decline endogenously in the EPPA model via learning and other factors such as adjustment costs (Morris et al. (2019b)). Traditional iron and steel in the EPPA model is representative of all current iron and steel production technologies including BF-BOF, DRI-EAF and scrap steel EAF.

Many integrated assessment models represent energy intensive sectors as one aggregated entity but here I aim to represent specific technologies. The EPPA model represents conventional iron and steel technologies as well as low carbon advanced steel technologies (DRI-EAF with CCS and H_2 DRI-EAF). In addition, hydrogen production pathways for Blue hydrogen and Green hydrogen are also represented

in the model. The EPPA model is also capable of representing different policy scenarios. In this research I explore the deployment of low carbon technologies under an aggressive climate policy scenario termed the Accelerated Action scenario (Paltsev et al. (2021b)). This scenario aims to limit global warming to below 1.5 Celsius with greater emission reductions in the short term (2025-2030) than has been expressed in the current Nationally Determined Contributions.

Chapter 4

Integrated Assessment Modeling Results

4.1 Iron and Steel Sector Decarbonization Policy Scenarios

I incorporated advanced technology pathways for low-emission steelmaking and hydrogen production into the MIT Economic Projection and Policy Analysis (EPPA) model (Morris et al. (2021); Paltsev et al. (2021a); Chen et al. (2022)). I assessed the steel decarbonization pathways in a policy scenario termed Accelerated Action as described in Section 3.4.1 (Paltsev et al. (2021b)). This scenario abates global CO_2 emissions by 80% in year 2050 and 98% in year 2070; relative to the base year of 2020. The direct global CO_2 emissions from the iron and steel sector are reduced from about 1.8 Gt CO_2 in 2020 to about 0.9 Gt in 2050 and 0.1 Gt in 2070 (when assuming the base costs for both the advanced steel technologies and hydrogen production). I assume no deployment of negative emissions technologies in these base cases but I do conduct a sensitivity analysis to explore a scenario where bioelectricity with CCS (BioCCS) is an available technology.

Table 4.1: Model Scenarios Assessed 2020-2050

Policy	**Advanced Steel Production Non-energy Input Costs**	**H_2 Production Cost**
Reference	Base Cost	Base Cost
Accelerated Action	Base Cost Reduced Cost Base Cost Reduced Cost	Base Cost Base Cost Reduced Cost Reduced Cost
Accelerated Action with Inflation Reduction Act Applied to U.S. Steel Sector	Base Cost	Base Cost
Accelerated Action with BioCCS	Base Cost	Base Cost

4.1.1 Model Scenario Assumptions

The model scenarios that I assessed are summarized in Table 4.1. I explored several cost reduction scenarios using the same policy assumptions but different technology cost assumptions. Base costs represent the cost premiums determined from our levelized cost calculations. Reduced non-energy input cost for advanced steel production represents a scenario in which the non-energy input costs are equal to that of traditional steelmaking. Reduced cost of H_2 production assumes a cost of \$1/kg H_2. This would be a significant reduction of the current cost of green hydrogen and a modest reduction of the blue hydrogen cost. This ambitious reduction in hydrogen production cost aligns with the current cost of Grey hydrogen and with the U.S. Department of Energy's "Hydrogen Shot" goal which aims to reduce the cost of clean hydrogen to \$1/kg H_2 (DOE (2021)). This low hydrogen production cost reduces the input share required for hydrogen feedstock in the H_2 DRI-EAF pathway.

I also explored two scenarios where the Accelerated Action policy case has been altered. One scenario incorporates the Inflation Reduction Act tax credits indefinitely for hydrogen and steel production in the United States. I applied the full 45 Q tax

credit of \$85/t captured CO_2 to both the DRI-EAF with CCS technology and the Blue H_2 production technology. In addition, this scenario applies the full 45 V tax credit of \$3/kg to the Green H_2 production cost. Lastly, I conducted a sensitivity analysis to see how the system responds when a negative emission technology such as BioCCS is available for deployment.

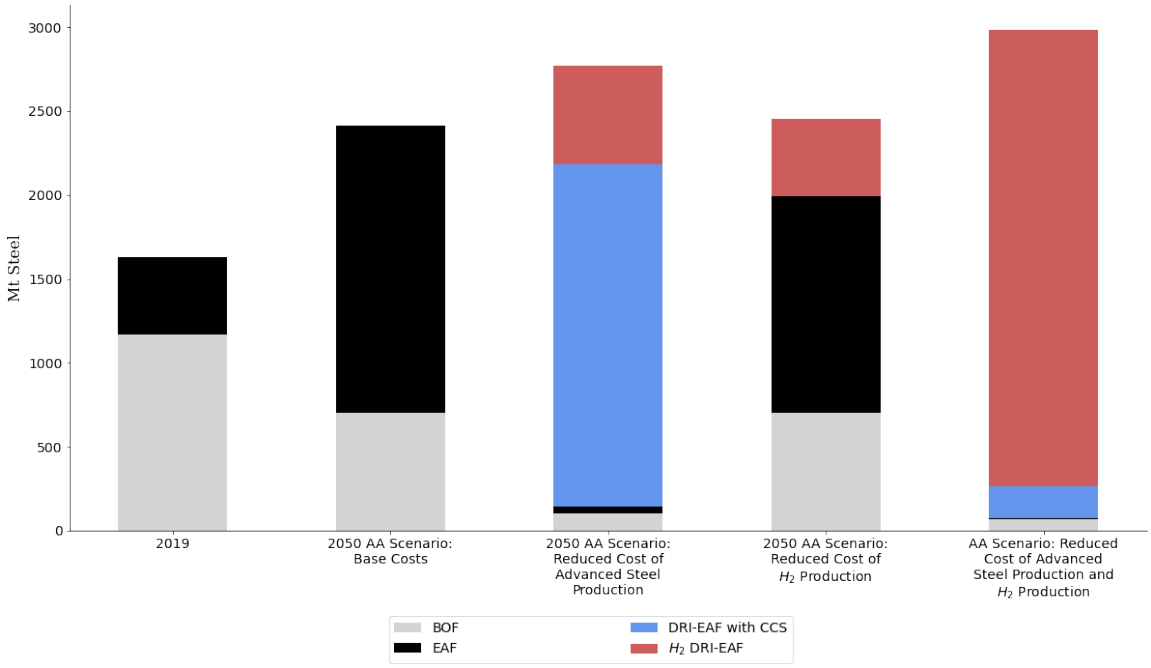

Figure 4-1: Global steel production by process under the different cost reduction scenarios described in Table 4-1

4.2 Global Results

4.2.1 Reference Case

In the Reference scenario in 2050, the share of global steel production by process only slightly changed from the process share in 2019. The share of EAF pathways increases from 28% to 34%. None of the low carbon advanced steel technologies are deployed. The direct emission intensity of the steelmaking is 1.16 tCO_2/t steel in 2020 and 1.21 tCO_2/t steel in 2050 (Figure 4-5). The energy intensity is also relatively unchanged with a slight increase from a global average of 17.3 to 17.7 GJ/t steel (Figure 4-3).

4.2.2 Accelerated Action: Base Costs

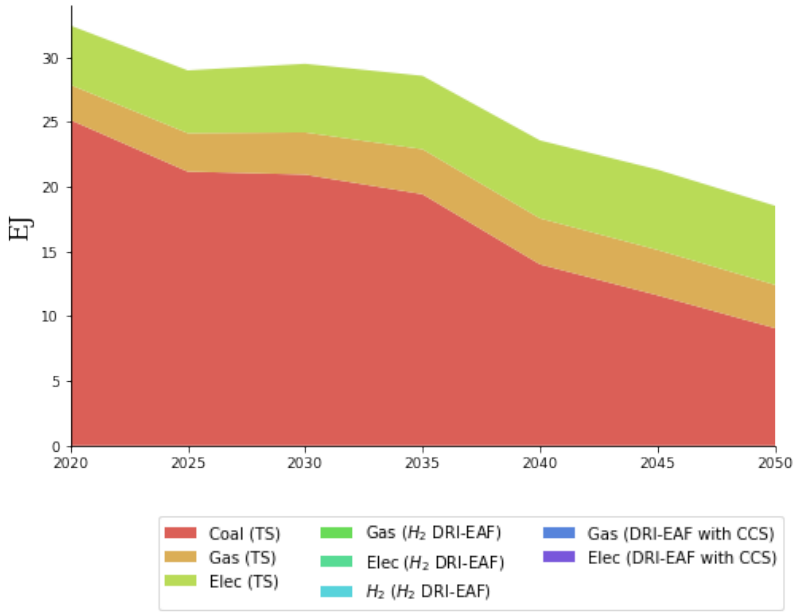

Figure 4-2: Energy consumed by global iron and steel production by type of energy input. The scenario modeled is the Accelerated Action policy case with Base Cost assumptions. Legend refers to the energy input to specific steel production pathways. TS = Traditional Steel.

Figure 4-1 shows that in the Accelerated Action policy scenario, when assuming base costs, the DRI-EAF with CCS pathway is only minimally deployed by 2050 (0.06 Mt steel). Additional sensitivity analysis revealed that at base costs the CCS technology would make up 2% of total production by 2060 and 4% by 2070. My analysis however focuses on the time frame from 2020 to 2050 as this is when the IPCC has identified that significant decarbonization must take place to minimize global warming below 1.5 Celsius.

Figure 4-4 demonstrates that in the base costs scenario even without significant adoption of the advanced low carbon steelmaking technologies there is a substantial emission reduction potential in the iron and steel sector. In the EPPA model, direct CO_2 emissions from iron and steel production are significantly reduced by an increase in energy efficiency and electrification in traditional steelmaking (Figure 4-2, 4-3).

Global average energy intensity reduces from 17.3 to 7.7 GJ/t steel (Figure 4-3). The electricity share of total energy used in the traditional steelmaking increases from

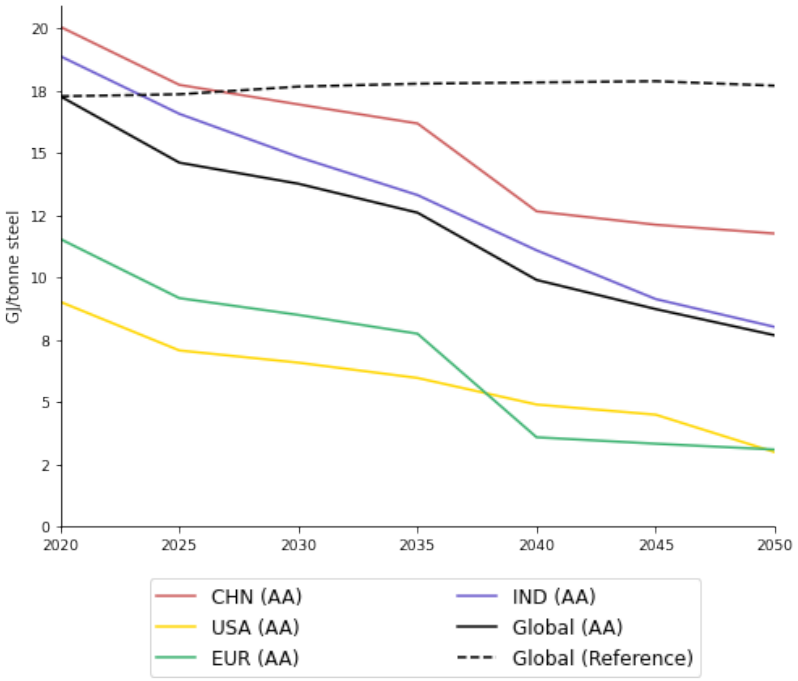

Figure 4-3: Energy intensity of iron and steel production. The scenario modeled is the Accelerated Action policy case with Base Cost assumptions.

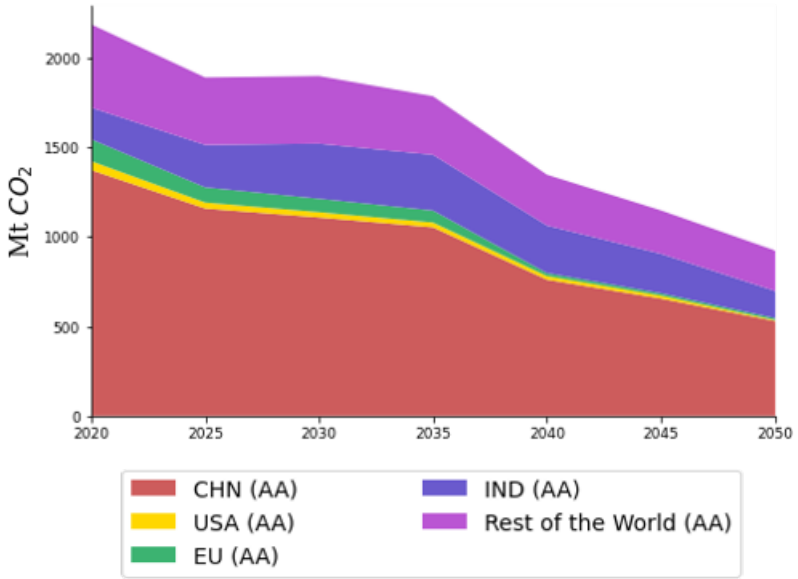

Figure 4-4: Total direct CO_2 emissions from iron and steel production. The scenario modeled is the Accelerated Action policy case with Base Cost assumptions.

14% to 33% (Figure 4-2), and correspondingly the share of total production that is produced via an EAF pathway is calculated to increase from 28% to 71% (Figure 4-1). By 2050, the direct CO_2 emission intensity of global iron and steel production

reduces from 1.16 to 0.38 tCO_2/t steel (Figure 4-5). In Section 4.7, I will delve deeper into how traditional steel making technologies achieve decarbonization in the model via energy efficiency, EAF pathway share/electrification, and scrap usage.

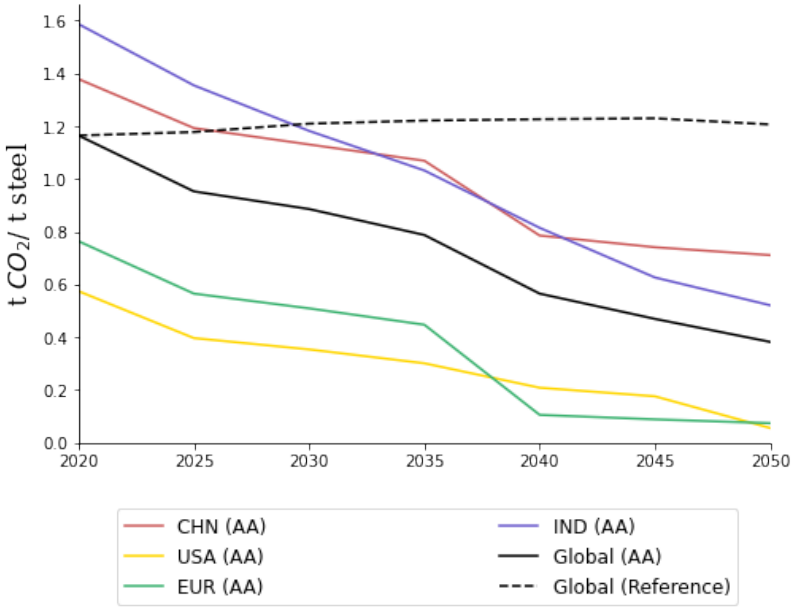

Figure 4-5: Direct CO_2 emission intensity of iron and steel production. The scenario modeled is the Accelerated Action policy case with Base Cost assumptions.

Accelerated Action: Base Costs with BioCCS Deployment

As a sensitivity to the Accelerated Action base costs scenario, I also explored the impact of deploying Bioelectricity with CCS (BioCCS). The EPPA model predicts a heavy reliance on the BioCCS technology in order to achieve emission reduction goals. When BioCCS is a technology option, then the model does not deploy the advanced low carbon steel technologies even when modeled out to 2070. Globally the iron and steel sector does slightly increase its share of the EAF pathway and reduces its energy intensity. Global average direct CO_2 emission intensity reduces to 0.43 tCO_2/t steel by 2050. This is slightly higher than in the scenario described without BioCCS technology. Furthermore, steel demand is slightly higher in the scenario with BioCCS particularly by year 2070 where it aligns more with the reference case. Figures in the appendix detail how the emission intensity of grid electricity decreases

over this time frame with and without BioCCS (Figures B-1, B-2, B-3, B-4).

4.2.3 Accelerated Action: Reduced Cost of Advanced Steel Production

Figure 4-1 shows that if the non-energy input costs of advanced steel production are reduced, then the DRI-EAF with CCS pathway becomes the dominant production pathway in EPPA (∼74% of global production) and H_2 DRI-EAF is also deployed in this scenario (∼21% of global production). The use of DRI-EAF with CCS in this pathway results in about 1000 Mt of CO_2 captured in the year 2050. To produce this amount of steel via the H_2 DRI-EAF pathway requires 47 Mt of H_2. Current H_2 demand for all sectors globally is about 70 Mt (IEA (2019)). The model supplies the H_2 in year 2050 via the Blue H_2 production pathway which is more cost competitive than the Green H_2. Approximately, 450 Mt of CO_2 will be captured during the Blue H_2 production in 2050. In this scenario, iron and steel production's global average direct CO_2 emission intensity is reduced to 0.1 tCO_2/t steel by 2050. Faster deployment of the advanced low carbon steelmaking results in greater emissions intensity reductions by 2050 than in the base costs scenario. The energy intensity doesn't decrease as much as in the bases costs scenario because the EAF pathway doesn't play as large of a role. As I will discuss further in Section 4.7, the EAF pathway has the potential to have a much lower energy intensity than the other pathways.

4.2.4 Accelerated Action: Reduced Cost of H_2 Production

In the scenario where I assume that all H_2 production costs are reduced to \$1/kg then the EPPA model predicts ∼19% of global steel production will be produced via the H_2 DRI-EAF pathway (Figure 4-1). This results in an annual H_2 demand of 37 Mt for steelmaking. All of the hydrogen is supplied via the Green H_2 production route because this pathway has no direct emissions, electricity generation is becoming increasingly decarbonized and because the scenario assumes the Green and Blue H_2

have equivalent production costs. This scenario assumes base costs for the non-energy inputs for the advanced steel making pathway so we see that the DRI-EAF with CCS pathway only contributes ∼0.06 Mt, which is well below 1% of total production. In 2050, ironmaking and steelmaking have decreased their direct CO_2 emissions intensity to 0.32 tCO_2/t steel. The EAF pathway plays a role in decarbonization in this scenario as this pathway can be very efficient and is a low carbon process in comparison to the traditional BOF pathway.

4.2.5 Accelerated Action: Reduced Cost of Advanced Steel Production and H_2 Production

In the final scenario, I assume that the advanced steelmaking non-energy costs are reduced and that the cost of H_2 production is reduced. This results in significant global shares of the H_2 DRI-EAF pathway (∼90%) and a hydrogen demand of 217 Mt (Figure 4-1). As seen in the previous scenario when the hydrogen production pathways are of equivalent costs then we see in year 2050 that all of this hydrogen production is via the Green H_2 production pathway. The global steel production is also made up of a smaller share of the DRI-EAF with CCS pathways (∼6%), resulting in 102 Mt of CO_2 captured annually (Figure 4-1). Direct CO_2 emissions intensity of iron and steel production is reduced to 0.08 tCO_2/t steel.

4.2.6 Summary of Global Results for Accelerated Action Policy Case with Different Cost Reduction Assumptions

I compare the CO_2 abatement potential of the iron and steel sector under the different cost reduction scenarios. In Figure 4-6, each color represents a different cost reduction scenario. The fraction of abated CO_2 that is graphed is calculated as the direct CO_2 emissions that have been abated relative to the base year of 2020. The marker size represents the approximate global CO_2 price in that year. In the scenarios assuming base costs the sector achieves 58% abatement and when assuming reduced cost of H_2 production it reaches 64% abatement of direct CO_2 emissions by 2050. In the

scenarios where I assume reduced cost of advanced steel production, the low carbon advanced steel technologies are deployed more rapidly. The scenario with reduced cost of advanced steel achieves 88%. When assuming reduced cost of advanced steel and reduced cost of H_2 production then the sector achieves 89% abatement.

In addition to the global analysis I also analyzed selected regions to understand how regional steel decarbonization pathways may differ. I analyze China, India, the European Union and the U.S. because these regions are all top steel producers and consumers (WSA (2022b)).

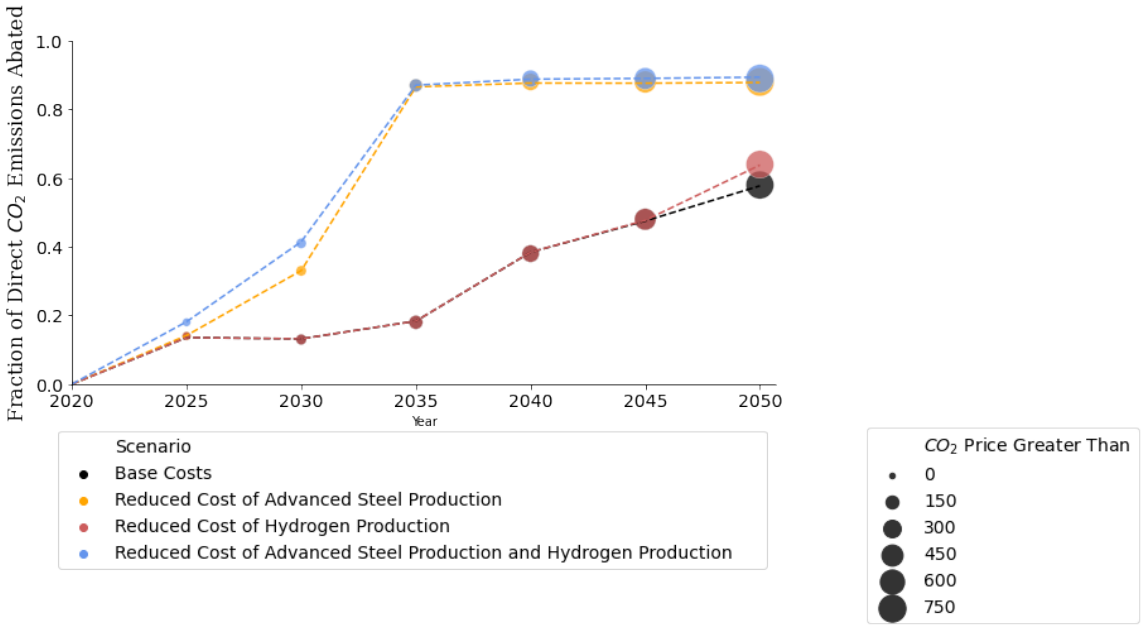

Figure 4-6: Abatement of direct CO_2 emissions from iron and steel production relative to the base year of 2020. The different cost scenarios are represented. Bubble size represents the approximate global CO_2 price for that year

4.3 China

In 2019 China produced more than 50% of global steel production (WSA (2022b)). China is currently a net exporter although the majority of the steel they produce is used domestically (WSA (2022b)). While, China's steel sector saw rapid growth in the early 2000s their rate of growth is anticipated to slow as described in Section 4.7.2. Currently, China produces 90% of its steel using the BF-BOF pathway and

relies heavily on coal (WSA (2022b)). This makes their steel production very emission intensive as demonstrated in Figure 4-5. Figure 4-7 shows that in the Accelerated

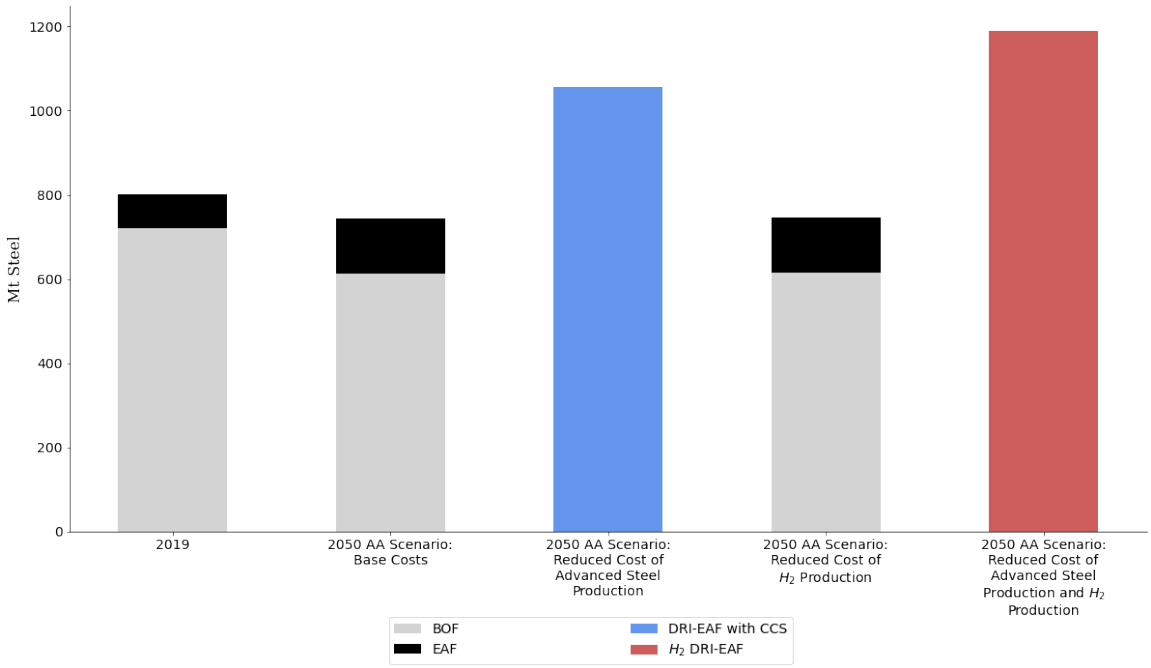

Figure 4-7: China's steel production by process under different scenarios described in Table 4-1

Action (AA) Scenario with base costs, the conventional EAF pathway grows its share of production from 10% to 17.6 %. In the AA scenario assuming reduced cost of advanced steel production, the DRI-EAF with CCS scenario makes up over 99% of the production with the remaining shares produced from the H_2 DRI-EAF pathway. In the AA scenario assuming reduced cost of H_2 production, the model produces the same results as in the base cost scenario where the share of conventional EAF pathways increases to 17.6%. In the final scenario, with reduced cost of both advanced steel production and H_2 production, the H_2 DRI-EAF pathway makes up 100% of the production.

These different scenarios also result in different regional production levels. Figure 4-8 details how China's share of total global production varies in the different cost reduction scenarios. In the reference scenario in 2050, China's production is 41% of global production. In both the base costs scenario and reduced cost of H_2 production scenario, China's production is reduced to 31% and 30% respectively. In

the reduced cost of advanced steel, 38%. And in the scenario assuming reduced cost of advanced steel and hydrogen production, China's production is 40% of the global production.

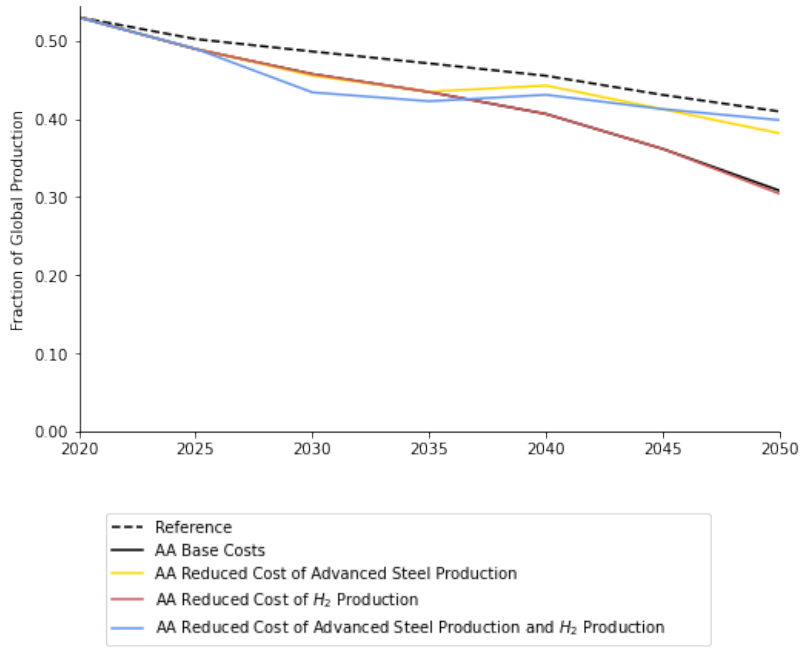

Figure 4-8: China's total steel production as a fraction of total global production under different scenarios described in Table 4-1

4.4 India

India is also currently a net exporter of steel. The country's economy is rapidly expanding and the IEA forecasts that India's steel production will increase 3-4 times by 2050 (IEA (2020)). In 2019, India produced 100 Mt of steel making up about 6% of global production (WSA (2022b)). India's current production is about 44% via BOF, 27% via coal-based DRI-EAF and 28% scrap-based EAF (WSA (2022b)). India's DRI shaft furnaces primarily use coal as the reducing agent and energy supply which differs from other regions which primarily use natural gas in the DRI process (IEA (2020); Paltsev et al. (2021a)).

In the Accelerated Action scenario assuming base costs, India's steel production increases and they increasingly switch away from coal energy. Figure 4-9 shows that

in the base cost scenario, the share of conventional EAF produced steel increases from 56% to 100 %. When assuming reduced cost of advanced steel production, 93% of production is via the DRI-EAF with CCS pathway and remaining share of 7% from BOF based pathways. Assuming reduced cost of hydrogen production results in the H_2 DRI-EAF pathway producing 84% of production and the remaining 16 % via conventional EAF pathways. And in the scenario assuming reduced cost of advanced steel and hydrogen production, 100 % of production is via the H_2 DRI-EAF pathway.

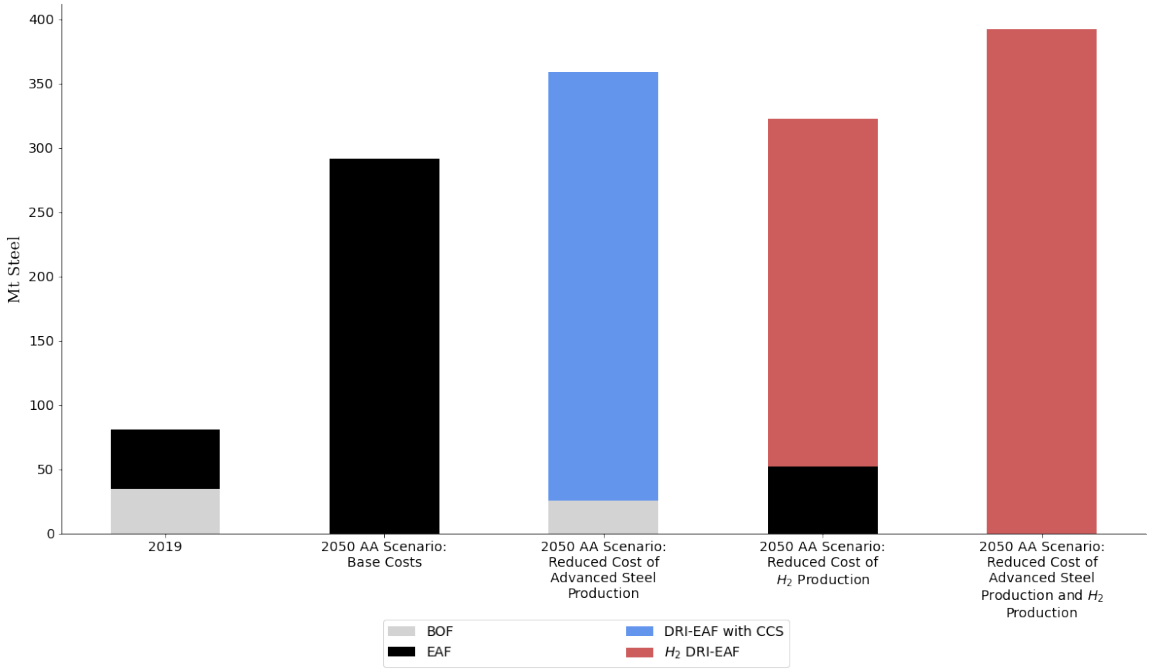

Figure 4-9: India's steel production by process under different scenarios described in Table 4-1

Figure 4-10 details how India's share of total global production varies in the different cost reduction scenarios. In the reference scenario in 2050, India's production increases to 17% of global production. In the base cost scenario, India's share of global production increases to 12 %. In all of the cost reduction scenarios, India's share of global production is 13% in 2050.

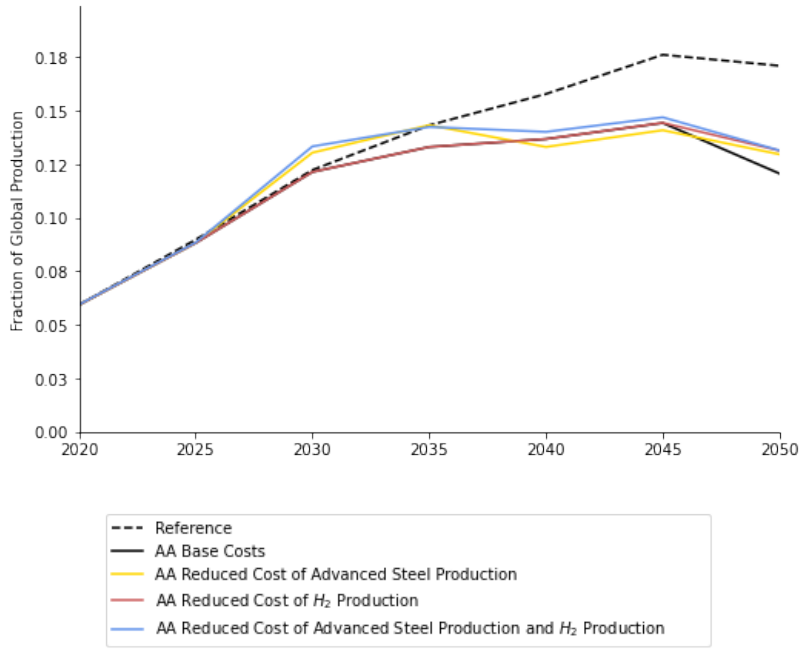

Figure 4-10: India's total steel production as a fraction of total global production under different scenarios described in Table 4-1

4.5 European Union

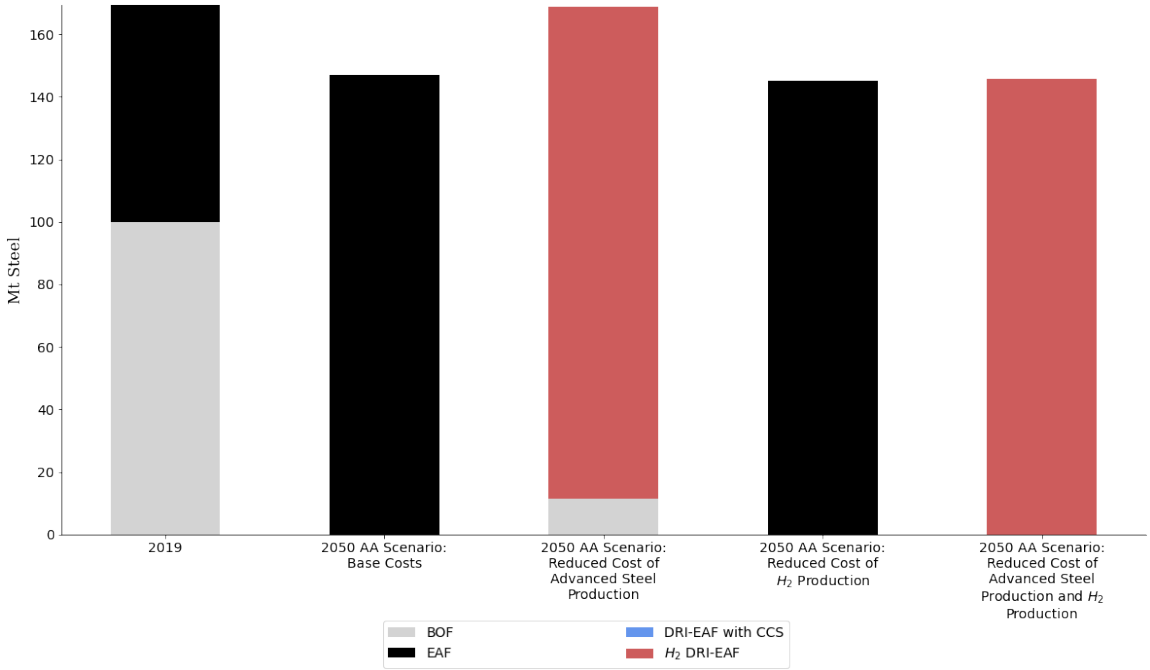

Figure 4-11: EU's steel production by process under different scenarios described in Table 4-1

The European Union (EU) is currently a net importer and produces about 8.5% of global steel production (WSA (2022b)). In the base year the EU produces 40% of their steel via the EAF pathway and 60% via the BOF pathway (WSA (2022b)). Figure 4-11 demonstrates that in the Accelerated Action scenario when assuming base costs by year 2050 that 100% of the EU's steel is produced via the conventional EAF pathways.

When assuming reduced cost of advanced steel technologies, then 93% of production is via the H_2 DRI-EAF pathway and 7% from conventional BOF pathways. Assuming reduced cost of H_2 production, the EU uses conventional EAF pathways to produce 100% of total production. Lastly, when assuming reduced cost of advanced steel production and reduced cost of H_2 production then 100% of production is via the H_2 DRI-EAF pathway.

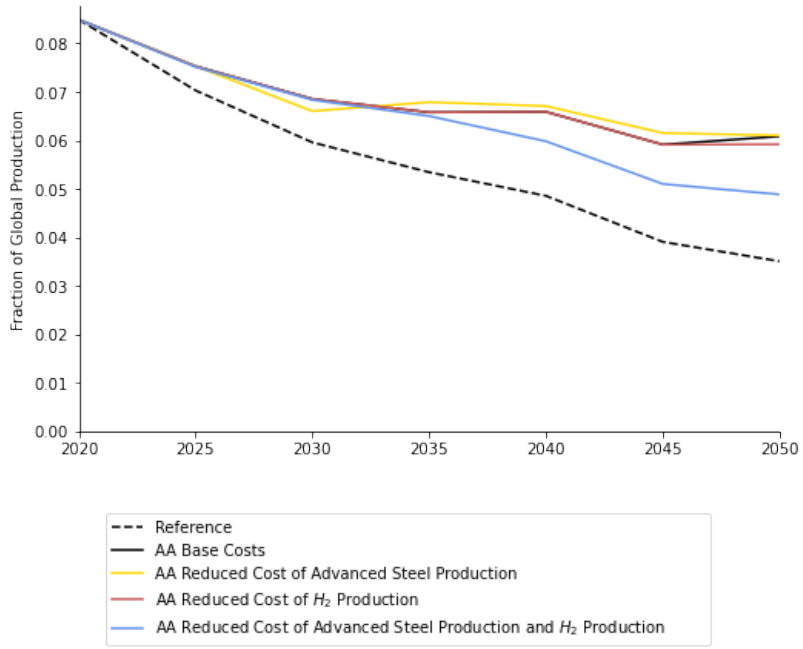

Figure 4-12: EU's total steel production as a fraction of total global production under different scenarios described in Table 4-1

Figure 4-12 details how the EU's share of total global production varies in the different cost reduction scenarios. In year 2050 in reference scenario, the EU's steel production makes up 3.5% of global production. The EU has a 6% share of global production under the Accelerated Action base cost, reduced cost of advanced steel

and reduced cost of H_2 production. When assuming reduced cost of both advanced steel production and H_2 production then the EU's share of global steel production is 5%.

4.6 USA

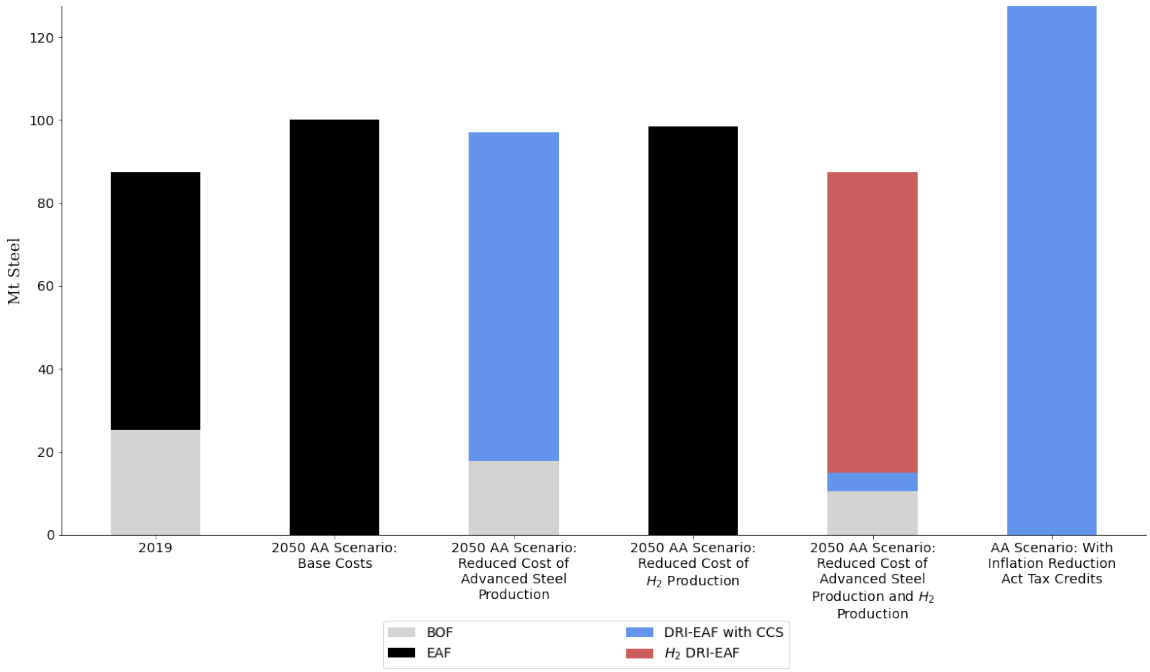

Figure 4-13: United States' steel production by process under different scenarios described in Table 4-1

The U.S. is currently a net importer and produces about 4.5% of global steel production. In 2019, 67% was produced via the scrap-based EAF pathway, 30% via the BOF pathway and 3% via the DRI-EAF pathway (WSA (2022b)). Figure 4-13 shows that in the Accelerated Action base costs scenario in year 2050, the U.S. produces 100% of its steel via conventional EAF pathways. When assuming reduced cost of advanced steel production then 82% is produced from the DRI-EAF with CCS pathway and 18% via conventional BOF pathways. Assuming reduced cost of H_2 production, then 100% of production is via conventional EAF pathways. When assuming reduced cost of both advanced steel production and H_2 production then

83% is produced from H_2 DRI-EAF pathways, 12% via conventional BOF pathways and 5% from DRI-EAF with CCS pathways.

4.6.1 Impact of the Inflation Reduction Act

I also explored the impact of the Inflation Reduction Act (IRA) tax credits on the cost of CCS steel and H_2 production. This scenario is based on the Accelerated Action policy scenario but also incorporates the IRA 45 Q tax credits of \$85/t captured CO_2 to both the DRI-EAF with CCS technology and the Blue H_2 production technology. In addition, this scenario applies the full 45 V tax credit of \$3/kg to the Green H_2 production cost. The tax credits are implemented indefinitely with no end date. The tax credits reduce the H_2 production costs by 42% for the Blue and 52% for the Green H_2

These tax credits resulted in a percent reduction of 7% for the DRI-EAF with CCS pathway, 9% reduction for the Blue H_2 DRI-EAF and 23% reduction of the Green H_2 pathway. However, the DRI-EAF with CCS is still the cheapest option with a total steel production cost that is 7% cheaper than the Blue H_2 DRI-EAF. Figure 4-13 shows that when these tax credits are implemented in the U.S. that it results in deployment of the DRI-EAF with CCS route. By 2050, this pathway makes up 100% of the process share for steel production in the United States.

Figure 4-14 details how the USA's share of total global production varies in the different scenarios. In the reference scenario in 2050, steel production from the U.S. makes up 2% of global production. The U.S. produces 4% of global steel production in the Accelerated Action base cost scenario and the AA reduced cost of H_2 steel scenario. The AA reduced cost of advanced steel results in a production share of 3.5%. In the AA reduced cost of advanced steel and H_2 production scenario, the U.S. produces 3% of global production. Lastly, in the AA with IRA scenario, U.S. steel production is 5% of global production.

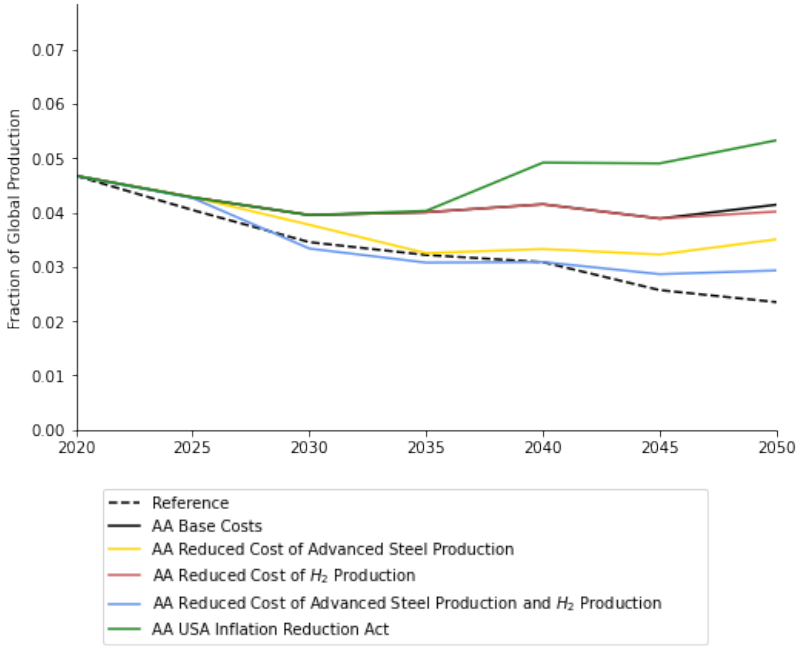

Figure 4-14: United States' total steel production as a fraction of total global production under different scenarios described in Table 4-1

4.7 Discussion

4.7.1 The Role of Conventional Steelmaking Processes in Decarbonization

Even in the scenarios where the advanced low carbon steel technologies are not deployed, the steel sector still achieves significant reduction of CO_2 emissions (Figure 4-1, 4-4). This is accomplished in several ways. One being increasing energy efficiency of the conventional pathways. In addition, in these deep decarbonization scenarios, the emission intensity of electricity generation is decreasing rapidly. Therefore, electrification by switching from BOF to EAF pathways enables the steel production to utilize lesser amounts of fossil fuels. Then, by increasing the use of scrap steel, the sector is able to reduce emissions even further. The EAF process is capable of utilizing a feedstock of 100% scrap steel. The BOF pathway can also reduce energy intensity by utilizing scrap but the current process can only replace metallic input at a fraction of its feed (25-30%) (Cavaliere (2019)).

The energy required for EAF operations with high scrap input (up to 100%) is approximately 4.5 GJ/thrs as compared to the ∼17 GJ/thrs required for natural gas based DRI-EAF and the BF-BOF process (WSA (2014); Cavaliere (2019); IEA (2020)). As a result, advanced steel technologies compete with traditional steelmaking that is increasingly efficient and has reduced emissions intensity. However, a 100% scrap-based EAF pathway cannot replace all primary steel production because there is insufficient scrap steel available to meet steel demand (See Section 4.7.2). In addition, traditional steel making cannot fully electrify with existing commercial technology because electrification of the iron making process is not yet commercialized.

The low carbon advanced steelmaking technologies that I have modeled still utilize natural gas for heating in the finishing steps and for temperature control in the H_2 DRI-EAF pathway. However, this fuel could be replaced with alternative low carbon fuels or theoretically with electric heating, which could further reduce direct emissions. In addition, electric arc furnaces have process emissions as discussed in Section 2.2 that are not currently accounted for in the model. However, even if the modelling of the traditional steel is calibrated to prevent complete electrification of the traditional steel sector, the electric arc furnace still plays a major role in lowering sectoral emissions in our scenarios.

4.7.2 Forecasts for Steel Demand and Scrap Availability

Although the electric arc furnace provides a pathway with lower energy intensity and potentially lower carbon emissions than the BF-BOF or DRI-EAF pathways, it cannot be the sole steel production process because of the limited availability of scrap steel. In 2019, about 1/3 of the total metallic input to make steel was sourced from scrap with the remainder being produced from iron ore (in the form of pig iron or direct reduced iron). In addition, scrap steel cannot achieve the highest steel quality needed for some applications due to contaminants often found in end of life scrap (IEA (2020)).

As seen in Figure 4-15, China currently produces ∼54% of global steel production (WSA (2022b)); which ties the future of steel strongly to the future of steel production

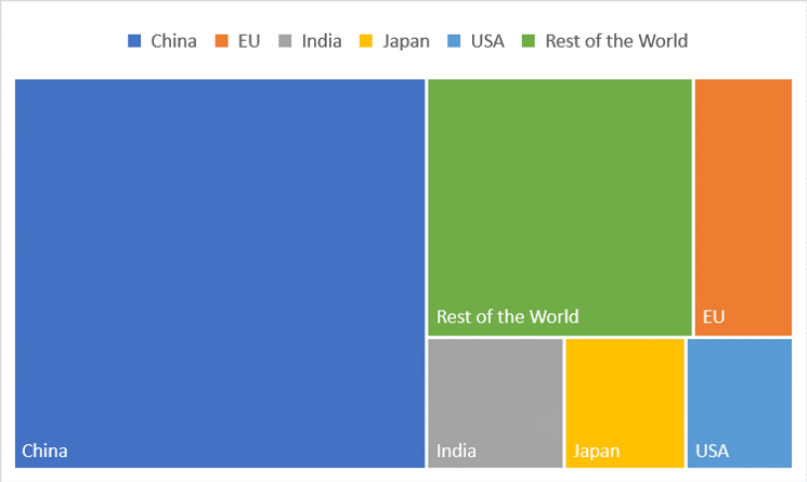

Figure 4-15: Global steel production by region in 2019. (Figure based on data from the WSA (2022b))

in China. However, the steel marketplace is still highly competitive because the top ten steel producing companies only produce ∼25% of steel production, and steel is traded as an international commodity (IEA (2020)). IEA estimates that the growth of primary steel demand will slow in the coming decades. In their Stated Policies Scenario they predict that in the year 2050, global steel end use demand will be 2,500 Mt and in their more aggressive decarbonization policy scenario (Sustainable Development Scenario) they predict that steel demand will be only 2,100 Mt (IEA (2020)). The reduced steel demand in this scenario is primarily due to assumptions around greater material efficiencies and higher recycle rates of scrap steel (IEA (2020)).

But, both of the IEA scenarios assume that there will be an increase in available scrap which will reduce the need for primary production of steel (IEA (2020)). Other forecasts assume greater steel demand in the future such as the World Steel Association's forecast from their report "Energy Use in the Steel Industry", which cites a prediction of 2,460 Mt for global steel production in 2030 (WSA (2014)). Both the IEA and WSA predictions assume that there will be increases in scrap availability and secondary steel production in the future, particularly in China as steel stock produced in the early 2000s reaches its end of life. Theoretical global available scrap was 865 Mt in 2019 (IEA (2020)); however, in 2021 the World Steel

Association estimated that only 680 Mt of scrap steel were utilized (Ciftci (2021)). Figure 4-16 illustrates the World Steel Association's forecast for available end of life scrap steel, which could increase to 900 Mt by 2050 and potentially upwards of 1300 Mt when accounting for all scrap available in 2050 (Ciftci (2018, 2021)). However, this future scrap supply still falls short of meeting even the current steel demand which was 1950 Mt in 2021 (WSA (2022b)) and a metallic input of 1.05-1.2 tonnes is required to produce a tonne of steel (IEA (2020)).

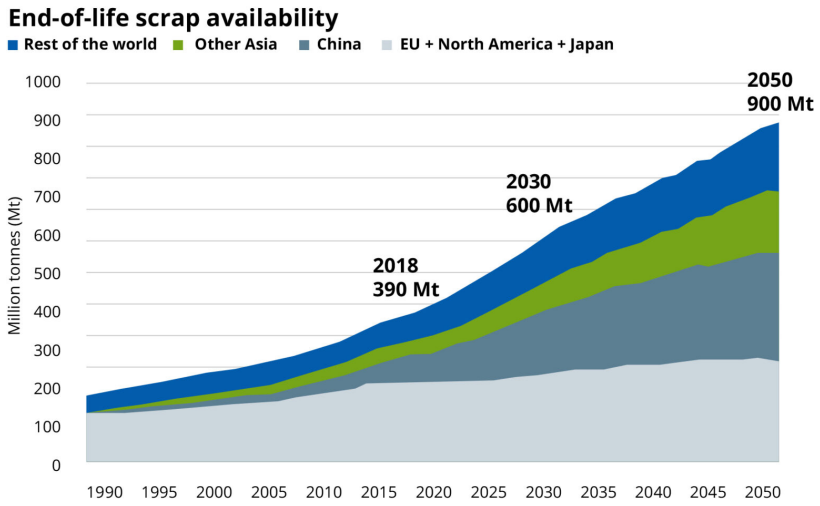

Figure 4-16: End of life scrap availability forecast from World Steel Association (Figure from Ciftci (2021))

4.7.3 Regional Decarbonization Pathways

It is apparent from the results that the decarbonization pathways are regionally specific. Regional differences in the cost of natural gas, electricity, hydrogen and CO_2 transport & storage (T&S) also inform which pathways are more economical. In the EU, the price of natural gas is more expensive than in China or the U.S., and the assumed cost of CO_2 T&S is more expensive than the other regions I analyzed in this thesis. This plays a role in the EU's lack of adoption of the DRI-EAF with CCS route as compared to other regions. India also has a high natural gas price and when the price of hydrogen is reduced it becomes competitive for steelmaking. As stated previously in the scenario of reduced cost of H_2, the price is assumed to be

$1/kg ($7/GJ HHV) for both Blue and Green H_2 this would be a drastic price cut particularly for the Green H_2 production (Currently $5.80/kg); however, this cost is still much higher than the price of natural gas in many regions. The price of natural gas in the U.S. and China notably are on the order of $4/GJ.

Also, the results show that regional steel demand can be influenced by the policy scenario and processes deployed in that region. Steel is an internationally traded commodity and its production is highly competitive. If only one region attempts to implement a carbon price it could result in that region's steel being less competitive. However, in a policy scenario where all regions are subject to the same CO_2 price the results from EPPA show that regions that are able to quickly deploy low carbon steelmaking have an advantage and increase their share of global steel production.

The U.S. and the EU currently produce more steel via the EAF pathway and recycle more steel than in China or India. The lower emission intensity of steel production in these regions is an advantage under the Accelerated Action scenario. This advantage decreases if we assume that all regions now have access to low carbon advanced steel making at a reduced cost. However, in the scenario I model where the U.S. implements the Inflation Reduction Act tax credits, they gain an additional advantage over other regions and in 2050 have a higher share of global steel production than they would in the reference case. The increase in steel demand could be driven by international trading as well as an increase in domestic use.

4.7.4 Sectoral Decarbonization

The Accelerated Action scenario prescribes emission reductions for each region. However, there are not specific emission caps for each sector. This means that the level of decarbonization between different sectors can vary based on relative marginal abatement costs. In addition, not only do the technologies that are available within a sector matter but the technologies available to other sectors also have an impact. When BioCCS is available to the electricity generation sector it also impacts the pathways that the steel sector selects to reduce emissions. BioCCS is able to achieve negative emissions which lessens the emission reductions needed to be achieved in

other sectors. It should be noted that actual sustainable implementation of BioCCS will be challenging as the supply of sustainable biomass will be competitive as will land availability.

Furthermore, other sectors may also implement carbon capture. There can be advantages to this in the form of economies of scale for CO_2 transportation infrastructure. But, this could also result in increasing competition for CO_2 storage. The model scenario which adopted the most DRI-EAF with CCS by year 2050 results in approximately 1000 Mt of CO_2 captured annually from the steel sector. As comparison, the Emirates Steel facility which injects CO_2 for enhanced oil recovery has a CO_2 capture rate of 0.8 Mt annually and is currently the only steel facility considered to store captured CO_2 (IEA (2020)). The IEA forecasts in their Sustainable Development Scenario (SDS) that by 2050 there will be 400 Mt of CO_2 captured annually by the steel sector (IEA (2020))

Chapter 5

Conclusion

5.1 Key Findings

Low carbon H_2 production costs need to be lowered significantly if H_2 is to play a significant role in decarbonizing heavy industry applications such as steel production or high temperature heating. Both Blue and Green hydrogen production pathways are currently more expensive than conventional fossil fuels (Figure 3.1). Emission intensive heavy industry applications like steel, cement, and petrochemical production are highly competitive global commodities and any increase in cost relative to the conventional pathway will be very unfavorable. Low carbon H_2 production costs may decrease in the future due to technological advances or become more competitive if carbon prices are implemented. Targeted policies such as the U.S.'s Inflation Reduction Act (IRA) can lower H_2 production costs significantly, however they will be in competition with the other IRA tax credits such as the 45 Q tax credit for carbon capture (See Section 4.6.1).

High temperature heating with low carbon hydrogen is still significantly more expensive than heating with conventional fossil fuels due to the high cost of producing low carbon hydrogen. Heating with hydrogen will not be cost competitive unless there are reductions in cost due to technological advances or implementation of carbon policy mechanisms (See Section 3.3).

The DRI-EAF with CCS pathway is currently more cost-competitive

than the H_2 DRI-EAF pathway. This is made apparent in both the levelized cost calculations (Section 3.2) and in the scenarios modeled via the EPPA model (Section 4). If the cost of H_2 production is reduced then the H_2 DRI-EAF pathway is deployed in certain regions. However, even in this scenario the cost of \$1/kg (or \$7/GJ) still exceeds the price of natural gas in many regions such as China and the United States (Figure 4-7 and 4-13).

The steel sector can reduce its CO_2 emission intensity using conventional steelmaking pathways. BF-BOF, DRI-EAF and scrap-based EAF pathways can achieve greater energy efficiencies and thus use less fossil fuels. The use of scrap steel can also further reduce energy usage. The scrap-based EAF pathway is more energy efficient than the BOF pathway and switching to this pathway further reduces energy consumption. Furthermore, under a decarbonization policy scenario the electricity generation sector is also decarbonizing which makes electrification of steelmaking increasingly advantageous. However, as discussed in Section 4.7, scrap steel stock is limited and, as seen in Figure 4-6, more rapid decarbonization can be enabled by adopting low carbon advanced steelmaking technologies if their costs are reduced.

The optimal decarbonization pathway is region specific. Sections 4.3-4.6 demonstrate how under the same scenarios each region has a different response. This is influenced by the region's currently deployed steel production processes and by their regional prices. For example, India's current reliance on coal for the DRI-EAF pathway can be altered by gradual switching to natural gas and biofuels. Regional differences in the types of processes deployed also influence that region's competitiveness with other regions. In the reference case, production pathways that are cheaper even though they may have higher emission intensities maintain their advantage which results in regions with those production pathways achieving a greater share of global production. But, under deep decarbonization policy scenarios, pathways with lower emission intensities are more advantageous to deploy and this yields a higher share of global steel production to the regions that can economically deploy them.

When negative emission technologies are deployed in a given sector

they can impact the technologies that are deployed in that sector as well as affecting the deployment of low carbon technologies in other sectors. When exploring this sensitivity in Section 4.2.2, I found that bio-electricity with CCS (BioCCS) results in the electricity generation sector achieving negative emissions and the steel sector deploys less of the low carbon advanced steelmaking pathways because negative emissions generated by BioCCS leave more room for the remaining emissions in other sectors of the economy.

5.2 Future work

The exact pathway for deployment of hydrogen is still speculative at this point. This uncertainty can be reduced by understanding how H_2 production costs could decrease in the future due to technology advances. Green H_2 in particular is anticipated to decrease in cost as module stack sizes increase, manufacturing facilities achieve economies of scale and operations increase efficiencies (IRENA (2020)). If these gradual cost decreases can be modeled, it may better mirror the actual dynamics of the future reductions in cost of hydrogen production. Furthermore, region specific renewable energy costs (and dealing with their intermittency) could be explicitly modeled as inputs to the Green H_2 production. Since Green H_2 relies on renewable electricity, its price and capacity factor will impact the overall cost of the Green H_2. Certain regions have very high renewable resources resulting in low electricity prices as well as curtailed electricity. These areas may present greater promise for incorporating electrolytic H_2 production.

Future work could also delve further into the limits of emission reduction via conventional steelmaking pathways. For one, the modeling of scrap steel stock will vary by region. The availability of scrap steel is the main limiting factor in the deployment of secondary steel production. Representation of other adaptations to conventional steelmaking that can reduce energy use and decrease emissions could also be explicitly represented in an integrated assessment model. Process changes such as blending of hydrogen into existing processes and BF top gas recycling are examples of such process changes (Cavaliere (2019)). In some cases, retrofit costs may be more cost effective than greenfield construction.

In addition, further exploration is needed to understand the decarbonization pathways for high temperature heating. Similar to my thesis work on steelmaking; the levelized cost assessments for advanced low carbon heating technologies could be incorporated into the EPPA model to analyze how they would compete for deployment. In my thesis, I assessed the heating cost associated with clinker kilns and glass furnaces, however there are other applications for high temperature heat such as

ammonia production or other petrochemical processes. Low carbon hydrogen heating would be in competition with other promising low carbon heating pathways including electrification and CCS. These technologies should also be included in the modeling to determine the optimal decarbonization pathway across different regions. There may also be potential emission reductions from conventional fossil fuel heating technologies similar to the results from my analysis of steelmaking via increased energy efficiencies and process optimizations. Regional variations will play a role in which technologies are adopted; as will the stringency of the carbon policy.

This research explores only two applications for hydrogen in decarbonizing heavy industry. Future work in this area could replicate this type of analysis to explore applications of low carbon hydrogen in other hard to abate industrial processes. For example, applications include high temperature heating for other industrial processes, power generation, and chemical production (CCUS and H_2). Utilizing integrated assessment models can assist in comparing the economic competitiveness of different decarbonization pathways including low carbon H_2. Economy-wide models like the EPPA model are also able to capture inter-sectoral interactions which can be critical in predicting which low carbon technologies are deployed. As described in Section 4.2.2, this interaction can be impactful and can result in certain sectors accounting for a greater share of the region's decarbonization. The type of analysis that I conducted in my thesis can assist policymakers and industry stakeholders in better understanding which pathways are most promising and how policies will impact deployment.

5.3 Policy Applications and Considerations

The findings from this research emphasize the importance of implementing policy that will support advanced low carbon technologies. Since, many of these technologies are currently more expensive than conventional technologies, they will not be implemented without cost reductions via policy assistance or technological advances. In the EPPA model, our decarbonization scenario relies primarily on a global carbon tax instrument that is enacted on all sectors of the economy. This carbon tax

increases over time to progressively cut greenhouse gases. By applying a cost to greenhouse gas emissions, the low carbon technologies become more competitive. For products that are traded globally such as steel, it is crucial that climate policies protect against carbon leakage. Carbon leakage is defined by the IPCC as an increase in CO_2 emissions in regions with less stringent carbon policies in response to other regions implementing more stringent carbon policies (IPCC (2007)). This increase in emissions can result from manufacturers relocating to regions with less stringent carbon policies where production costs are cheaper. It can also be due to decreased fossil fuel prices because of lower demand for fossil fuels; making it favorable for regions without mitigation requirements to increase fossil fuel consumption. In the policy scenario I modeled in this thesis work, there is a uniform global carbon price and all regions are pressured to decarbonize. However, realistically we will likely see a segmented world, where many emerging regions might implement very mild if any climate policy actions.

Countries that do implement carbon taxes will then have higher costs for their domestic production and they risk losing manufacturers to areas without carbon policies. One solution is to implement carbon border adjustment mechanisms; this is currently being developed in the European Union (EU Commission (2022)). Carbon border adjustment mechanisms implement a fee equal to the carbon price on imported goods based on their embedded greenhouse gas emissions (EU Commission (2022)). Importers would be responsible for reporting the greenhouse gas emissions embedded in imported products however, while the EU includes indirect emissions, at this point it is not certain how exactly the indirect emissions from electricity usage would be accounted for (EU Commission (2022)). For electricity intensive processes like EAF or Green H_2 production, the indirect emissions can be sizeable. Carbon border adjustment mechanisms would require a complex accounting practice to ensure that emissions are reported accurately. Despite potential implementation challenges, carbon border mechanisms provide a practical way to account for emissions from imports and ensure that domestic production is still competitive.

A carbon tax (or a carbon price resulting from an emission trading scheme) will

drive up costs for emission intensive processes and competing low carbon technologies will be deployed at particular costs. My thesis work sought to explore the role that hydrogen could play in decarbonization. Hydrogen is seen as being a versatile solution that could be applied to a number of processes and currently 26 countries have already adopted national hydrogen strategies aimed at utilizing hydrogen for various decarbonization pathways (Bermudez et al. (2022); DOE (2022)). But adoption of new applications has not progressed as much yet and today hydrogen is still primarily used for chemical and petrochemical production (namely ammonia). Also, the production of hydrogen is currently still reliant on fossil fuels and annually its production results in 830 Mt of CO_2 (IEA (2019)). Decarbonizing current hydrogen production should be prioritized.

Another priority should be to create a more rigorous system to define what qualifies as "low carbon" or "clean" hydrogen. The current informal color labeling system lacks the specificity needed. Furthermore, policies will need to include a method to actually verify and certify the emission intensity of hydrogen production pathways. So called Blue hydrogen represents a potential transition fuel for the Oil & Gas sector and could enable continued use of existing infrastructure. But, because Blue hydrogen relies on methane for its production, the upstream emissions intensity should be considered as well as requiring a certain minimum capture rate to ensure that the hydrogen production itself is a low emission process.

It is extremely difficult to pinpoint which technology will be superior for the next decade or longer. In the case of steelmaking, my thesis work showed that the optimal mix of decarbonization technologies is region specific and influenced by the presence of other technology deployment (such as BioCCS). My work also demonstrated that while hydrogen is promising in some aspects, its application in steelmaking is not currently the primary solution due to its high costs. CCS is currently a more cost competitive option and conventional steelmaking has potential for further emissions reductions. If policy would be formulated as more technology agnostic, it would allow for the deployment of new superior technologies. For example, technologies like iron ore electrolysis which today are still in development may one day be ready at a

commercial scale. If policies are too rigid, then they will not be able to adapt to new technological advances. Policy actions should also consider the advances that can be made to conventional pathways in order to achieve cost effective emission reductions using the existing infrastructure.

Hydrogen is not (and most likely will not) be the silver bullet to solving climate change but it can be one of the tools that are utilized. It is important to decarbonize the current uses of hydrogen and also focus on applications in hard to abate sectors where electrification and other solutions are not feasible. To limit global warming to 1.5 Celsius will require that we achieve net zero GHG emissions by mid-century (IPCC (2022)). Given that many hard to abate sectors have plants that have long lifetimes, the turnover rate will be slow. The average age of blast furnaces in China is only 12 years old and these facilities can last upwards of 20 years (IEA (2020)). If we want to achieve real progress by 2050, then we need policy that will allow for the most cost effective and low emission processes to be deployed starting this decade. My thesis adds to the existing literature by providing a rigorous exploration of different aspects of decarbonization of heavy industry.

Appendix A

Tables

Table A.1: Hydrogen production cost financial assumptions

Financial Parameters	**Value**	**Reference**
Interest Rate for Construction Period	4%	Morris et al. (2019a)
Discount Rate	8.5%	Morris et al. (2019a)
Currency	2016 USD	N/A
Grid Electricity Cost	$69/MWh	EIA (2023)
Natural Gas Cost	$4/MMBtu	EIA (2022b)
Project Lifetime	20 years	Khan et al. (2021) Mallapragada et al. (2022)

Table A.2: Natural gas reforming hydrogen production cost assumptions

Parameter	**Units**	**Blue H_2**	**Grey H_2**	**References**
Actual H_2 Production	kt/yr	217	159	
Capacity factor	%	90	90	
Overnight Capital Cost	\$/GJ H_2 HHV/yr	28.20	14.66	Lewis et al. (2022)
Construction Years	Years	3	3	Lewis et al. (2022)
Total Capital Req.	\$/GJ H_2 HHV/yr	30.16	15.69	
Capital Recovery Req.	\$/GJ H_2 HHV	2.71	1.66	
Fixed O&M	\$/GJ H_2 HHV	0.77	0.45	Saur et al. (2018) NREL (2021) Lewis et al. (2022)
Variable O&M	\$/GJ H_2 HHV	0.44	0.28	Saur et al. (2018) NREL (2021) Lewis et al. (2022)
Hourly Electricity Demand	MW/h	110	12.65	Saur et al. (2018) Lewis et al. (2022)
Hourly Heat Rate	MMBtu/h	4804	3518	Lewis et al. (2022)
CO_2 Transportation & Storage Cost	\$/tCO_2	10.53	N/A	Smith et al. (2021)
Levelized Cost of H_2 Production	\$/GJ H_2 HHV	11.95	7.62	
Ratio relative to Baseline Technology	unitless	3.2	2.0	-

Table A.3: Electrolytic hydrogen production cost assumptions

Parameter	**Units**	**Green H_2**	**Yellow H_2**	**References**
Actual H_2 Production	kt/yr	92	92	
Capacity factor	%	57	90	
Overnight Capital Cost	\$/GJ H_2 HHV/yr	124.08 H_2 *plant* 139.05 *Wind Plant*	78.59	ISPT (2020); NREL (2021)
Construction Years	Years	1 H_2 *plant* 3 *Wind Plant*	1	ISPT (2020); NREL (2021)
Total Capital Req.	\$/GJ H_2 HHV/yr	284.78	81.73	
Stack Replacement Cost	\$/GJ H_2 HHV/yr	25.32	16.04	Derived from Khan et al. (2021) Saur et al. (2018) Chardonnet et al. (2017)
Capital Recovery Req.	\$/GJ H_2 HHV	27.42	6.94	
Stack Lifetime	Years	12	7.6	Saur et al. (2018) IEA (2019)
Stack Capital Recovery Req.	\$/GJ H_2 HHV	3.44	2.95	
Fixed O&M	\$/GJ H_2 HHV	5.54 H_2 *plant* 4.45 *Wind Plant*	3.51	Saur et al. (2018) NREL (2021)
Variable O&M	\$/GJ H_2 HHV	0.08	0.08	Saur et al. (2018) NREL (2021)
Hourly Electricity Demand	MW/h	1000	633	Saur et al. (2018)
Levelized Cost of H_2 Production	\$/GJ H_2 HHV	40.92	39.83	
Ratio relative to Baseline Technology	unitless	10.8	10.6	-

Table A.4: Wind capacity factors

Resource Level	**Capacity Factor**	**Location**
Low	35 %	33.07868615030591, -95.44870293943644
Average U.S. Wind Resource Level	43%	34.88447558813019, -97.21912666481369
High	56%	64.34776768088481, -17.713612479642226
2019 Dataset: Merra 2	Land Based Wind Turbines: Vestas V90 2000 Turbine Height: 90m	Pfenninger & Staffell (2022); Staffell & Pfenninger (2016); Pfenninger & Staffell (2016)

Table A.5: Iron and steel production cost financial assumptions

Financial Parameters	**Value**	**Reference**
Interest Rate for Construction Period	4%	Morris et al. (2019a)
Discount Rate	8.5%	Morris et al. (2019a)
Currency	2016 USD	N/A
Plant Lifetime	25 years	IEA (2019)
Construction Time	3 years	Hughes & Zoelle (2022)
Grid Electricity Cost	\$69/MWh	EIA (2023)
Natural Gas Cost	\$4/MMBtu	EIA (2022b)
Coal Cost	\$1.83/GJ	EIA (2022a)
Coke Cost	\$6.64/GJ	De Clercq et al. (2022)
Iron Ore Cost *(DRI grade)*	\$144/tonne	Vogl et al. (2018)
Iron Ore Cost *(BOF grade)*	\$134/tonne	Vogl et al. (2018) Barrington (2018) S&P Global (2023a)
Electrode Cost	\$ 5.78/kg	Vogl et al. (2018)
Lime Cost	\$0.14/kg	Vogl et al. (2018)
Alloy Cost	\$2.57/kg	Vogl et al. (2018)
Scrap Steel Cost	\$304/t	USGS (2019b)

Table A.6: DRI & EAF material usage rates

Material	**Units**	**Value**	**Reference**
Iron Ore	t/tcs	1.5	Vogl et al. (2018)
Graphite Electrode	kg/tcs	2	Vogl et al. (2018)
Lime	kg/tcs	50	Vogl et al. (2018)
Alloy	kg/tcs	11	Vogl et al. (2018)
Scrap Steel	t/tcs	1.1	100% scrap feed WSA (2014)

Table A.7: BF material usage rates

Material	**Units**	**Value**	**Reference**
Iron Ore	t/tcs	1.4	WSA (2014)

Table A.8: Conventional iron and steel production cost assumptions

Parameter	**Units**	**DRI-EAF**	**EAF Scrap**	**BF-BOF**	**References**
Steel Production	Mtpa	2	2	2	Midrex (2019)
Capacity Factor	%	90	90	90	IEA (2019) James et al. (2019)
Overnight Capital Cost	$/tcs/yr	578.20	266	588	IEA (2019) Dahlmann et al. (2015)
Total Capital Req.	$/tcs	70.31	32.34	71.50	-
Fixed O&M	$/tcs	21.59	8.87	19.60	3% of total CapEx (Vogl et al. (2018))
Labor	$/thrs	79.26	78.02	62.53	14% of total cost (Vogl et al. (2018))
Electricity Usage	kWh/tcs	109	0	97.2	Cavaliere (2019); WSA (2014)
Ironmaking					
Steelmaking	kWh/tcs	753	520	77.7	Vogl et al. (2018); WSA (2014)
hot rolling	kWh/thrs	110	110	110	Duarte & Becerra (2011)
Natural Gas	GJ HHV/tcs	11.52	0	0.008	Cavaliere (2019); WSA (2014)
Ironmaking					
Steelmaking	GJ HHV/tcs	0	0.65	0.062	WSA (2014)
hot rolling	GJ HHV/thrs	1.05	1.05	1.05	Duarte & Becerra (2011)
Coal Usage	GJ HHV/tcs	0	0.53	5	WSA (2014)
Coke Usage	GJ HHV/tcs	0	0	9.78	WSA (2014)
Levelized Cost of Steel	$/thrs	563	566	453	-
U.S. (2019) Steel Production by Process	%	3	67	30	WSA (2022b)

Table A.9: Low carbon iron and steel production cost assumptions

Parameter	**Units**	**DRI-EAF with CCS**	H_2 **DRI-EAF**	**References**
Steel Production	Mtpa	2	2	Midrex (2019)
Capacity Factor	%	90	90	IEA (2019) James et al. (2019)
Overnight Capital Cost	\$/tcs/yr	578.20 127.91 (CC)	578.20	IEA (2019)
Total Capital Req.	\$/tcs	85.86	70.31	N/A
Fixed O&M	\$/tcs	21.59	21.59	3% of total CapEx (Vogl et al. (2018))
CCS Fixed O&M	\$/tcs	2.53	N/A	James et al. (2019)
Labor	\$/thrs	79	79	Vogl et al. (2018)
CCS Variable O&M	\$/tcs	2.28	N/A	James et al. (2019)
H_2 Usage	kg/tcs	N/A	80.89	IEA (2019) Cavaliere (2019)
Elec. Usage *DRI*	kWh/tcs	314	109	Cavaliere (2019); James et al. (2019)
EAF	kWh/tcs	753	753	Vogl et al. (2018)
hot rolling	kWh/thrs	110	110	Duarte & Becerra (2011)
Natural Gas Usage *DRI*	GJ HHV /tcs	11.52	1.89	Cavaliere (2019); James et al. (2019)
hot rolling	GJ HHV/thrs	1.05	1.05	Duarte & Becerra (2011)
CO_2 Capture Rate	%	90	N/A	IEA (2020)
CO_2 T&S Costs	\$/tCO_2	10.53	N/A	Smith et al. (2021)
Levelized Cost of Steel	\$/thrs	605	667 (Blue H_2) 1010 (Green H_2)	
Ratio of Cost to Weighted Average Cost of Traditional Steel	unitless	1.14	1.25 (Blue H_2) 1.9 (Green H_2)	

Table A.10: Regional steel production by process type in 2019. Data derived from the World Steel Association (WSA (2022b))

Region	**BOF [Mt]**	**DRI-EAF [Mt]**	**EAF [Mt]**
China	896	0	100
European Union	94	1	65
India	49	31	32
Japan	75	0	24
USA	26	3	59
Russia	47	7	18
S. Korea	49	0	23
Other Eurasia	37	0	28
Middle East	3	36	6
Dynamic Asia	14	1	21
Brazil	25	0	7
Other East Asia	13	0	14
Africa	4	6	9
Mexico	4	5	9
Canada	8	1	4
Other Latin America	7	1	2
Indonesia	4	0	5
Australia and New Zealand	5	0	1

Table A.11: Heat demand assumptions for selected industrial processes

Process	**Units**	**Heat Demand**	**Reference**
Clinker Kiln	GJ/t	3.444	Friedmann et al. (2019)
Glass Furnace	GJ/t	6.858	Friedmann et al. (2019)

Appendix B

Figures

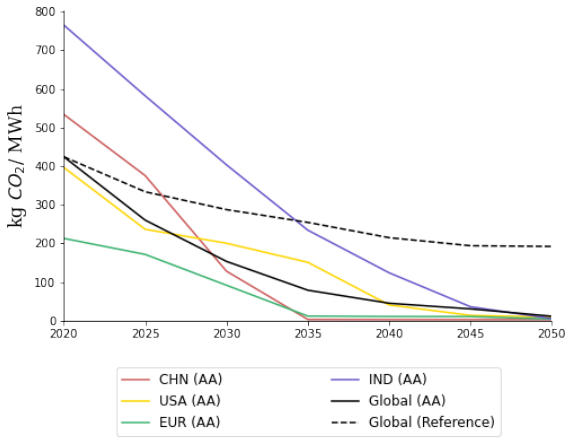

Figure B-1: Direct CO_2 emission intensity of electricity generation. The scenario modeled is the Accelerated Action policy case with base cost assumptions

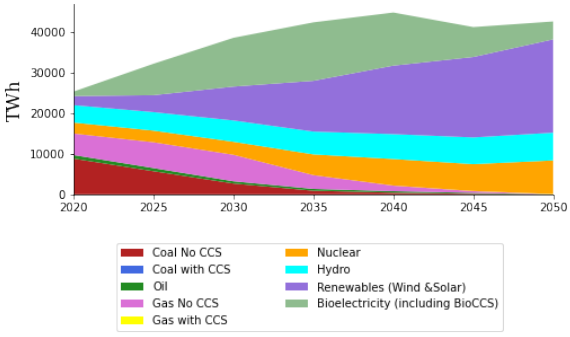

Figure B-2: Global total electricity produced by generation type. The scenario modeled is the Accelerated Action policy case with base cost assumptions

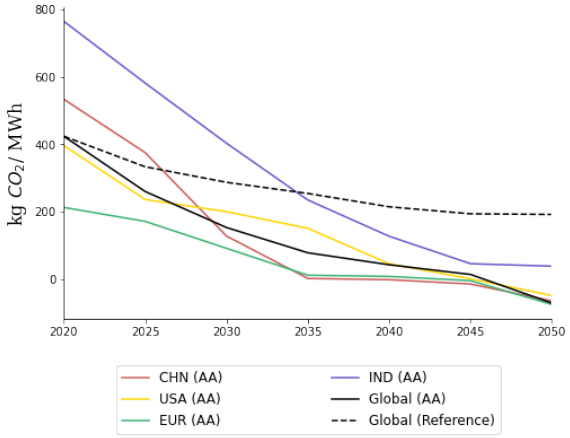

Figure B-3: Direct CO_2 emission intensity of electricity generation. The scenario modeled is the Accelerated Action policy case with base cost assumptions and includes deployment of bioelectricity with CCS (BioCCS)

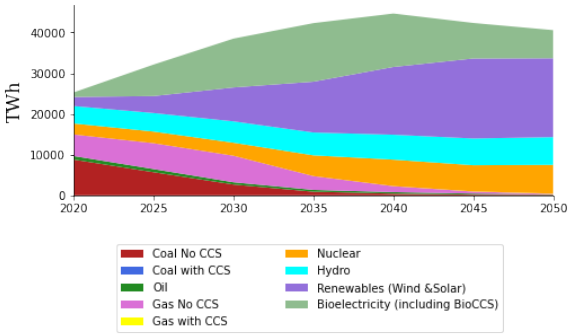

Figure B-4: Global total electricity produced by generation type. The scenario modeled is the Accelerated Action policy case with base cost assumptions and includes deployment of bioelectricity with CCS (BioCCS)

Bibliography

Aguiar A, M Chepeliev, E Corong, R McDougall, & D van der Mensbrugghe 2019 'The GTAP Data Base: Version 10' *Journal of Global Economic Analysis* 4(1):1–27 doi:10.21642/JGEA.040101AF URL https://jgea.org/ojs/index.php/jgea/article/view/77 number: 1.

Arrigoni A & L Bravo Diaz 2022 'Hydrogen Emissions from a Hydrogen Economy and their Potential Global Warming Impact' Technical report European Commission. Joint Research Centre. LU URL https://data.europa.eu/doi/10.2760/065589.

Barrington C 2018 'DR-Grade Iron Ore Pellets - A Supply Overview' URL https://www.midrex.com/tech-article/dr-grade-iron-ore-pellets-a-supply-overview/.

Bellevrat E & K West 2018 'Clean and efficient heat for industry – Analysis' Technical report International Energy Agency URL https://www.iea.org/commentaries/clean-and-efficient-heat-for-industry.

Bermudez J, S Evangelopoulou, & F Pavan 2022 'Hydrogen: Energy Stem Overview' Technical report International Energy Agency (IEA) URL https://www.iea.org/reports/hydrogen.

Bhaskar A, M Assadi, & H Nikpey Somehsaraei 2020 'Decarbonization of the Iron and Steel Industry with Direct Reduction of Iron Ore with Green Hydrogen' *Energies* 13(3):758 doi:10.3390/en13030758 number: 3 Publisher: Multidisciplinary Digital Publishing Institute.

Breckel A, N Britton, S Comello, T Green, & A Maranville 2021 'The Future of Clean Hydrogen in the United States: Views from Industry, Market Innovators, and Investors' Technical report Energy Futures Initiative URL https://energyfuturesinitiative.org/wp-content/uploads/sites/2/2022/03/The-Future-of-Clean-Hydrogen-in-the-U.S._Report-1.pdf.

Cavaliere P 2019 *Clean Ironmaking and Steelmaking Processes* Springer International Publishing doi:10.1007/978-3-030-21209-4_9 URL https://doi.org/10.1007/978-3-030-21209-4_9.

Chardonnet C, V Giordano, L De Vos, F Genoese, G Roig, F Bart, J Lanoix, T De Lacroix, T Ha, & B Van Genabet 2017 'Study on Early Business Cases for H2 in Energy Storage and More Broadly Power to H2 Applications' Technical report Fuel Cells and Hydrogen Joint Undertaking/Tractebel Engineering URL https://hsweb.hs.uni-hamburg.de/projects/star-formation/hydrogen/P2H_Full_Study_FCHJU.pdf.

Chen H, S Paltsev, A Gurgel, J Reilly, & J Morris 2022 'A Multisectoral Dynamic Model for Energy, Economic, and Climate Scenario Analysis' *Low Carbon Economy* 13(02):70–111 doi:10.4236/lce.2022.132005.

Ciftci BB 2018 'Blog: The Future of Global Scrap Availability' URL https://worldsteel.org/media-centre/blog/2018/future-of-global-scrap-availability/.

Ciftci BB 2021 'Raw Materials' URL https://worldsteel.org/steel-topics/raw-materials/.

Collins L 2022 'Sinopec Partners with Cummins to Build 1GW Hydrogen Electrolyser Factory in China' URL https://www.upstreamonline.com/hydrogen/sinopec-partners-with-cummins-to-build-1gw-hydrogen-electrolyser-factory-in-china/2-1-1139182 section: hydrogen.

Dahlmann P, H Bodo Lungen, J Ghenda, M Wortler, F Schuler, N Voigt, & T Schmidt 2015 'Steel's Contribution to a Low-Carbon Europe 2050: Technical and Economic Analysis of the Steel Sector's CO2 Abatement Potential' *Association for Iron and Steel Technology* 12(4):62–72 URL https://imis.aist.org/store/detail.aspx?id=MAGAPR15.

Davey E 2023 'US Company Gets $120 Million Boost to Make 'Green Steel" URL https://apnews.com/article/production-facilities-climate-and-environment-business-d095684168e9f6a2634ee9316007f994.

De Clercq F, A Doyle, & T Voet 2022 'High Coking Coal Prices Provide Glimpse into Steelmaking's Future' URL https://www.mckinsey.com/industries/metals-and-mining/our-insights/high-coking-coal-prices-provide-glimpse-into-steelmakings-future.

DOE 2021 'Hydrogen Shot Summit' URL https://www.energy.gov/eere/fuelcells/hydrogen-shot-summit.

DOE U 2022 'DOE National Clean Hydrogen Strategy and Roadmap' Technical report U.S. Department of Energy (DOE) URL https://www.hydrogen.energy.gov/pdfs/clean-hydrogen-strategy-roadmap.pdf.

Duarte PE & J Becerra 2011 'Decrease of GHG emissions through the Carbon Free Emissions ENERGIRON DR Scheme in Integrated Mills' *HYL Technologies*

:8URL https://www.energiron.com/wp-content/uploads/2019/05/2011-Decrease-of-GHG-emissions-through-the-Carbon-Free-Emissions-ENERGIRON-DR-Scheme-in-Integrated-Mills.pdf.

Duarte PE, A Tavano, & E Zendejas 2010 'Achieving Carbon Free Emissions via the ENERGIRON DR Process' Technical report Energiron URL https://www.energiron.com/wp-content/uploads/2019/05/2010-Achieving-Carbon-Free-Emissions-via-the-ENERGIRON-DR-Process.pdf.

Egenhofer C, DL Schrefler, A Marcu, S Roth, & W Stoefs 2014 'For a Study on Composition and Drivers of Energy Prices and Costs in Energy Intensive Industries: The Case of the Flat Glass Industry' Technical report Centre for European Policy Studies URL https://op.europa.eu/en/publication-detail/-/publication/b43ca37c-ae26-49f3-9341-7558a75d52da.

EIA 2022a 'Annual Coal Reports - U.S. Energy Information Administration (EIA)' URL https://www.eia.gov/coal/annual/index.php.

EIA 2022b 'U.S. Natural Gas Prices' URL https://www.eia.gov/dnav/ng/ng_pri_sum_dcu_nus_m.htm.

EIA 2023 'Electric Power Monthly - U.S. Energy Information Administration (EIA)' URL https://www.eia.gov/electricity/monthly/epm_table_grapher.php.

EU Commission E 2022 'Carbon Border Adjustment Mechanism' URL https://taxation-customs.ec.europa.eu/green-taxation-0/carbon-border-adjustment-mechanism_en.

Fischedick M, J Marzinkowski, P Winzer, & M Weigel 2014 'Techno-economic Evaluation of Innovative Steel Production Technologies' *Journal of Cleaner Production* 84:563–580 doi:10.1016/j.jclepro.2014.05.063.

Friedmann SJ, Z Fan, & K Tang 2019 'Low-Carbon Solutions for Heavy Industry: Source, Options, and Costs Today' Technical report Columbia Center on Global Energy Policy URL https://www.energypolicy.columbia.edu/publications/low-carbon-heat-solutions-heavy-industry-sources-options-and-costs-today.

FuelCellsWorks 2022 'The World's Largest Green Hydrogen Project With A 150MW Electrolyser Comes Online In China' URL https://fuelcellsworks.com/news/the-worlds-largest-green-hydrogen-project-with-a-150mw-electrolyser-comes-online-in-china-el-periodico-de-la-energia/ section: China.

Glass Alliance Europe G 2023 'What is Glass?' URL https://www.glassallianceeurope.eu/en/what-is-glass.

Gross S 2021 'The Challenge of Decarbonizing Heavy Industry' URL https://www.brookings.edu/research/the-challenge-of-decarbonizing-heavy-industry/.

H2GreenSteel 2022 'The Colors of Hydrogen' URL https://www.h2greensteel.com/articles/the-colors-of-hydrogen.

H2GreenSteel 2023 'About us' URL https://www.h2greensteel.com/about-us.

Ho MT, A Bustamante, & DE Wiley 2013 'Comparison of CO2 Capture Economics for Iron and Steel Mills' *International Journal of Greenhouse Gas Control* 19:145–159 doi:10.1016/j.ijggc.2013.08.003.

Hodges L & J Anton 2022 'Prices Soften on Weaker Steel Demand Outlook' URL https://www.spglobal.com/marketintelligence/en/mi/solutions/steel-forecast.html.

Hosford WF 2012 *Iron and Steel* Cambridge: Cambridge University Press doi:10.1017/CBO9781139086233.002 URL https://www.cambridge.org/core/books/iron-and-steel/general-introduction/D7E0036B39F9BA5FE016F0520723F18E.

Hughes S & A Zoelle 2022 'Cost of Capturing CO2 from Industrial Sources' Technical report National Eenergy Technology Laboratory (NETL) URL https://netl.doe.gov/projects/files/CostofCapturingCO2fromIndustrialSources_071522.pdf.

Hybrit 2022 'Fossil-free steel – a joint opportunity!' URL https://www.hybritdevelopment.se/en/.

Iberdola 2022 'Iberdrola and H2 Green Steel Sign 2.3 Billion Euros Green Hydrogen Deal' URL https://www.iberdrola.com/press-room/news/detail/deal-green-hydrogen-iberdrola-h2-green-steel.

IEA 2018a 'Industrial Heat Demand by Temperature Range' URL https://prod.iea.org/data-and-statistics/charts/industrial-heat-demand-by-temperature-range-2018.

IEA 2018b 'Technology Roadmap - Low-Carbon Transition in the Cement Industry' Technical report International Energy Agency URL https://www.iea.org/reports/technology-roadmap-low-carbon-transition-in-the-cement-industry.

IEA 2019 'The Future of Hydrogen' Technical report International Energy Agency URL https://www.iea.org/reports/the-future-of-hydrogen.

IEA 2020 'Iron and Steel Technology Roadmap - Towards more sustainable steelmaking' Technical report International Energy Agency URL https://www.iea.org/reports/iron-and-steel-technology-roadmap.

IEA 2021 'World Energy Outlook 2021 – Analysis' Technical report URL https://www.iea.org/reports/world-energy-outlook-2021.

IEA 2022 *Achieving Net Zero Heavy Industry Sectors in G7 Members* OECD doi:10.1787/f25c9648-en URL https://www.oecd-ilibrary.org/energy/achieving-net-zero-heavy-industry-sectors-in-g7-members_f25c9648-en.

IEA 2022a 'Defying Expectations, CO2 Emissions From Global Fossil Fuel Combustion Are Set to Grow in 2022 by Only a Fraction of Last Year's Big Increase' URL https://www.iea.org/news/defying-expectations-co2-emissions-from-global-fossil-fuel-combustion-are-set-to-grow-in-2022-by-only-a-fraction-of-last-year-s-big-increase.

IEA 2022b 'Gas Market Report Q4 2022 including Global Gas Security Review 2022' URL https://www.iea.org/reports/gas-market-report-q4-2022.

IEA 2022c 'Hydrogen Projects Database - Data product' URL https://www.iea.org/data-and-statistics/data-product/hydrogen-projects-database.

IPCC 2007 'AR4 WGIII Chapter 11: Mitigation from a cross-sectoral perspective - 11.7.2 Carbon leakage' Technical report Intergovernmental Panel on Climate Change URL https://archive.ipcc.ch/publications_and_data/ar4/wg3/en/ch11-ens11-7-2.html.

IPCC 2022 'Climate Change 2022: Impacts, Adaptation and Vulnerability. In IPCC 6th Assessment Report' Technical report Intergovernmental Panel on Climate Change URL https://www.ipcc.ch/report/ar6/wg2/.

IRENA 2020 'Green Hydrogen: A Guide to Policy Making' Technical report International Renewable Energy Agency (IRENA) URL https://www.irena.org/publications/2020/Nov/Green-hydrogen.

ISPT 2020 'Gigawatt Green Hydrogen Plant: State of the Art Design and Total Installed Capital Costs' Technical report Institute for Sustainable Process Technology URL https://ispt.eu/media/ISPT-public-report-gigawatt-green-hydrogen-plant.pdf.

Iyer RK, J Kelly, & A Elgowainy 2022 'Electrolyzers for Hydrogen Production: Solid Oxide, Alkaline, and Proton Exchange Membrane' .

James R III, D Keairns, M Turner, M Woods, N Kuehn, & A Zoelle 2019 'Cost and Performance Baseline for Fossil Energy Plants Volume 1: Bituminous Coal and Natural Gas to Electricity' Technical Report NETL-PUB-22638, 1569246 doi:10.2172/1569246 URL https://www.osti.gov/servlets/purl/1569246/.

Khan MHA, R Daiyan, Z Han, M Hablutzel, N Haque, R Amal, & I MacGill 2021 'Designing Optimal Integrated Electricity Supply Configurations for Renewable

Hydrogen Generation in Australia' *iScience* 24(6):102539 doi:10.1016/j.isci.2021.102539.

Kirschen M, K Badr, & H Pfeifer 2011 'Influence of Direct Reduced Iron on the Energy Balance of the Electric Arc Furnace in Steel Industry' *Energy* 36(10):6146–6155 doi:10.1016/j.energy.2011.07.050.

Krey V, O Masera, G Blanford, T Bruckner, R Cooke, K Fisher-Vanden, H Haberl, E Hertwich, E Kriegler, D Mueller, S Paltsev, L Price, S Schlomer, D Ürge Vorsatz, D van Vuuren, & T Zwickel 2014 'Annex II: Metrics & Methodology. In: Climate Change 2014: Mitigation of Climate Change. Contribution of Working Group III to the Fifth Assessment Report of the Intergovernmental Panel on Climate Change' Technical report Intergovernmental Panel on Climate Change URL https://archive.ipcc.ch/pdf/assessment-report/ar5/wg3/ipcc_wg3_ar5_annex-ii.pdf.

Laguna JC, J Duerinck, F Meinke-Hubeny, & J Valee 2021 *Carbon-free Steel Production: Cost Reduction Options and Usage of Existing Gas Infrastructure.* LU: Panel for the Future of Science and Technology (European Parliamentary Research Services) URL https://data.europa.eu/doi/10.2861/01969.

Lazard 2021 'Lazard's Levelized Cost of Hydrogen Analysis' Technical Report v. 2.0 Lazard URL https://www.lazard.com/media/451922/lazards-levelized-cost-of-hydrogen-analysis-version-20-vf.pdf.

LBNL 2010 'The State–of-the-Art Clean Technologies (SOACT) for Steelmaking Handbook' Technical report Lawrence Berkeley National Laboratory (LBNL). Prepared for Asia Pacific Partnership for Clean Development and Climate URL https://www.jisf.or.jp/business/ondanka/eco/docs/SOACT-Handbook-2nd-Edition.pdf.

Lewis E, S McNaul, M Jamieson, M Henriksen, H Matthews, L Walsh, J Grove, T Shultz, & R Stevens 2022 'Comparison of Commercial, State-of-the-Art, Fossil-Based Hydrogen Production Technologies' Technical Report DOE/NETL-2022/3241, 1862910 doi:10.2172/1862910 URL https://www.osti.gov/servlets/purl/1862910/.

Mallapragada D, E Gencer, & P Insinger 2022 'Can Industrial-Scale Solar Hydrogen Supplied from Commodity Technologies Be Cost Competitive by 2030?: Cell Reports Physical Science' *Cell Reports Physical Science* doi:https://doi.org/10.1016/j.xcrp.2020.100174 URL https://www.cell.com/cell-reports-physical-science/fulltext/S2666-3864(20)30185-5.

Mandova H, T Vass, A Fernandez-Pales, P Levi, & T Gul 2020 'The Challenge of Reaching Zero Emissions in Heavy Industry – Analysis' Technical report International Energy Agency (IEA) URL https://www.iea.org/articles/the-challenge-of-reaching-zero-emissions-in-heavy-industry.

Midrex 2019 '2019 World Direct Reduction Statistics' Technical report Midrex URL https://www.midrex.com/wp-content/uploads/Midrex-STATSbook2019Final.pdf.

MIT Joint Program J 2023 'Integrated Global System Modeling (IGSM) Framework | MIT Global Change' URL https://globalchange.mit.edu/research/research-tools/global-framework.

Morris J, J Farrell, H Kheshgi, H Thomann, H Chen, S Paltsev, & H Herzog 2019a 'Representing the Costs of Low-Carbon Power Generation in Multi-Region Multi-Sector Energy-Economic Models' *International Journal of Greenhouse Gas Control* 87:170–187 doi:https://doi.org/10.1016/j.ijggc.2019.05.016.

Morris J, H Kheshgi, S Paltsev, & H Herzog 2021 'Scenarios for the Deployment of Carbon Capture and Storage in the Power Sector in a Portfolio of Mitigation Options' *Climate Change Economics* 12(1) doi:https://doi.org/10.1142/S2010007821500019.

Morris JF, JM Reilly, & YHH Chen 2019b 'Advanced Technologies in Energy-Economy Models for Climate Change Assessment' *Energy Economics* 80:476–490 doi:10.1016/j.eneco.2019.01.034.

NETL 2023 'NETL Patents Fiber Optic Sensor Technology for Hydrogen Leak Detection' URL https://netl.doe.gov/node/12415.

NREL 2021 'Annual Technology Baseline (ATB) Cost and Performance Data for Electricity Generation Technologies' URL https://dx.doi.org/10.25984/1807473.

Paltsev S, A Gurgel, J Morris, H Chen, S Dey, & S Marwah 2021a 'Economic Analysis of the Hard-to-Abate Sectors in India' *Energy Economics* 112:34 doi:https://doi.org/10.1016/j.eneco.2022.106149.

Paltsev S, A Schlosser, H Chen, X Gao, A Gurgel, H Jacoby, J Morris, R Prinn, A Sokolov, & K Strzepek 2021b '2021 Global Change Outlook: Charting the Earth's Future Energy, Managed Resources, Climate, and Policy Prospects' Technical report MIT Joint Program on the Science and Policy of Global Change URL https://globalchange.mit.edu/sites/default/files/newsletters/files/2021-JP-Outlook.pdf.

Parfomak PW 2021 'Pipeline Transportation of Hydrogen: Regulation, Research, and Policy' Technical report U.S. Congressional Research Service URL https://crsreports.congress.gov/product/pdf/R/R46700.

Pfenninger S & I Staffell 2016 'Long-term Patterns of European PV Output Using 30 Years of Validated Hourly Reanalysis and Satellite Data' *Energy* 114:1251–1265 doi:10.1016/j.energy.2016.08.068.

Pfenninger S & I Staffell 2022 'Hourly Output from Wind and Solar Plants' URL https://www.renewables.ninja/.

Purdue University DoAE 2023 'Global Trade Analysis Project (GTAP) Data Base 10' URL https://www.gtap.agecon.purdue.edu/databases/v10/index.aspx.

Reimink H & F Maciel 2021 'CO2 Data Collection' *World Steel Association* :25.

Rubin E, C Short, G Booras, J Davison, C Ekstrom, M Matuszewski, & S McCoy 2013 'A Proposed Methodology for CO2 Capture and Storage Cost Estimates' *International Journal of Greenhouse Gas Control* 17:488–503 doi:https://doi.org/10.1016/j.ijggc.2013.06.004.

Sadler D & HS Anderson 2018 'H21 North of England Report' Technical report URL https://www.h21.green/app/uploads/2019/01/H21-NoE-PRINT-PDF-FINAL-1.pdf.

Saur G, T Ramsden, B James, & W Colella 2018 'Current Central Hydrogen Production from Grid PEM Electrolysis' URL https://www.nrel.gov/hydrogen/h2a-production-models.html.

Schmidt O, A Gambhir, I Staffell, A Hawkes, J Nelson, & S Few 2017 'Future Cost and Performance of Water Electrolysis: An Expert Elicitation Study' *International Journal of Hydrogen Energy* 42(52):30470–30492 doi:10.1016/j.ijhydene.2017.10.045.

Smith E, J Morris, H Kheshgi, H Teletzke, H Herzog, & Paltzev 2021 'The Cost of CO2 Transport and Storage in Global Integrated Assessment Modeling' *International Journal of Greenhouse Gas Control* 109 doi:https://doi.org/10.1016/j.ijggc.2021.103367.

S&P Global CI 2023a 'Specifications Guide: Global Iron Ore' URL https://www.spglobal.com/commodityinsights/PlattsContent/_assets/_files/en/our-methodology/methodology-specifications/global_iron_ore.pdf.

S&P Global CI 2023b 'Steel Scrap Prices US Midwest' URL https://www.spglobal.com/commodityinsights/en/our-methodology/price-assessments/metals/the-price-of-us-midwest-shredded-steel-scrap.

Staffell I & S Pfenninger 2016 'Using Bias-Corrected Reanalysis to Simulate Current and Future Wind Power Output' *Energy* 114:1224–1239 doi:10.1016/j.energy.2016.08.068.

USGS 2019a 'Cement Statistics and Information: Annual Publications: Mineral Yearbook' Technical report U.S. Geological Survey (USGS) URL https://www.usgs.gov/centers/national-minerals-information-center/cement-statistics-and-information.

USGS 2019b 'Iron and Steel Scrap Statistics and Information' Technical report U.S. Geological Survey (USGS): National Minerals Information Center URL https://www.usgs.gov/centers/national-minerals-information-center/iron-and-steel-scrap-statistics-and-information.

van Beek L, M Hajer, P Pelzer, D van Vuuren, & C Cassen 2020 'Anticipating Futures Through Models: the Rise of Integrated Assessment Modelling in the Climate Science-Policy Interface Since 1970' *Global Environmental Change* 65:102191 doi:10.1016/j.gloenvcha.2020.102191.

Vine D 2021 'Clean Industrial Heat: A Technology Inclusive Framework' Technical report Center for Climate and Energy Solutions URL https://www.c2es.org/wp-content/uploads/2021/10/Clean_Industrial_Heat_A_Technology_Inclusive_Framework.pdf.

Vogl V, M Ahman, & L Nilsson 2018 'Assessment of Hydrogen Direct Reduction for Fossil-free Steelmaking' *Journal of Cleaner Production* 203 doi:10.1016/j.jclepro.2018.08.279.

Wood L 2023 'China Cement Clinker Import Industry Report 2023: Due to the Lower Price of Imported Cement Clinker, Companies Import Cement Clinker as a Raw Material to Reduce Costs' URL https://www.businesswire.com/news/home/20230118005609/en/China-Cement-Clinker-Import-Industry-Report-2023-Due-to-the-Lower-Price-of-Imported-Cement-Clinker-Companies-Import-Cement-Clinker-as-a-Raw-Material-to-Reduce-Costs---ResearchAndMarkets.com.

World Bank W 2022 'World Bank Commodity Price Data (The Pink Sheet)' URL https://www.worldbank.org/en/research/commodity-markets.

Worrell E, L Price, M Neelis, C Galitsky, & N Zhou 2007 'World Best Practice Energy Intensity Values for Selected Industrial Sectors' Technical Report LBNL–62806, 927032 doi:10.2172/927032 URL http://www.osti.gov/servlets/purl/927032-RWG8Cg/.

WSA 2014 'Energy Use in the Steel Industry' Technical report World Steel Association.

WSA 2021 'Fact Sheet: Steel and Raw Materials' URL https://worldsteel.org/wp-content/uploads/Fact-sheet-steel-and-raw-materials.pdf.

WSA 2022a 'Sustainability Indicators: 2022 Report' Technical report World Steel Association URL https://worldsteel.org/wp-content/uploads/Sustainability-Indicators-2022-report-1.pdf.

WSA 2022b 'World Steel in Figures 2022' Technical report World Steel Association URL https://worldsteel.org/wp-content/uploads/World-Steel-in-Figures-2022-1.pdf.

WSA 2023 'The Steelmaking Process' URL https://worldsteel.org/about-steel/about-steel/steelmaking/.

Yan H, R Wang, S Du, B Hu, & Z Xu 2021 'Analysis and Perspective on Heat Pump for Industrial Steam Generation' *Advanced Energy and Sustainability Research* 2(5) doi:https://doi.org/10.1002/aesr.202000108.

Yu S, J Lehne, N Blahut, & M Charles 2021 '1.5C Steel: Decarbonizing the Steel Sector in Paris Compatible Pathways' Technical report Pacific Northwest National Laboratory URL https://e3g.wpenginepowered.com/wp-content/uploads/1.5C-Steel-Report_E3G-PNNL-1.pdf.